INTEGRATED RECEIVER CHANNEL CIRCUITS AND STRUCTURES FOR A PULSED TIME-OF-FLIGHT LASER RADAR

TARMO RUOTSALAINEN

Department of Electrical Engineering

OULU 1999

TARMO RUOTSALAINEN

INTEGRATED RECEIVER CHANNEL CIRCUITS AND STRUCTURES FOR A PULSED TIME-OF-FLIGHT LASER RADAR

Academic Dissertation to be presented with the assent of the Faculty of Technology, University of Oulu, for public discussion in Raahensali (Auditorium L 10), Linnanmaa, on May 19th, 1999, at 12 noon.

OULUN YLIOPISTO, OULU 1999

Manuscript received 9.4.1999
Accepted 14.4.1999

Communicated by
Professor Kari Halonen
Professor Franco Maloberti

ISBN 951-42-5216-0
(URL: http://herkules.oulu.fi/isbn9514252160/)

ALSO AVAILABLE IN PRINTED FORMAT

ISBN 951-42-5215-2
ISSN 0355-3213 (URL: http://herkules.oulu.fi/issn03553213/)

OULU UNIVERSITY LIBRARY
OULU 1999

Ruotsalainen, Tarmo: Integrated receiver channel circuits and structures for a pulsed time-of-flight laser radar
Department of Electrical Engineering, University of Oulu, P.O.B. 4500, FIN-90401, Oulu, Finland
1999
Oulu, Finland
(Manuscript received 9 April 1999)

Abstract

This thesis describes the development of integrated structures and circuit implementations for the receiver channel of portable pulsed time-of-flight laser rangefinders for industrial measurement applications where the measurement range is from ~ 1 m to ~ 100 m to noncooperative targets and the required measurement accuracy is from a few millimetres to a few centimetres. The receiver channel is used to convert the current pulse from a photodetector to a voltage pulse, amplify it, discriminate the timing point and produce an accurately timed logic-level pulse for a time-to-digital converter.

Since the length of the laser pulse, typically 5 ns, is large compared to the required accuracy, a specific point in the pulses has to be discriminated. The amplitude of the input pulses varies widely as a function of measurement range and the reflectivity of the target, typically from 1 to 100 ... 1000, so that the gain of the amplifier channel needs to be controlled and the discrimination scheme should be insensitive to the amplitude variation of the input signal. Furthermore, the amplifier channel should have low noise in order to minimize timing jitter.

Alternative circuit structures are discussed, the treatment concentrating on the preamplifier, gain control circuitry and timing discriminator, which are the key circuit blocks from the performance point of view. New circuit techniques and structures, such as a fully differential transimpedance preamplifier and a current mode gain control scheme, have been developed. Several circuit implementations for different applications are presented together with experimental results, one of them being a differential BiCMOS receiver channel with a bandwidth of 170 MHz, input referred noise of 6 pA/$\sqrt{Hz}$ and maximum transimpedance of 260 kΩ. It has an accuracy of about +/- 7 mm (average of 10000 measurements), taking into account walk error with an input signal range of 1:624 and jitter (3σ).

The achievable performance level using integrated circuit technology is comparable or superior to that of the previously developed commercially available discrete component implementations, and the significantly reduced size and power consumption open up new application areas.

Keywords: laser rangefinding, transimpedance preamplifier, gain control, timing discrimination

Acknowledgements

This thesis is based on research work carried out at the Electronics Laboratory of the Department of Electrical Engineering, University of Oulu.

I wish to express my deepest gratitude to my supervisor, Professor Juha Kostamovaara, for his tireless encouragement and guidance. I am also grateful to Professor Timo Rahkonen and Dr. Kari Määttä for their help and support. I thank my colleagues at the Electronics Laboratory for the pleasant working atmosphere and for their assistance, especially Mr. Pasi Palojärvi and Mr. Tero Peltola. My family deserve my warmest thanks for their support during these years.

I wish to thank Professors Franco Maloberti and Kari Halonen for examining this thesis, and Mr. Malcolm Hicks for revising the English of the manuscript.

This work was supported financially by the Technology Development Centre of Finland, the Academy of Finland, the Emil Aaltonen Foundation, the Oulu University Research Foundation and the Tauno Tönning Foundation, all of which are gratefully acknowledged.

Oulu, April 1999 Tarmo Ruotsalainen

List of terms, symbols and abbreviations

The following definitions for the various terms describing the performance of measurement equipment are given in the IEEE Standard Dictionary (IEEE 1984).

- Accuracy is the degree of correctness with which a measured value agrees with the true value.
- Drift is the gradual change in the output over a period of time due to change or aging of circuit components, all other variables being held constant.
- Precision is the quality of coherence or repeatability of measurement data, customarily expressed in terms of the standard deviation of an extended set of measurement results.

A/D	=	**a**nalog-to-**d**igital
AMS	=	**A**ustrian **M**ikro **S**ysteme
BiCMOS	=	**bi**polar-**CMOS**, semiconductor process containing both bipolar (usually only high quality npn) and both types of MOS-transistors
BW	=	**b**and**w**idth
CLCC	=	**c**eramic **l**eaded (or **l**eadless) **c**hip **c**arrier
CMOS	=	**c**omplementary **MOS**, semiconductor process containing both types of MOS-transistors
D/A	=	**d**igital-to-**a**nalog
ECL	=	**e**mitter **c**oupled **l**ogic, logic circuit family
Euro1	=	standardized printed circuit board size, 100 mm x 160 mm
FWHM	=	**f**ull **w**idth at **h**alf **m**aximum
GBW	=	**g**ain-**b**and**w**idth product
IEEE	=	**I**nstitute of **E**lectrical and **E**lectronics **E**ngineers, Inc.
I/O	=	**i**nput/**o**utput
MOS	=	**m**etal-**o**xide-**s**emiconductor
MSM	=	**m**etal-**s**emiconductor-**m**etal
NMOS	=	**n**-channel **MOS**
PCB	=	**p**rinted **c**ircuit **b**oard
PMOS	=	**p**-channel **MOS**
PSD	=	**p**osition-**s**ensitive photo**d**etector
PSRR	=	**p**ower **s**upply **r**ejection **r**atio
PTAT	=	**p**roportional **t**o **a**bsolute **t**emperature

RC	=	**r**esistor-**c**apacitor
RF	=	**r**adio **f**requency
SNR	=	**s**ignal to **n**oise **r**atio, here often peak signal voltage to rms noise ratio
TDC	=	**t**ime-to-**d**igital **c**onverter
TOF	=	**t**ime-**o**f-**f**light

A	=	voltage gain
A_0	=	low frequency voltage gain of the core amplifier
A_u	=	voltage gain of the core amplifier
B	=	constant depending on the structure, bandwidth etc. of a comparator
c	=	speed of light, ~ $3x10^8$ m/s
C_{be}	=	base-to-emitter capacitance
C_{bc}	=	base-to-collector capacitance
C_{gs}	=	gate-to-source capacitance
C_{gd}	=	gate-to-drain capacitance
C_d	=	diode capacitance
C_p	=	parasitic capacitance in the input node
C_T	=	total capacitance in the input node
$F(M)$	=	excess noise factor
f	=	frequency
f_{h1},f_{h2}	=	bandwidth of the preamplifier
f_{p1},f_{p2}	=	poles of the core amplifier
g_m	=	transconductance
$h(t)$	=	combined impulse response for the amplifier channel and timing discriminator
$h_1(t)$	=	impulse response of the amplifier channel
$h_2(t)$	=	impulse response of the timing discriminator
$i_{in}(t)$	=	input pulse
i_{ni}	=	input referred noise current
i_{nR}	=	noise current of the feedback resistor
i_{nT}	=	input referred noise current of the core amplifier
i_{signal}	=	input current signal
$i_{signalmin}$	=	minimum input current signal
M	=	avalanche gain
N	=	number of measurements
$P_{rec}(R)$	=	received optical power as a function of the measurement range
P_T	=	output power of the laser diode
q	=	electronic charge, ~ $1.6x10^{-19}$ C
Q	=	quality factor
r	=	radius of the receiver lens
R	=	measurement range
R_0	=	responsivity of the photodetector
R_{fb}	=	feedback resistor
R_l	=	load resistor
t_{dcomp}	=	delay of a comparator
t_{dmin}	=	fixed part of the delay of a comparator

t_f = fall time, from 90 % to 10 %
$t_{doffset}$ = change in the timing point caused by the offset voltage V_{offset}
t_p = timing point
t_r = rise time, from 10 % to 90 %
T_s = shift in time
t_w = pulse width, from 50 % to 50 %
u_{nT} = input-referred noise voltage of the core amplifier
V_{offset} = offset voltage
v_p = peak amplitude of a pulse
V_{th} = threshold voltage (e.g. in a timing discriminator)
Z = transimpedance gain
Z_{cl} = closed loop transimpedance
Z_{ol} = open loop transimpedance

β = feedback factor
ε = reflectivity of the target
θ = angle
λ = mean flow rate of electrons in the input of the receiver channel
σ_t = standard deviation of the timing point
σ_v = noise power
τ_T = transmission of the transmitter optics
τ_R = transmission of the receiver optics

Contents

List of original papers

I Ruotsalainen T & Kostamovaara J (1994) A 50 MHz CMOS Amplifier Channel for a Laser Radar. Journal of Analog Integrated Circuits and Signal Processing, Kluwer Academic Publishers, 5(3): 257-264.

II Ruotsalainen T & Kostamovaara J (1994) A 50 MHz CMOS Differential Amplifier Channel for a Laser Rangefinding Device. Proc. IEEE International Conference on Circuits and Systems, London, United Kingdom, 5: 89-92.

III Ruotsalainen T, Palojärvi P & Kostamovaara J (1997) A BiCMOS Differential Amplifier and Timing Discriminator for the Receiver of a Laser Radar. Journal of Analog Integrated Circuits and Signal Processing, Kluwer Academic Publishers, 13(3): 341-352.

IV Palojärvi P, Ruotsalainen T & Kostamovaara J (1997) A Variable Gain Transimpedance Amplifier Channel with a Timing Discriminator for a Time-of-Flight Laser Radar. Proc. Twenty-Third European Solid-State Circuits Conference, Southampton, United Kingdom, 1: 384-387.

V Ruotsalainen T, Palojärvi P & Kostamovaara J (1999) A Current-Mode Gain Control Scheme with Constant Bandwidth and Propagation Delay for a Transimpedance Preamplifier. Journal of Solid-State Circuits, 34(2): 253-258.

VI Pennala R, Ruotsalainen T, Palojärvi P & Kostamovaara J (1998) A 4 GHz Differential Transimpedance Amplifier Channel for a Pulsed Time-of-Flight Laser Radar. Proc. IEEE International Conference on Circuits and Systems, Monterey, California, USA, 1: 229-232.

VII Ruotsalainen T, Palojärvi P, Kostamovaara J & Peltola T (1996) Laser Pulse Timing Detector. Proc. Twenty-Second European Solid-State Circuits Conference, Neuchatel, Switzerland, 1: 108-111.

VIII Ruotsalainen T, Palojärvi P, Kostamovaara J & Peltola T (1997) A Low-Noise Receiver Channel For a Pulsed Laser Range-Finder. Proc. 40th Midwest Symposium on Circuits and Systems, Sacramento, California, USA, 2: 1395-1398.

The research work described in these papers was carried out at the Electronics Laboratory, Department of Electrical Engineering and Infotech Oulu, University of Oulu, Finland. The work was done mainly in the research projects NOPEL 1991-1992, NOPEL II 1992-1993, RF-ASIC 1993-1994, RF-ASIC II 1994-1995, ERFMI 1995-1996, FAMIC 1996-1997 and NOPSA 1997-1998, which were funded by the University of Oulu, TEKES

and several industrial companies. These project were headed by Prof. Juha Kostamovaara, who also supervised this work.

Papers I and II describe CMOS amplifier channels designed with a centimetre/decimetre distance measurement accuracy in mind. The research described in them was done by the author, who also prepared the manuscripts.

Papers III to V describe BiCMOS receiver channels designed with the aim of achieving millimetre/centimetre distance measurement accuracy in a wide input signal dynamic range. The research described in paper III was done by the author, while P. Palojärvi assisted in the measurements. The research described in Papers IV and V was done jointly by the author and P. Palojärvi.

Paper VI describes a bipolar receiver channel in which the main goal is to further improve accuracy by using very short laser pulses with fast edges. The circuit is implemented in a fast bipolar array to achieve the required wide bandwidth. The research was done jointly by the author, P. Palojärvi and R. Pennala.

Papers VII to VIII describe BiCMOS receiver channels in which main goal is maximization of the measurement range to noncooperative targets. To this end, the noise of the receiver channel is minimized. The research described was done by the author, who also prepared the manuscripts. P. Palojärvi and T. Peltola assisted in the measurements of the circuits.

1. Introduction

1.1. Aim and scope of this work

The aim of this work was to develop integrated electronics for the receiver channel of a portable pulsed time-of-flight (TOF) laser rangefinder for industrial measurement applications where the measurement range is from ~ 1 m to ~ 100 m to noncooperative targets and the required measurement accuracy is from a few millimeters to a few centimeters. The receiver channel converts the current pulse from a photodetector to a voltage pulse, amplifies it, discriminates the timing point and produces an accurately timed logic level pulse for a time-to-digital converter. The structure of the receiver channel, consisting of an amplifier channel, gain control circuitry, amplitude measurement, timing discriminator etc., along with experimental results from several implementations, are presented in this thesis.

New circuit techniques and structures, such as a fully differential transimpedance preamplifier and a current mode gain control scheme, are developed here. The electronic gain control structures enable the elimination of awkward optical ones in some applications, which along with the small size and power consumption achieved by the use of integrated technology, considerably simplifies the rangefinding devices. Furthermore, it will be shown that the achievable performance level using integrated circuit technology is comparable or superior to that of commercially available discrete component implementations described by Määttä (1995).

Laser radars have been a topic of extensive research at the Electronics Laboratory of the University of Oulu for two decades (Ahola 1979). A commercially available distance measurement device based on that work, shown in Fig. 1 a), achieves a centimeter-level measurement accuracy over a wide temperature range (Määttä 1995). The use of standard commercial linear and ECL components results in a large area and a high power consumption, however, the receiver channel and time-to-digital converter (TDC) alone taking up 2 - 3 Euro1-size printed circuit boards (PCB) and consuming in excess of 10 W. Furthermore, the assembly and component costs make these measuring instruments expensive, which restricts their use to demanding industrial applications.

The long-term aim of our work is to implement the whole measurement device with a

minimum number of components, such as two or three CMOS or BiCMOS full-custom integrated circuits, internal or external photodetectors, a laser diode, a few passive components and a microcontroller. The integrated circuits should be implemented using standard processes to keep the development and manufacturing costs down. A prototype receiver PCB based on a receiver circuit designed in this work (Chapter 5.1.4) and an integrated TDC circuit (Räisänen-Ruotsalainen 1998, Räisänen-Ruotsalainen *et al.* 1998b) is shown in Fig. 1 b). The significantly reduced power consumption, size and cost open up new application areas in consumer products, for example. Moreover, the small size permits the integration of an array of photodetectors, receiver channels and TDCs working in parallel on one chip. This may enable construction of new kinds of three-dimensional object recognition and machine vision systems without complicated mechanical scanning structures.

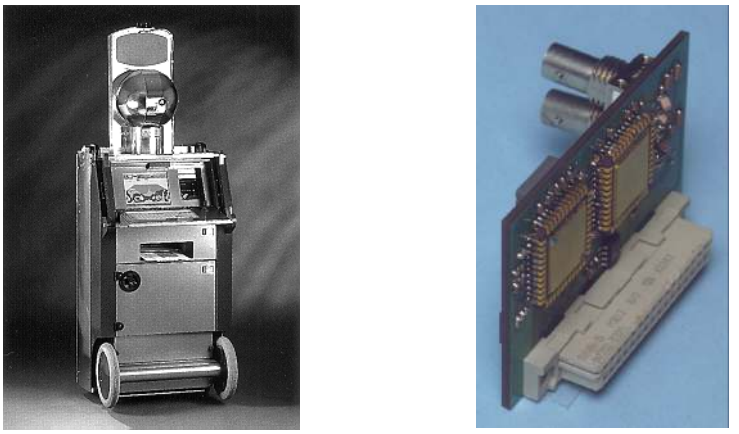

a) b)

Fig. 1. a) A commercially available pulsed time-of-flight laser rangefinder based on the use of discrete components. b) A prototype receiver PCB based on an integrated receiver channel and TDC.

Integration of the receiver electronics gives several advantages in addition to reduced size. As signals are mostly processed and transmitted between subsystems inside an integrated circuit, the power consumption, disturbances and timing errors associated with the input/output (I/O) buffering, circuit packages and wiring on a PCB are reduced. Furthermore, more complicated functions, such as amplitude measurement, noise measurement, automatic adaptation of the detection threshold and temporal masking of signals, can be incorporated in the receiver channel without appreciably increasing the area or complexity of the system. All this helps to improve the performance and versatility of the measurement devices.

The integration of the receiver channel introduces its own special problems, however. As the receiver channel contains several specialized subsystems with demanding specifications, such as low-noise wideband amplifiers, gain control circuitry with stable delay, accurate timing discriminators, amplitude and noise measurement circuits, standard

components from manufacturers' cell libraries can seldom be used. Instead, most of the circuit blocks have to be full-custom designed, which is time consuming. Furthermore, many components used in discrete implementations, such as accurate passive components or delay lines, are not available, so that alternative circuit techniques must be developed and used. Packaging of the receiver channel entails problems as well. The integrated circuit is fabricated on a semiconducting substrate, and the interactions of the various blocks on this common substrate are difficult to model accurately. Furthermore, these interactions depend greatly on the package and PCB parasitics, such as capacitances and wire inductances, which may be difficult to estimate accurately beforehand. Therefore extensive simulation and usually several design iterations are needed when developing specialized high performance analog integrated circuits.

1.2. Principle of a TOF laser rangefinder and its applications

The principle and block diagram of a pulsed time-of-flight laser radar is shown in Fig. 2. A short laser pulse, with a half value width of 5 ns, for example, is generated and transmitted to an optically visible target. A small part of the outgoing light pulse, the reference signal in Fig. 2, is taken directly to a photodetector, where it is converted to an electrical pulse. The electrical pulse is then amplified and an accurately timed logic-level pulse, the start pulse, is generated for a time interval measurement unit. In the same way a logic-level stop pulse is generated from the light pulse which is reflected from the target. The time between the start and stop pulses is measured and converted to a distance result. Due to the extreme speed of light, ~ 300 000 000 m/s, the time intervals to be measured are very short and the required timing accuracy and stability are very high, as ~ 7 ps in time corresponds to 1 mm in distance.

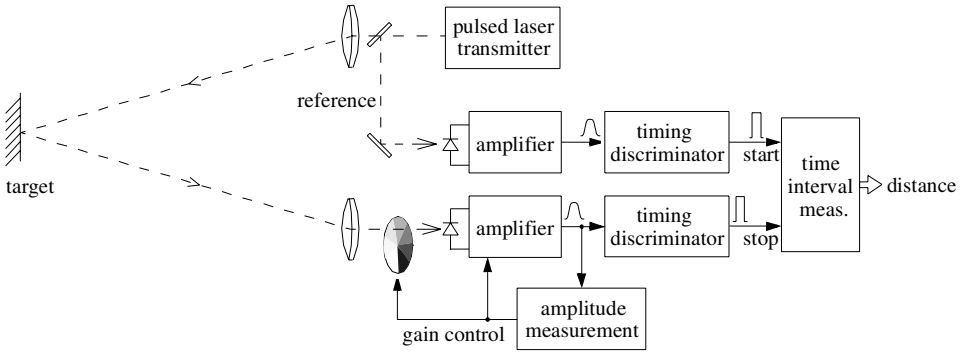

Fig. 2. Principle and block diagram of the pulsed time-of-flight laser rangefinder.

Laser radars can be used in many industrial measurement applications. Due to their non-contact nature, they are particularly suitable for measuring the profiles and dimensions

of large objects e.g. in shipyards (Kaisto *et al.* 1990, Kaisto *et al.* 1993), as shown in Fig. 3 a), or hot objects for example in steelworks (Määttä *et al.* 1993, Araki & Yoshida 1996), as shown in Fig. 3 b). As light pulses can be readily conveyed over long distances in optical fibers, the electronics parts can be located far away from the place where the measurement is made, and thus laser radars can be used to measure the level of flammable fluids in large tanks, e.g. in oil refineries or harbors (Määttä & Kostamovaara 1997). Thanks to the good focusability of the laser beam, the measurement can be made selective, which is useful in lidar systems for automotive speed detection, for example (Samuels *et al.* 1992, Leti product information). Three dimensional machine vision can be implemented using a scanning system or matrix of detectors, the advantage being that there is no unambiguity in the result. Scanning laser radars can also be used in automotive cruise control systems (Automotive Engineering 1997) or automatic warning and protection systems for hazardous areas (SICK product information), e.g. around unattended heavy machinery.

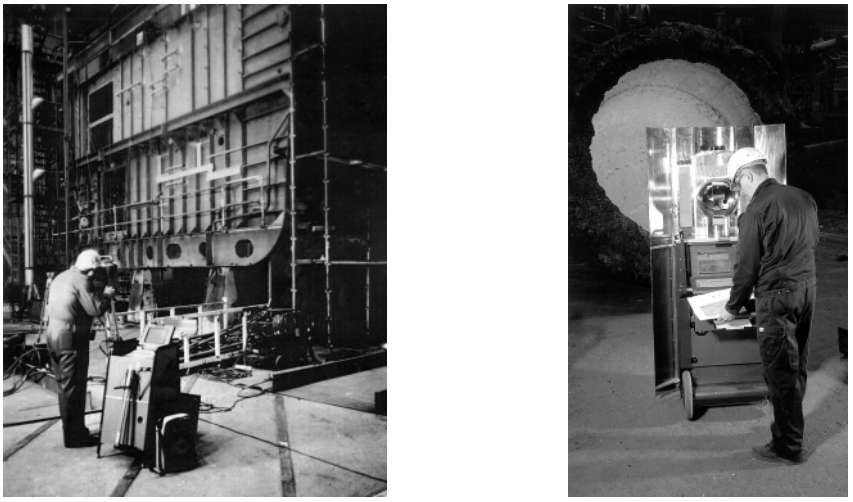

a) b)

Fig. 3. Laser rangefinders used a) in a shipyard to measure the dimensions of a large ship block and b) in a steelworks to measure the profile of a hot object.

1.3. Contents of this work

The organization of this thesis is as follows. Chapter 2 presents the structure, operation and requirements of the receiver channel of the pulsed time-of-flight laser radar in more detail. The main sources of error and ways to reduce them are also discussed. The amplifier channel of the receiver is discussed in Chapter 3, concentrating on the preamplifier and gain control circuitry, which are the key circuit blocks from the performance point of view. Alternative structures and their main features are considered. In addition, measurement of the amplitude of short pulses is discussed briefly. Chapter 4 presents alternative methods

for timing discrimination and discusses the structure of the timing comparator and its delay stability. The Chapter ends with a short treatment of interference issues which may ultimately limit the achievable accuracy. Chapter 5 contains short descriptions of several circuit implementations together with experimental results. More details can be found in the original papers at the end of the thesis. The results of the work are discussed in Chapter 6, and finally a summary of the work is given in Chapter 7.

2. The receiver channel of a pulsed time-of-flight laser radar

2.1. Structure and operation of the receiver channel

The structure of the receiver channel for a pulsed time-of-flight laser rangefinder as used in this work is shown in Fig. 4. It consists of two identical channels, one for the start pulse and the other for the stop pulse, preferably on the same chip so as to minimize errors caused by delay variations due to changes in temperature, supply voltage and process parameters. The incoming light pulse is converted to a current pulse in a photodetector, which is either a PIN or avalanche photodiode (APD). As this current pulse is too weak to be processed directly, it is first converted to a voltage pulse in a low-noise transimpedance preamplifier and then amplified in a voltage-type postamplifier.

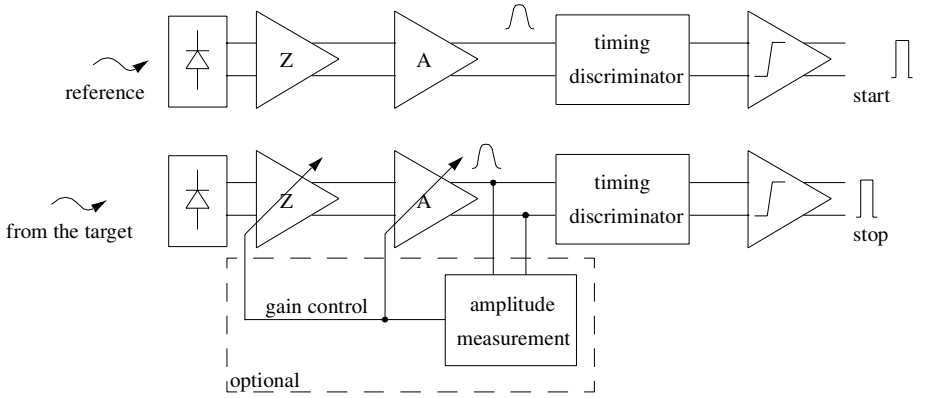

Fig. 4. Block diagram of the receiver channel of a pulsed time-of-flight laser rangefinder.

As the length of the laser pulses which can be readily generated using semiconductor lasers and handled using standard silicon technology is large compared to the intended centimetre/millimetre-level distance measurement accuracy, it is necessary to discriminate

a specific point of each analog timing pulse, such as the peak. Finally, the timing comparator generates a logic-level timing pulse for the TDC.

The level of the reference signal is relatively constant, whereas the level of the signal reflected from the target varies widely as a function of the measurement range, reflectivity and angle of the target etc. This problem can be addressed in several ways. One way is to amplify the signal in an amplifier channel with a fixed gain and discriminate the timing point with a leading edge discriminator having a constant threshold voltage, as shown in Fig. 5 b). Another way is to process it in a strictly linear manner with a variable gain amplifier channel followed by an amplitude-insensitive timing discriminator, as shown in Fig. 5 c).

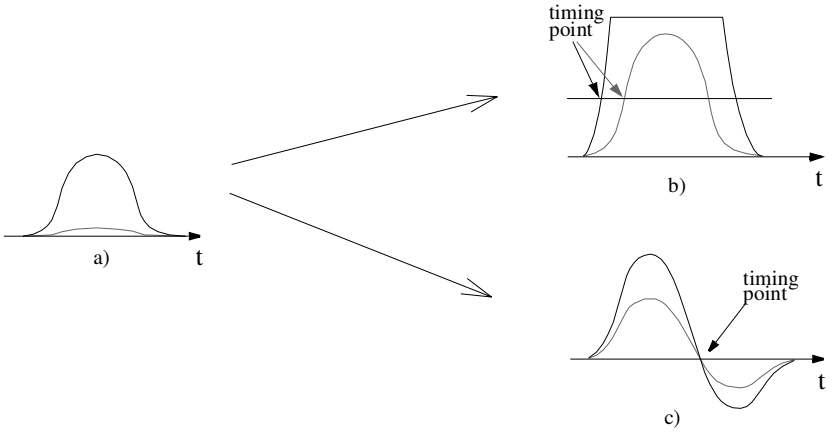

Fig. 5. Pulse shapes in different timing discrimination schemes, a) input signal with amplitude varying in a range from 1 to 10, b) amplifier channel with fixed gain followed by a leading edge discriminator with a constant threshold voltage and c) amplifier channel with variable gain followed by an amplitude insensitive timing discriminator.

In the former scheme only the leading edge of the pulse is used, so that distortion or clipping of large pulses does not affect the timing discrimination. However, any change in the signal amplitude directly affects the timing point, which causes signal-dependent error. In the latter scheme, where the timing point is detected near the top of the pulse or in its trailing edge, or at least some information on the amplitude of the pulse is used, the amplifier channel must always remain in the linear region. This scheme is more difficult to implement and often requires gain control circuitry with stable delay and bandwidth. The gain should be controlled as late in the amplifier channel as possible to minimize degradation of the SNR, but before any distortion occurs, so that several gain control blocks in different places may be needed.

The choice of discrimination scheme depends on the application and the required accuracy. The scheme based on an amplitude-insensitive timing discriminator often provides the best accuracy, but if the dynamic range of the input signal is excessively high, or if there is not enough time to use gain control circuitry to keep the amplifier channel linear, leading edge timing discrimination may be the best solution.

The primary parameters and features of the receiver channel from the performance point of view are the delay stability, noise and input dynamic range of the preamplifier, the bandwidth of the whole amplifier channel and the scheme used in timing discrimination. Other important factors affecting the feasibility and cost of the system are area, power consumption, supply voltage, and the technology and process used in the implementation, such as silicon, silicon-germanium, gallium-arsenide, CMOS, BiCMOS, HEMT, HBT etc. Issues affecting the accuracy are considered in more detail in the following sections. First the main sources of error are identified and then the requirements and specifications for the receiver channel are considered.

2.2. Main sources of error

The main factors limiting the accuracy of the receiver channel of a pulsed TOF laser radar are amplitude variation in the input signal, which causes systematic error, and noise, which causes random errors. Temperature and supply voltage variation will also cause systematic errors, and electrical disturbances may cause both random and systematic errors. The systematic errors can be minimized by continuously calibrating the measurement equipment, and the remaining random errors can be reduced by averaging.

2.2.1. Amplitude variation

Amplitude variation in the input signal causes systematic error in the measurement result, known as walk error or time slewing. The timing point usually moves earlier with increasing pulse amplitude. This error originates from distortion in the amplifiers, nonideal gain control, crosstalk, an amplitude-sensitive timing discrimination scheme and delay variation in the timing comparator with the rate of change and overdrive of the input signal. The dominant sources of error are usually the amplitude sensitivity of the discrimination scheme and timing comparator.

An example of walk error caused by the discrimination scheme is shown in Fig. 5 b), where the timing points of two pulses with different amplitudes are marked. This walk error can be partly compensated for by means of correction tables, provided the shape of the pulses does not vary too much and provided the amplitude of the signal can be measured accurately. Walk error caused by fast pulse-to-pulse amplitude variation may appear as jitter if the amplitude of each pulse cannot be measured accurately enough. Several timing discrimination schemes have been developed to avoid time slewing, and these are discussed in more detail in Chapter 4.1. These are referred to here in short as linear timing discrimination schemes, because they are often based on linear operations.

Even if the timing discrimination scheme itself is not sensitive to amplitude variation, the delay of the timing comparator will vary with the amplitude of the input signal, as shown in Fig. 6, increasing with decreasing input signal rate of change and overdrive, so that it is longest when the amplitude is low. This error can be minimized by maximizing the

speed of the timing comparator.

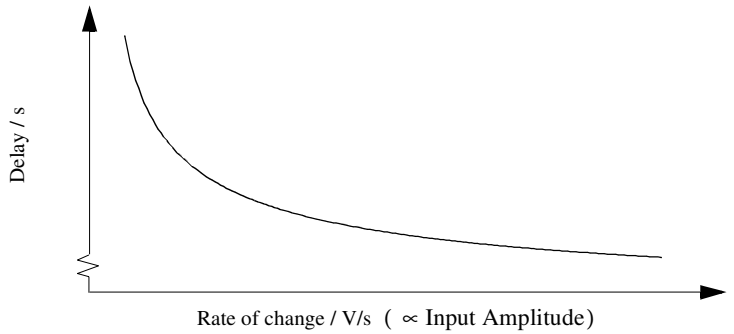

Fig. 6. Delay variation in a practical comparator as function of the rate of change in the input signal, which is directly proportional to the amplitude.

2.2.2. Noise

The pulses in a laser radar are corrupted by noise in the transmitter, in the flight path through the air (turbulence, dust particles etc.), in the target (an inhomogeneous and irregularly reflecting surface), in the receiver (noise from the detector and electronics) and in the time interval measurement unit, the dominant noise source often being the electronic noise of the receiver channel. Noise superimposed on the signal causes random variation, jitter, in the timing result, and therefore limits the precision of the measurement, as illustrated in Fig. 7.

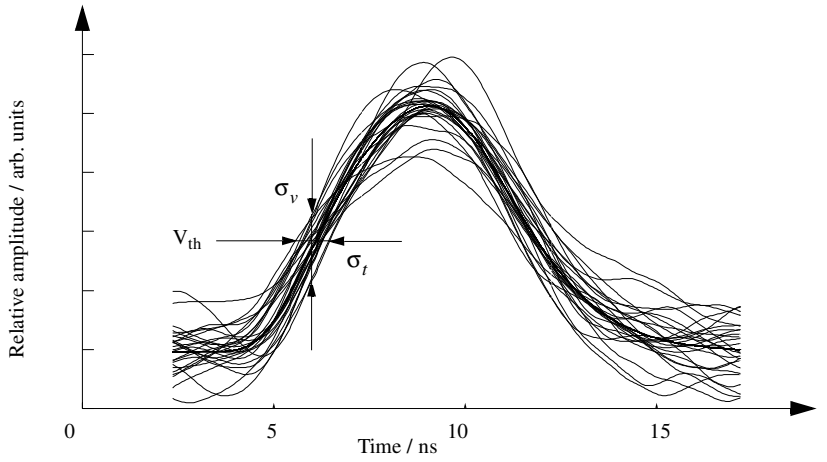

Fig. 7. Analog timing pulses at the output of the amplifier channel, SNR ~ 10 (25 simulated pulses superimposed).

The timing jitter can be approximated with the 'triangular rule' (Bertolini 1968)

$$\sigma_t = \frac{\sigma_v(t)\Big|_{t=t_p}}{\frac{d}{dt}v(t)\Big|_{t=t_p}} , \qquad (1)$$

where σ_t is the standard deviation of the timing point, $\sigma_v(t)$ is the instantaneous noise power at the timing point and $v(t)$ is the input signal at the input to the timing comparator. The noise power is composed of the noise of the electronics and the noise of the signal itself. The former can be calculated by standard circuit analysis techniques and the latter using Campbell's theorem with (Rehak 1983, Athanasios & Papoulis 1984)

$$\sigma_v^2(t) \approx \int_{-\infty}^{\infty} q\lambda(\alpha)h^2(t-\alpha)d\alpha , \qquad (2)$$

where $\lambda(t)$ is the mean flow rate of electrons in the input to the receiver channel, $h(t)$ is the combined impulse response for the amplifier channel and timing discriminator and q is the electronic charge.

If the variation is truly random, precision can be improved by averaging over several measurements, the precision in asynchronous measurement being inversely proportional to the square root of the number of samples (Hewlett-Packard AN. 162-1)

$$\sigma_{tN} = \frac{\sigma_t}{\sqrt{N}} , \qquad (3)$$

where σ_{tN} is the standard deviation in the timing point when averaging over N measurements.

The noise and its effect can be reduced by careful design of the preamplifier, which is often the dominant noise source when the signal is weak (see Fig. 12), optimization of the transfer function of the amplifier channel and the proper choice of timing discrimination scheme.

Noise can also cause a systematic change in the timing point as a function of signal amplitude, i.e. walk error. As the amplitude of the signal changes, so does its rate of change at the timing point. When the rate of change of the signal in the input to the timing comparator is high, the mean value of the timing points is not greatly affected by noise and the distribution of the timing points follows that of the noise (the two main noise sources at higher frequencies are thermal and shot noises, which have a Gaussian distribution). However, as the amplitude, and therefore also the rate of change of the signal is reduced, the timing discriminator tends to fire slightly earlier, i.e. the mean value moves earlier, which appears as walk error. Moreover, the distribution becomes distorted, i.e. it is narrower and skewed (Fleischer 1994).

The effect of walk error and jitter on the timing point is illustrated in Fig. 8. The timing point lies within the area bounded by the dashed lines. The variation in the mean value with signal amplitude is caused by walk error, whereas the funnel-shaped area around it is

caused by jitter.

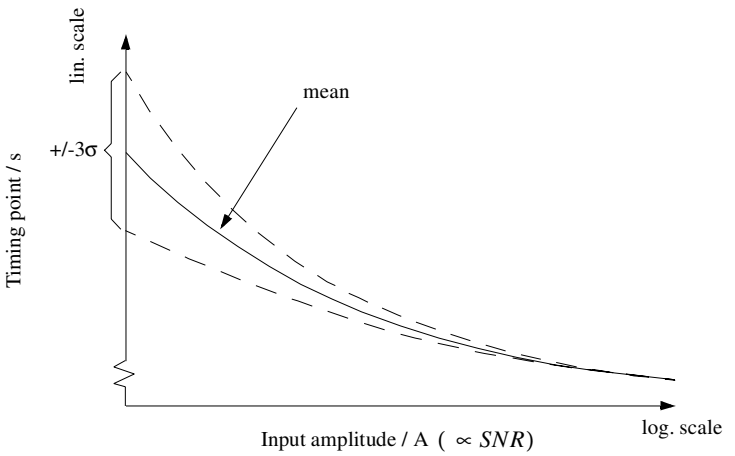

Fig. 8. Effect of jitter and walk error on the timing point.

2.2.3. Drift and disturbances

Temperature and supply voltage variations affect the bandwidth and delay of the amplifiers and comparators, which results in systematic errors, drift. Temperature drift is mainly caused by the temperature dependence of the transconductance of the transistors and the resistivity of the resistor materials. The drift with supply voltage is caused by the nonlinear junction capacitances of transistors and resistors. Changes in the supply voltage affect the operating point voltages, so that the capacitances in the circuit nodes limiting the bandwidth also change. These errors can be minimized by making the start and stop channels identical and integrating them on the same chip. This way only the mismatch of the drifts of the channels causes errors. The residual errors can partly be compensated for by measuring the ambient temperature and supply voltage and using correction tables.

Disturbances and cross-talk, and hence time jitter, can be reduced by using fully differential structures (Rein 1990). Differential circuits, both logic and analog blocks, are often based on differential pairs in which a constant current is steered from one branch to another. This produces less disturbances in the power supplies, substrate etc. than single-ended structures such as common source/emitter stages. Furthermore, the operation of differential structures is less affected by these disturbances, as they are picked off as a common mode signal. An added advantage of differentiality is that it improves linearity (even order harmonics are reduced), which in turn reduces the variation in the timing point of the pulses as a function of amplitude.

2.3. Requirements and specifications

The goal of this work is to develop circuit techniques for portable measurement devices with a centimetre/millimetre-level accuracy and a measurement range from ~ 1 m to ~ 100 m to noncooperative targets. The portability requirement places restrictions on the size and weight of the optics and battery, which in turn affects the design of the electronics.

2.3.1. Bandwidth

If the rate of change of the pulses at the input to the timing comparator is limited by the bandwidth of the amplifier channel and timing discriminator, the single shot precision given by (1) can be approximated in edge detection by (Kostamovaara *et al.* 1992)

$$\sigma_R \approx \frac{0{,}35 \cdot c}{2 \cdot BW \cdot SNR} \ , \qquad (4)$$

where c is the speed of light, BW is the bandwidth and SNR is the peak signal voltage to rms noise ratio. In practise, a minimum SNR of about 10 is required to keep the number of false detections caused by noise acceptable (Määttä *et al.* 1993).

According to (4), a single shot precision of 1 mm requires a bandwidth of ~5 GHz, which corresponds to a rise time of ~70 ps. The generation of laser pulses with sufficiently fast edges and the implementation of an integrated receiver channel with such a high bandwidth requires special techniques and processes, as documented in Vainstein & Kostamovaara (1998), Vainstein *et al.* (1998) and in Paper VI, respectively.

An example of a laser pulse which can be generated using a semiconductor laser diode (EG&G PGAS3S06) with a high enough power using more conventional techniques is shown in Fig. 9. The rise time t_r is seen to be ~3 ns and the half-value width t_w ~6 ns. With pulses of this kind the required precision can be achieved by performing several measurements and calculating the average, whereupon the precision improves as given in (3). The bandwidth of the receiver channel needed to preserve the edges can be approximated by (Ziemer & Tranter 1985)

$$BW \approx \frac{0{,}35}{t_r} \ \ldots \ \frac{0{,}44}{t_r} \ . \qquad (5)$$

In equation (5) the value 0.35 applies for a first order system and 0.44 for an ideal lowpass filter, so that a value somewhere between them is appropriate in a practical system. With the pulse shown in Fig. 9, equation (5) gives a bandwidth of ~115 - 145 MHz. The bandwidth should not be designed to be any larger than needed to prevent the noise from deteriorating the precision. If the bandwidth is increased above the optimum, noise increases faster than the rate of change of the signal. The optimal bandwidth, taking into account the characteristics of the noise spectrum, can be obtained with simulations. If, for example, the bandwidth was 100 MHz, which is much easier to achieve than 5 GHz, a precision of 1 mm would require ~2750 measurements. This would take about a quarter of

a second with a typical pulsing frequency of 10 kHz.

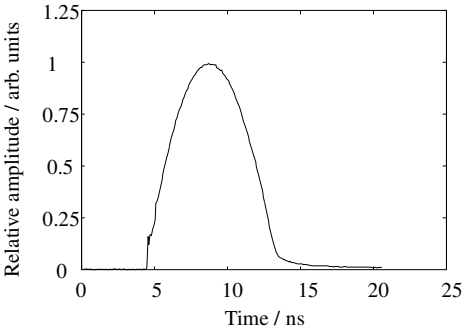

Fig. 9. A laser pulse used in rangefinding applications (laser diode EG&G PGAS3S06 pulsed with a ZTX 415 avalanche transistor).

2.3.2. Noise

The maximum measurement range is limited by noise. The received optical power $P_{rec}(R)$ as a function of the measurement range R can be estimated with the radar equation (the target area is assumed to be larger than the beam)

$$P_{rec}(R) = \frac{P_T \tau_T \varepsilon}{\pi} \cdot \frac{\pi r^2}{R^2} \cdot \tau_R \ , \qquad (6)$$

where P_T is the output power of the laser diode, τ_T and τ_R are the transmissions of the transmitter and receiver optics, ε is the reflectivity of the target and r is the radius of the receiver lens. This optical power gives rise to a signal current $i_{signal}(R)$

$$i_{signal}(R) = P_{rec}(R) \cdot R_0 \ , \qquad (7)$$

where R_0 is the responsivity of the photodetector.

Using values appropriate for our application, $P_T = 30$ W (laser diode with 3 stripes), $\tau_T = 0.85$, $\tau_R = 0.6$ (filter included), $\varepsilon = 0.1$ - 1, $r = 1$ cm (reasonable in a portable device), $R_0 = 50$ A/W (avalanche photodiode), and $R = 100$ m, the radar equation gives a minimum input current signal $i_{signalmin}$ of ~ 0.8 μA. Since in practise a minimum SNR of about 10 is required for reliable detection, the input-referred noise of the receiver channel should be less than 80 nA. If the bandwidth of the receiver channel is 100 MHz, for example, this corresponds to an input referred noise current density of 8 pA/$\sqrt{Hz}$.

2.3.3. Transimpedance gain and gain control

The weak input current pulse from the photodetector has to be amplified to a level which is suitable for timing discrimination and amplitude measurement. In practise, the timing

comparator and peak detector require an input signal of the order of 100 mV or more. With smaller pulses the delay of the comparator increases rapidly and the accuracy of the peak detector starts to deteriorate. If the minimum input signal is ~ 0.8 μA, the total transimpedance gain of the amplifier channel should be at least 100 kΩ. The gain should be kept to the minimum required, however, because crosstalk between stages may cause stability problems.

According to (6), the received optical power, and therefore also the amplitude of the current pulse from the photodetector, varies so as to be inversely proportional to the square of the distance. Thus if the measurement range varies from 1 m to 100 m, the amplitude of the signal current varies in a range from 1 to 10000. Furthermore, the reflectivity of natural targets can vary in a range from 0.1 to 1, or even more. All in all, the amplitude of the signal may vary in a range from 1 to 100000 or more. With suitably designed optics the variation can be reduced significantly, so that, depending on the application, the signal may vary in a range from 1 to 100 ... 10000.

This variation is a problem if a linear timing discrimination scheme is used. In practise these can handle an input signal variation from 1 to 10 ... 100, so that the transimpedance gain of the amplifier channel control needs to be controlled by at least 40 dB. The gain control circuitry should have a stable delay and the shape of the analog pulses should not be affected. Electronic gain control integrated within the receiver channel is preferable over optical gain control from the point of view of space and power consumption.

2.3.4. Power consumption

The power consumption of a portable device has to be minimized in order to achieve a long enough operating time and to keep the size and weight of the battery reasonable. The capacity of a battery of a portable phone or video camera, for example, is of the order of 1000 mAh (3 - 6 V), so that the average current consumption should not exceed a few tens of milliamperes.

However, low noise and high speed operation in analog signal processing often require high bias currents. In pulsed time-of-flight laser rangefinding the most effective way to save power without compromising accuracy is to power down the electronics between measurements. With a pulsing frequency of 10 kHz and a measurement range of 100 m, for example, the duty cycle is less than 1 %.

2.4. Other methods used in electronic distance measurement

Electronic distance measurement equipment can use either ultrasound or electromagnetic waves, usually microwaves or light, as the probe. Due to the moderate speed of sound, ~ 331 m/s under normal conditions (CRC 1993), the electronics used in ultrasound techniques are less demanding, but the accuracy is limited by the significant dependence of the speed of sound on temperature, relative humidity and atmospheric pressure. In contrast, the speed of electromagnetic waves is almost constant in air, so that much better accuracy

can be achieved. Furthermore, the better focusability of electromagnetic waves, especially light waves, enables more selective measurement, and the lower attenuation in air permits longer measurement ranges. Due to the extreme speed of light, however, rather involved circuit techniques are often required.

Modulated or unmodulated, continuous or pulsed light sources can be used in laser rangefinding techniques, and the measurement is based on detecting frequency, phase, time interval, or position and angle. A few alternative methods will be reviewed briefly below.

In the 'chirp-technique' the target is illuminated with continuous amplitude-modulated light, the modulation frequency of which is swept linearly with time. The light reflected from the target is converted to an electrical signal and mixed with the transmitted one, resulting in a frequency proportional to the distance. In another technique, the modulation frequency is constant and the phase difference between the transmitted and received waves is measured (Scott 1990). At least two modulation frequencies must be used to obtain an unambiguous result. In interferometric measurements, coherent unmodulated light is used. The distance traveled by the target or the measuring equipment can be calculated very accurately by measuring the numbers of interference minima and maxima (Rüeger 1990). The self-mixing effect inside a laser diode can also be exploited in rangefinding by using the same laser diode as the transmitter and the receiver at the same time. The laser is modulated with a slow triangular wave, which modulates the optical frequency of the transmitted light. The received light from the target causes marked variations in the optical output power, the beat frequency being proportional to the distance from the target (Bosch *et al.* 1996).

Position sensing techniques combined with triangulation can also be used. The light reflected from the target can be detected with a matrix of photodetectors (Gruss *et al.* 1991) or an analog PSD (Lindholm & Edwards 1991), and the distance can be calculated from the direction of the transmitted beam of light and the position of the received spot on the detector. Video systems using several stationary cameras or one moving one can be used to obtain multiple views of the object, from which the distance can be calculated (Heikkilä 1997). In these video systems the target can be illuminated with normal white light.

Several techniques involving pulsed light are also used. In the 'sing-around' technique (Acuity Research 1995) a single pulse is sent to the target and the reflected pulse is received and used to trigger the transmitter, which immediately sends a new pulse. Thus the distance can be calculated from the pulsing frequency. In the time-of-flight technique, as used in this work, the flight time of a single short laser pulse travelling to the target and back is measured.

The spread spectrum techniques used in modern telecommunications systems can be applied to range measurement as well. A specially designed pulse train having good autocorrelation properties, producing a single peak and low sidelobes, is sent to the target and the received signal is analyzed in a matched filter or correlator, which extracts the sequence and its timing from the noisy signal. The longer the sequence is, the lower the required SNR. In practise the SNR can be much less than 0 dB. (Dixon 1994)

Each technique has its pros and cons. A distinct advantage of the pulsed time-of-flight technique is that a single measurement can be made in a very short time, which is important in scanning safeguard systems or proximity detectors, for example (Automotive Engineering 1997). Also, the peak power of the pulses can be made much higher than the average power of a continuous wave without exceeding the limitations dictated by eye

safety, which is advantageous in noisy environments (Araki & Yoshida 1996). These powerful laser pulses can be generated with pulsed semiconductor laser diodes, which have a maximum obtainable output power two to three orders of magnitude higher than the power obtainable from continuous wave laser diodes. The advantage of high peak power is partly negated by the requirement of good SNR, in practice better than ~ 10, which is needed for reliable measurement. The time intervals to be measured in the time-of-flight technique are very short and the required accuracy is of the order of picoseconds, so that very fast and stable electronic and optoelectronic structures are needed.

3. The amplifier channel

The amplifier channel is used to match the current mode signal source with a capacitive output impedance to the voltage mode timing discriminator and to amplify the weak input signal to a level which is adequate for the timing comparator.

3.1. Transfer function

From the precision point of view it is important to minimize the timing jitter by optimizing the ratio of the rate of change in the pulse to the noise in the input to the timing comparator at the detection threshold, as given in (1). The optimum transfer function for the amplifier channel and timing discriminator depends on the shape and width of the input pulse, the properties of the dominant noise source, the feature of the rangefinder which needs to be optimized etc. Two cases can be recognized, according to whether or not the noise level depends on the signal level (this dependence is discussed in more detail in Section 3.2).

3.1.1. With signal independent dominant noise

If the dominant noise does not depend on the signal level, as is often the case when using PIN photodiodes (see Fig. 12), the optimum impulse response for the amplifier channel and timing discriminator from the precision point of view is a derivative of the impulse response of a matched filter, i.e. (Rehak 1983, Loinaz & Wooley 1995)

$$h(t) = \frac{d}{dt} i_{in}(T_s - t) \ , \qquad (8)$$

where $i_{in}(t)$ is the input pulse and T_s is a shift in time. If the noise spectrum in the input is not white, as is often the case, a noise whitening filter should be used (Rehak 1983) and $i_{in}(t)$ should be convolved with the impulse response of this filter before using (8).

The maximum measurement range is limited partly by the deterioration in precision and partly by the increase in the number of false detections caused by noise. The latter can be reduced by using an arming/noise comparator to enable the timing comparator when the amplitude and width, i.e. energy, of the pulse is higher than a preset threshold, as shown in Fig. 10. The probability of false detections can be further reduced by maximizing the signal-to-noise ratio in the input of the arming comparator. This can be achieved by matching the impulse response of the amplifier channel to the pulse, i.e. the impulse response of the amplifier channel $h_1(t)$ should be that of a matched filter as given by (Haykin 1983, Rehak 1983, Arbel 1990)

$$h_1(t) = i_{in}(T_s - t) \ . \qquad (9)$$

A noise whitening filter is again needed if the noise is not white (Arbel 1990). To optimize the timing precision at the same time, the impulse function of the timing discriminator $h_2(t)$ should be designed so that the convolution of $h_1(t)$ and $h_2(t)$ equals $h(t)$ as given by (8).

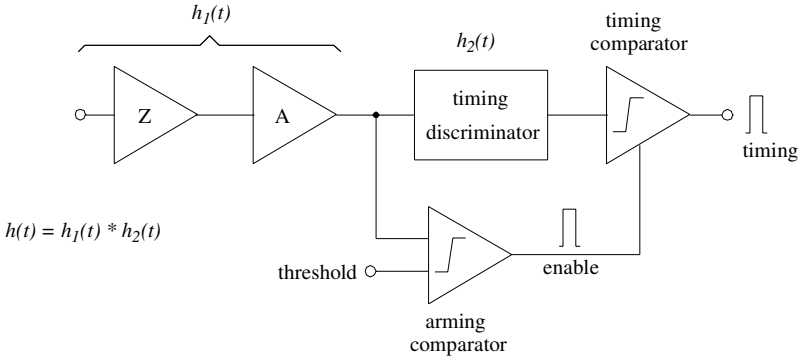

Fig. 10. Block diagram of the receiver channel showing the structure of the timing discriminator.

In practise it may be difficult, or even impossible, to achieve the transfer functions (8) or (9) accurately. For instance, for a typical laser pulse used in rangefinding applications, as shown in Fig. 9, the frequency response of the receiver channel given by (8) is as in Fig. 11. The rising and falling edges of the amplitude response can be approximated with simple passive RC sections, but the notches at high frequencies are too difficult to produce accurately. Furthermore, the shape and width of the input pulses and the frequency response of the receiver channel may change with the properties of the target, time, temperature, supply voltage, process parameters etc., so that complicated real-time tuning may be needed. Fortunately, a simple lowpass filter in pulsed applications may yield a SNR quite close to the optimum achieved by the more complicated matched filter given by (9)

(Arbel 1980).

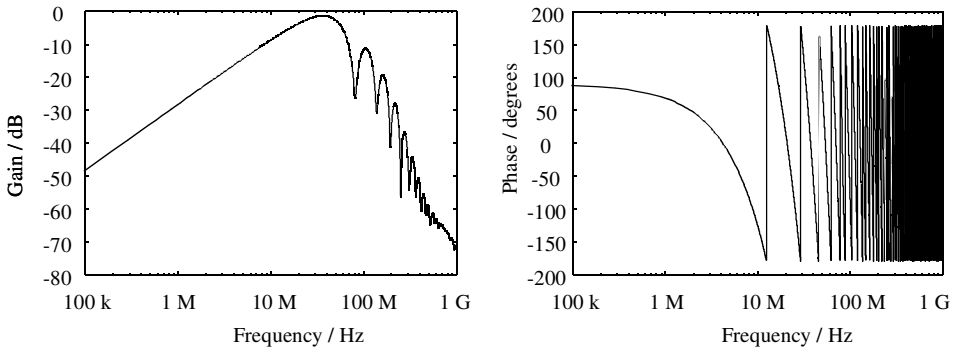

Fig. 11. Amplitude and phase response of the receiver channel given by (8), when the input pulse is as shown Fig. 9.

3.1.2. With signal dependent dominant noise

If the dominant noise level depends on the signal level, as is often the case when an APD is used and the signal is large (see Fig. 12), optimization of the transfer function of the amplifier channel and the choice of discrimination scheme is not so straightforward. The optimum depends on the characteristics and magnitude of the pulse and the noise sources.

If the input signal has a fast leading edge, for example, a leading edge discriminator with a proper threshold may be optimal (Gatti & Svelto 1966). In this case it is important for the fast edges of the input pulse to be preserved in the amplifier channel and for the output noise to be minimized at the same time. Thus the bandwidth of the amplifier channel should be limited to the minimum value which is needed to pass the input pulse unimpaired. The required bandwidth can be approximated using (5). The frequency response can be optimized with Monte Carlo simulations, taking into account the shape of the noise spectrum and the dependence of the noise level on the signal amplitude. In practice, interferences and disturbances may affect the optimal bandwidth (Simpson & Paulus 1998).

3.2. The photodetector

The optical input signal is converted to an electrical one by a photodetector, which in fast applications is usually a reverse-biased APD or PIN photodiode. Owing to the avalanche multiplication of the current carriers, the responsivity of an APD may be two orders of magnitude or so higher than that of a PIN photodiode (~ 50 A/W versus ~ 0.5 A/W @ λ ~ 850 nm), which is beneficial with noncooperative targets. The advantage is partly offset by the higher noise of the APD, however, as shown in Fig. 12, which compares the

sensitivities of receiver channels using PIN and avalanche photodiodes.

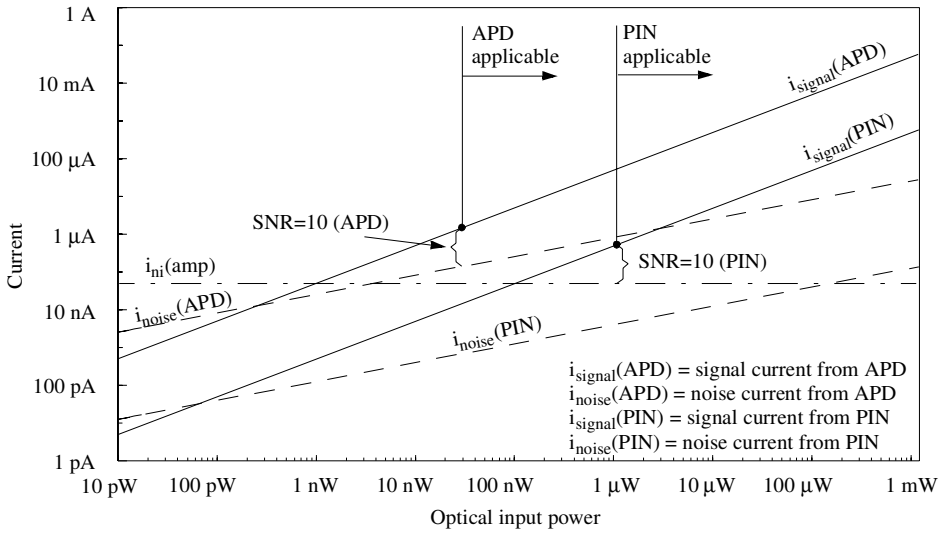

Fig. 12. Comparison of the sensitivity of the amplifier channel with PIN and avalanche photodiodes (*BW* = 100 MHz, responsivity = 0.5 A/W, avalanche gain *M* = 100, excess noise factor *F(M)* = 4, input referred noise current of the electronics i_{ni} = 5 pA/$\sqrt{Hz}$).

It is seen that the sensitivity of a receiver using a PIN photodiode is dictated by the electronic noise of the amplifier channel, whereas that of a receiver channel using an APD may be limited by the noise in the output current of the photodetector, which is caused by the randomness of the photon current and avalanche gain. Optimum sensitivity with an APD is achieved when the noise contributions of the amplifier channel and the APD are equal (Muoi 1984, Senior 1992). This can be achieved by first minimizing the noise of the amplifier channel and then selecting the proper bias voltage for the APD (the excess noise factor depends on the avalanche gain, which in turn depends on the bias voltage). In practise the sensitivity of a receiver channel using an APD is about 10 to 20 times better than that of one using a PIN photodiode (Muoi 1984).

The major disadvantage of an APD is that it requires a very high, temperature-dependent bias voltage, often in excess of ~ 150 V, the generation of which is cumbersome and may cause disturbances, and also necessitates the use of high voltage capacitors and resistors. In addition, APDs are more expensive than PIN photodiodes.

One special feature of laser rangefinders in typical industrial measurement applications is that they need photodiodes with a large active area (∅ ~ 500 µm), and consequently a high capacitance (C_d ~ 2 pF). In fiberoptic communications, for example, the diodes are often much smaller. The high capacitance has a significant effect on the performance and design of the preamplifier.

3.3. The transimpedance preamplifier

The current mode signal from the photodetector is converted to a voltage mode signal in the preamplifier. Optimization of this preamplifier is important, as it often limits the performance of the whole receiver channel. At the same time the preamplifier is often the most difficult circuit block to design, due to the partly conflicting requirements, such as low noise and wide dynamic range, wide bandwidth and good stability, etc. Furthermore, operation of the preamplifier is affected by various external parasitics, the exact values of which are not always known beforehand.

3.3.1. Preamplifier types

Several types of preamplifier can be used, as shown in Fig. 13, the main ones being transimpedance and high impedance preamplifiers. A transimpedance preamplifier is composed of a core amplifier of either the voltage or transimpedance kind and a feedback resistor in which the input current is converted to a voltage. The transimpedance preamplifier employs shunt-shunt feedback to reduce the input impedance so as to achieve a wide bandwidth, and it is often preferred in wideband receivers (Senior 1992), as it offers a relatively wide dynamic range and high-speed operation without equalization (Unwin 1982). The transimpedance preamplifier must be designed carefully to avoid the stability problems associated with feedback systems.

A high impedance preamplifier is composed of a high-valued load resistor, in which the input current is converted to a voltage, and a voltage amplifier (Personick 1973, Yano *et al.* 1990). As its bandwidth is limited because of the pole in the input node, equalization is needed to restore the bandwidth. High impedance preamplifiers are used in applications where maximum sensitivity is required (Smith & Personick 1980). One of the main problems is that it is difficult to design and maintain accurate equalization with changing process parameters, temperature, supply voltage etc. (Smith & Personick 1980). Furthermore, the pole frequency in the input node depends on the capacitance of the photodetector and the various parasitic capacitances, the values of which are difficult to estimate accurately.

In principle both transimpedance and high impedance preamplifiers offer the same sensitivity (Kasper 1988). The main noise sources are the same, and if the signal transfer functions are made identical, so are the noise transfer functions. In practise, however, the load resistor of a high impedance preamplifier can be made larger than the feedback resistor of a transimpedance preamplifier, which results in better sensitivity (the limited gain-bandwidth product (GBW) of the core amplifier of a transimpedance preamplifier limits the value of the feedback resistor). This increased sensitivity is achieved at the expense of a reduced dynamic range (Smith & Personick 1980), as the latter is inversely proportional to the value of the load or feedback resistors.

The low impedance and current preamplifiers shown in Fig. 13 are less popular topologies. The structure of a low impedance preamplifier is similar to that of a high impedance one, except that a load resistor with a much lower value is used, often 50 Ω. As the low load resistance results in a wide bandwidth, no equalization is needed. Another

advantage of this structure is that the photodetector may be connected to the preamplifier with a transmission line, e.g. a 50 Ω cable. Due to the high noise of the low valued load resistor, however, the sensitivity of a low impedance preamplifier is inferior to that of a transimpedance one (Vella-Coleiro 1988, Senior 1992), so that this type of preamplifier is impractical for low-noise wideband systems (Senior 1992). Current amplifiers are often too noisy to be used in preamplifiers (Chang & Sansen 1991). Rogers reported in (1984) on a transimpedance preamplifier in which the output is taken as a current instead of a voltage. The structure combines the good noise performance of a transimpedance preamplifier with a current-mode output, which may be useful for gain control purposes, for instance.

Only transimpedance preamplifiers are used here, because they provide low-noise wideband operation without equalization. In addition, the width of the dynamic range is often as important a parameter as the sensitivity, so that a medium-valued load/feedback resistor is used anyway. The sensitivity degradation compared with a high impedance preamplifier can be rendered insignificant with proper design, and the difference is negligible at high frequencies, above 1 GHz (Muoi 1984).

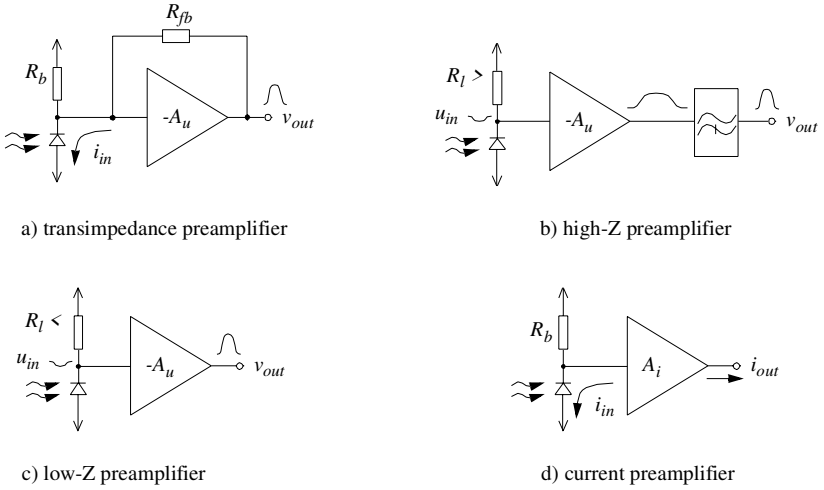

Fig. 13. Various types of preamplifier.

3.3.2. Transimpedance preamplifier structures with bipolar inputs

The core amplifier of a transimpedance preamplifier is either a voltage or transimpedance amplifier, usually the former. In high frequency applications the core amplifier should have a wide bandwidth to ensure the stability of the feedback loop, which means that relatively simple circuit structures must be used. In bipolar technology the amplifier is often composed of one amplifying input stage and a buffer stage. Various types of input stage are shown in Fig. 14, the most popular one being the common emitter input stage as shown in Fig. 14 a) (Meyer & Blauschild 1986). A cascode transistor may be added to the basic structure to reduce the input capacitance by reducing the Miller effect (El-Diwany *et al.*

1981), or a Darlington pair may be used in place of the input transistor to reduce the shot noise of the base current as a result of the reduced bias current (Aiki 1985). The Darlington input may also yield a larger GBW, so that a larger feedback resistor may be used, resulting in reduced thermal noise.

Another widely used input structure is the common collector input stage as shown in Fig. 14 b) (Sibley *et al.* 1984), where the input capacitance is reduced because the Miller effect is eliminated and the base-emitter capacitance is bootstrapped. Furthermore, the emitter follower may be biased with a lower current than the common emitter stage, which reduces the shot noise of the base current. On the other hand, as the input stage has no voltage gain, the input-referred voltage noise caused by the input transistor of the following stage increases. The emitter follower can be used to bootstrap the capacitance of the photodetector, too, as shown in Fig. 14 c) (Abraham 1982).

A common base stage may be used either as an input stage of the core amplifier, as shown in Fig. 14 d) (Wilson & Darwazeh 1987), or as a current buffer in front of a transimpedance preamplifier, as shown in Fig. 14 e) (Vanisri & Toumazou 1995). As the input resistance of the common base stage is inherently low, the preamplifier is affected less by the capacitance in the input node, allowing the use of a larger feedback resistance. A distinct drawback of the common base input is that it is very difficult to construct a low noise bias current source within a single 5 V power supply, and in practice an extra negative supply is needed. The common base amplifier can also be used in an open loop, as shown in Fig. 14 f), resulting in a very wide bandwidth (Hamano *et al.* 1991).

It is difficult to achieve a meaningful comparison of the reported performances of the various input stages, because the specifications, such as diode capacitance, parasitic capacitances, bandwidth, transimpedance, phase margin etc. are different. Furthermore, the selected components or technology may favor one of the structures. For example, the base resistance of the input transistor may be the dominant noise source due to nonoptimal base doping and structure, which may favor the use of a common emitter input over a common collector one. The achievable noise performance (Vanisri & Toumazou 1992), which is of great importance in many applications, nevertheless appears to be fairly similar.

Differential implementations of the common emitter input, i.e. a differential pair, both with and without cascode transistors, are used in the present work, together with a differential structure containing current mode gain control circuitry as shown in Fig. 21 b)

and documented in Paper V.

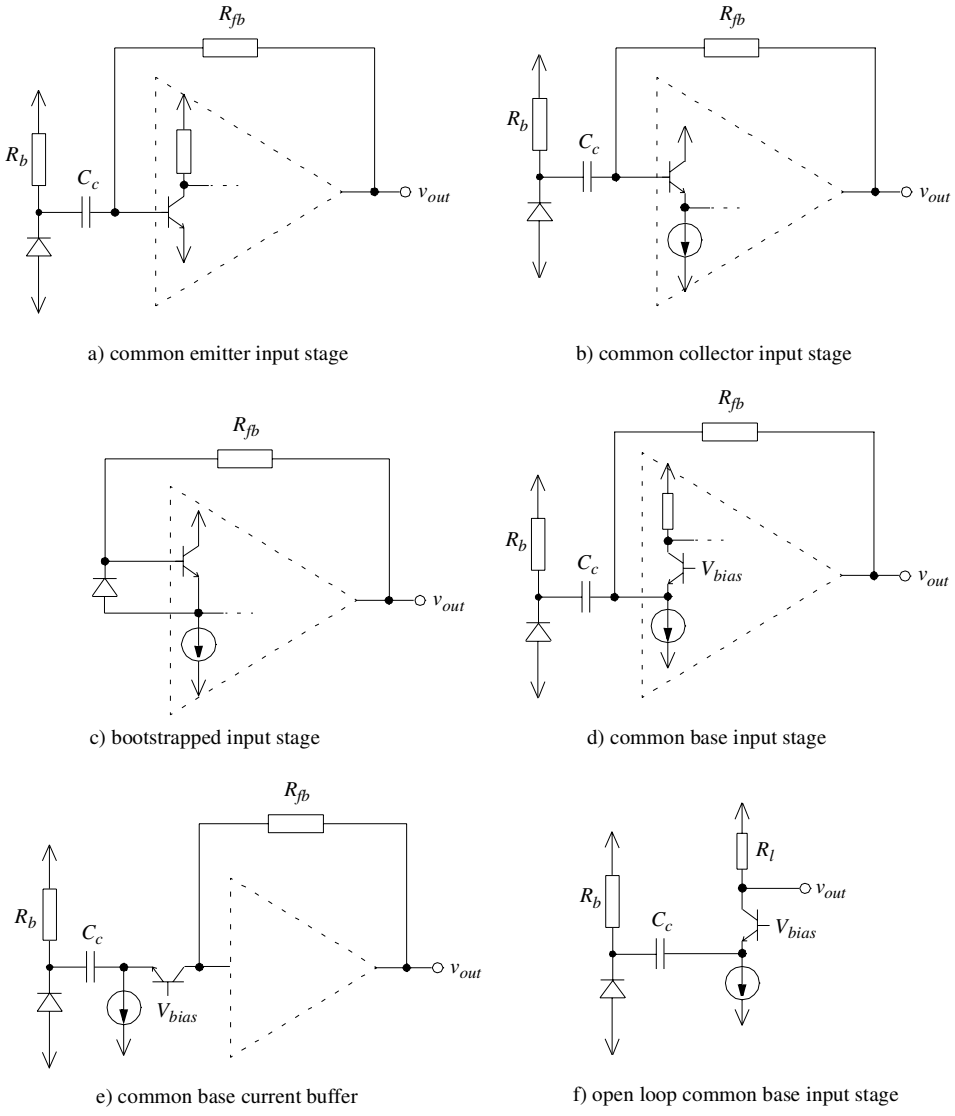

a) common emitter input stage

b) common collector input stage

c) bootstrapped input stage

d) common base input stage

e) common base current buffer

f) open loop common base input stage

Fig. 14. Various types of transimpedance preamplifier for use in bipolar technology.

3.3.3. Transimpedance preamplifier structures with MOS inputs

In MOS technology the core amplifier is often composed of several amplifying stages, because it is more difficult to achieve the required GBW due to the lower transconductance of MOS transistors. The number of inverting amplifier stages must be odd in single-ended

structures to facilitate the negative feedback. The optimal number depends on the specifications and technology, and can be estimated using the equations given by Jindal (1987) and Pietruszynski *et al.* (1988). The common source amplifier in its different forms, some of which are shown in Fig. 15, is the most popular amplifier structure (Kasper 1988). The load of the amplifier stages can be either a resistor or a diode-connected transistor, as shown in Fig. 15 a) and b), the advantage of the latter being that its transconductance tracks that of the input transistor, which helps to stabilize the gain. The amplifier stages used by Pietruszynski *et al.* (1988) are biased with constant current sources and the diode-connected transistor loads are folded as shown in Fig. 15 c). In this structure both the currents and voltages can be easily controlled, which helps dc biasing. Ingels *et al.* (1994) used a push-pull inverter in place of a single input transistor to maximize the transconductance of the amplifier stages, and hence the GBW, as shown in Fig. 15 d). The problem with this structure is that the bias current varies over a wide range with the process parameters, temperature and supply voltage, and the power supply rejection ratio is rather poor.

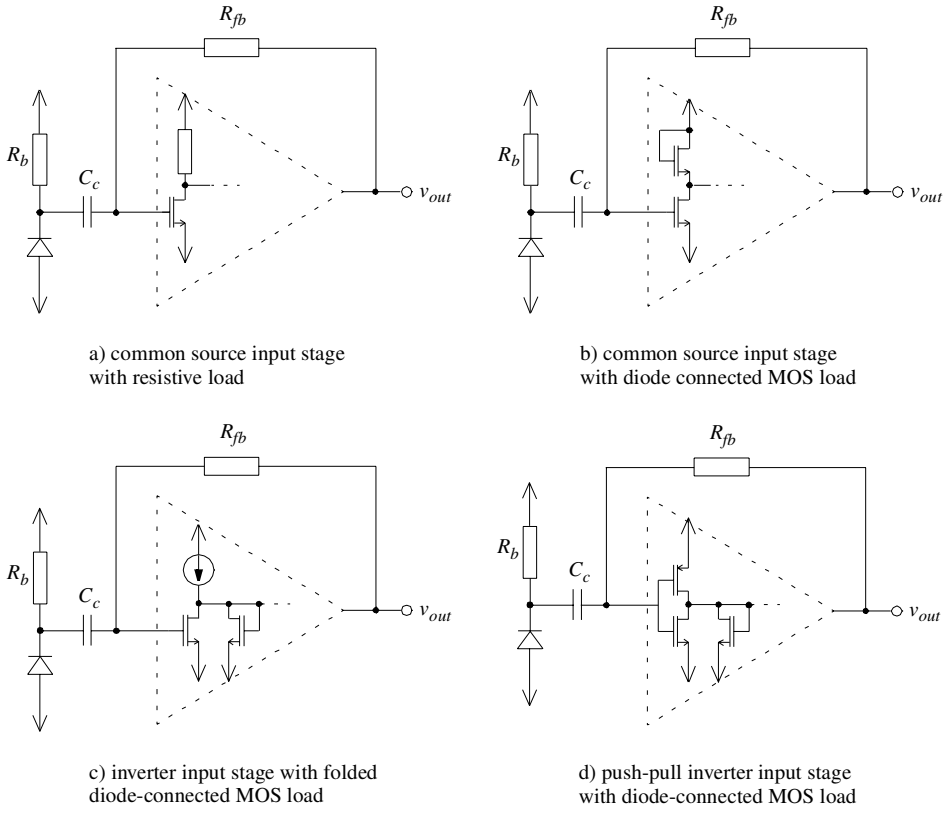

Fig. 15. Various types of transimpedance preamplifier for use in MOS technology.

Common gate input stages similar to the common base ones shown in Fig. 14 can also

be used, either in the core amplifier (Vanisri & Toumazou 1992, 1995) or as a current buffer in front of the preamplifier (Park & Toumazou 1998). The input impedance can be further reduced by using a regulated cascode in the input, as proposed by Park & Toumazou (1998).

The structure shown in Fig. 15 c) was used in this work, both in single-ended and in pseudo-differential form, as documented in Paper I and Paper II, respectively. This structure was chosen mainly because the voltage gain of the core amplifier is well defined despite large variations in the properties of MOS transistors with temperature and process parameters. This helps to make the preamplifier stable, as discussed further in Section 3.3.5. A differential implementation of the common source input, i.e. a differential pair, is also used.

3.3.4. Parasitics

The operation of the preamplifier is greatly affected by the various parasitics associated with the external packaged components, PCB, lead frame, bondwires, I/O protection structures etc. The diode and parasitic capacitances, along with the bondwire inductances, limit the achievable bandwidth and transimpedance, deteriorate the noise performance and stability, and may cause resonances and peaking in the frequency response. An example of a model of the input to a preamplifier, based on information found in the literature, manufacturers data sheets (EG&G 1994) and schematic libraries (AMS), application notes (Pearson & Beckwith 1992) and the author's own experimental results, is shown in Fig. 16.

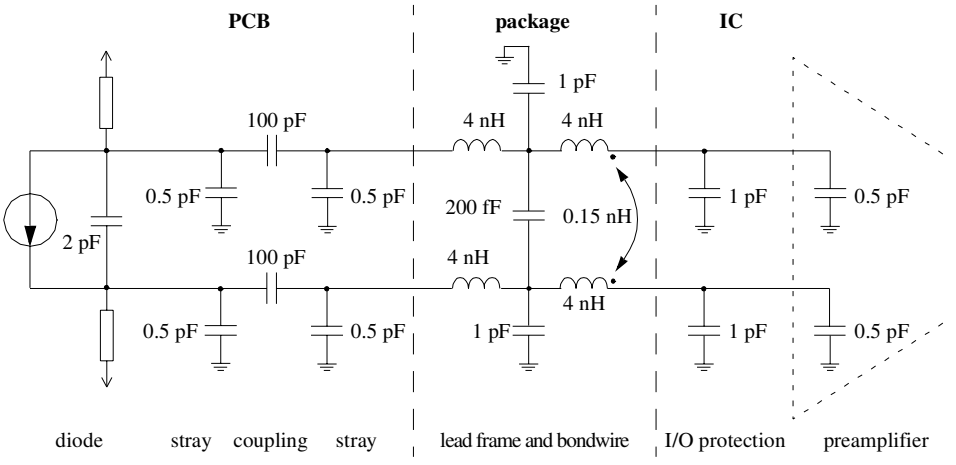

Fig. 16. Example of a model of the input to the receiver channel. The photodiode is packaged, the biasing resistors and coupling capacitors are surface mounted devices, and the integrated circuit (AMS 0.8 mm BiCMOS process) is mounted in a CLCC package.

The parasitics and their effect can be reduced by using unpackaged chips and bonding

them directly on a PCB or a ceramic substrate with minimum length bondwires. The effective inductance of the bondwires is reduced in the case of differential inputs due to the effect of the mutual inductance, and the inductances could be further reduced by using a flipchip photodiode mounted directly on the receiver chip (Hamano *et al.* 1991), or a photodetector integrated on the same chip as the receiver channel (Palojärvi *et al.* 1997c).

3.3.5. Stability

The transimpedance preamplifier employs feedback to achieve stable transimpedance gain and a wide bandwidth, but this feedback may cause stability problems. The open loop transimpedance gain, feedback factor and closed loop transimpedance gain are shown in Fig. 17. In high frequency applications the dominant pole of the open loop frequency response is located in the input node and the nondominant poles (f_{p1}, f_{p2} ...) are the poles of the core amplifier. The open loop frequency response is affected by the external parasitics, the exact values of which are unknown, and the gain A_0 and pole locations of the core amplifier, which may vary with temperature, supply voltage, process parameters etc. The inverse of the feedback factor is ideally just the feedback resistor R_{fb}, but in practise the phase lag of the distributed RC delay line of the feedback resistor (Ghausi & Kelly 1968) or the MOS feedback resistor (Jindal 1987) must be taken into account.

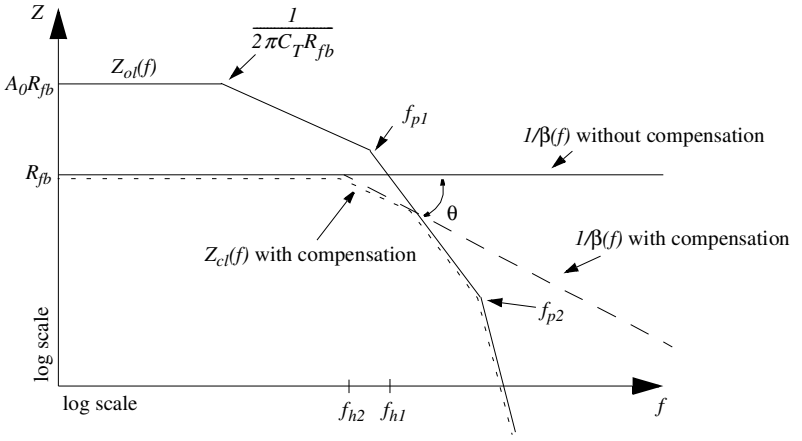

Fig. 17. Open loop transimpedance $Z_{ol}(f)$, the inverse of the feedback factor $1/\beta(f)$ and closed loop transimpedance $Z_{cl}(f)$ in a transimpedance preamplifier. C_T is the total capacitance in the input node.

The poles of the core amplifier should reside at high enough frequencies, preferably well above the cut-off frequency f_{h1} as shown in Fig. 17 to ensure stability. Therefore low-gain wideband amplifier stages need to be used. This is especially important in CMOS technology due to the lower achievable GBW per stage and large variation in component properties. The pole locations of the core amplifier can be designed to give stable response

(Abraham 1982), or even maximally flat closed loop frequency response (Das *et al.* 1995).

It may not be possible in practise to design the core amplifier so that the closed loop response is unconditionally stable. The stability can be improved by using a compensation capacitor in parallel with the feedback resistor, the effect of which is shown in Fig. 17. This compensation reduces the bandwidth of the preamplifier (f_{h2}), however, and overcompensation cannot usually be afforded in high frequency applications, as it is often the preamplifier in which the required bandwidth is hardest to achieve (Rein 1990). Peaking should not be used to widen the bandwidth, as it results in a poor pulse response (Paulus 1985).

3.3.6. Noise

The noise of the preamplifier often limits the sensitivity of the receiver channel, as shown in Fig. 12, and therefore also the maximum measurement range. The noise performance of the receiver channel can have a significant effect on the cost and feasibility of the whole receiver, as it affects the required optical output power of the laser pulser, the size and cost of the optics, the choice of photodetector etc. When optimizing the noise of the preamplifier both the magnitude of the noise sources and their transfer functions to the output, as shown in Fig. 18, must be considered. The primary noise sources of the transimpedance preamplifier are the thermal noise of the feedback resistor i_{nR} and the input-referred noise current i_{nT} and voltage u_{nT} of the core amplifier. i_{nT} and u_{nT} are often caused mainly by the input transistor. These noise sources are discussed next, first the feedback resistor, and then both a bipolar and MOS input transistor.

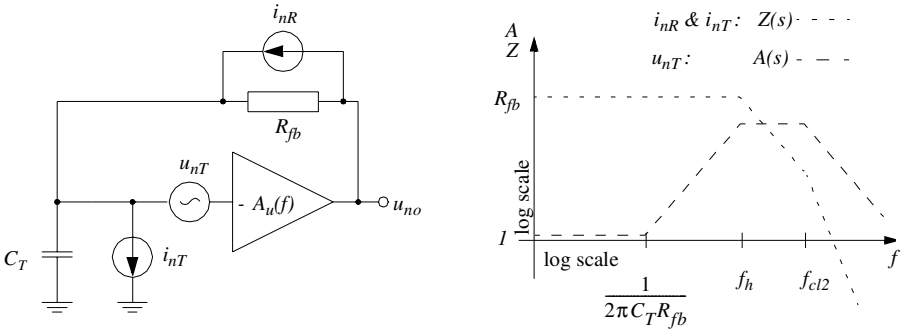

Fig. 18. Noise sources in a transimpedance preamplifier and their transfer functions to the output.

The noise of the feedback resistor is white and can be reduced by increasing the resistance, although the maximum resistance value is often limited by the conflicting requirements of wide bandwidth and wide dynamic range. Since the transfer function for this noise source is almost identical to the signal transfer function, the only way to minimize the output noise is to limit the bandwidth to the minimum value which is needed to pass the input pulse.

The primary noise sources of a bipolar input transistor are the thermal noise of the base

resistance, the shot noise of the base current and the shot noise of the collector current (Gray & Meyer 1984). The 1/f noise is very low and can be neglected in high frequency applications. The optimum value for the bias current of the input transistor in a common emitter input stage (shown in Fig. 14 a)) has been derived by Smith & Personick (1980) and by El-Diwany *et al.* (1981) and is directly proportional to the total capacitance in the input node and the bandwidth. The optimum is quite shallow, however, (Muoi 1984), so that the bias current can be tailored to meet other specifications, such as low power consumption or wide bandwidth.

From the noise performance point of view the figure of merit for a bipolar transistor in a common emitter input stage (shown in Fig. 14 a)) is $\sqrt{\beta}/(C_{be} + C_{bc})$ (Smith & Personick 1980), where C_{be} and C_{bc} are the base-to-emitter capacitance and base-to-collector capacitance. In addition, it is important that the base resistance should be minimized with a proper doping concentration and layout. The total output noise increases rapidly with the total capacitance in the input node and bandwidth, being proportional to the square of the capacitance and to the square of the bandwidth, or, if the noise of the base resistance dominates, to the cube of the bandwidth (Smith & Personick 1980).

The primary noise sources of a MOS input transistor are the thermal noise of the resistive channel and the 1/f noise (Gray & Meyer 1984). The 1/f noise, although much higher than in bipolar transistors, is not a problem in the frequency range of interest, i.e. above several MHz, especially as the input transistors are in practise relatively wide. Other noise sources which may become significant at higher frequencies in short channel transistors are the thermal noise of the gate resistance (Thornber 1981, Jindal 1984), the shot noise of the substrate currents (Jindal 1985a), the thermal noise of the substrate resistance (Jindal 1985b) and the excess noise (Jindal 1986).

The contribution of the thermal noise of the resistive channel, which is the main noise source in a MOS transistor in the frequency range of interest, can be minimized in a common source input stage (shown in Fig. 15 a)) by matching the input capacitance of the input transistor to the diode and parasitic capacitances (Jindal 1987a). As the diode capacitance in our application is high, the optimum input transistor may be excessively wide, and as the current density needs to be relatively high to achieve a wide bandwidth, the power consumption may become too high. Furthermore, the large input capacitance of the wide input transistor and the inductance of the bonding wires may result in resonance at the signal frequencies. The optimum is shallow, however, and the noise performance is quite close to the optimum when (Abidi 1987)

$$0{,}2(C_d + C_p) < (C_{gs} + C_{gd}) < 2(C_d + C_p)\,, \qquad (10)$$

where C_{gs} is the gate-to-source capacitance, C_{gd} is the gate-to-drain capacitance, C_d is the diode capacitance and C_p is the parasitic capacitance in the input node. A capacitance value near the minimum is practical. The noise of the resistive gate and substrate can be minimized by layout techniques (Chang & Sansen 1991), and the 1/f noise can be filtered out with ac coupling or cancelled out with offset compensation.

From the noise performance point of view, the figure of merit for a MOS transistor in a common source input stage (shown in Fig. 15 a)) is $g_m/(C_{gs} + C_{gd})^2$ (Smith & Personick 1980), where g_m is the transconductance. This can be maximized by using a minimum channel length and large bias current. Again, the total output noise increases rapidly with the total capacitance in the input node and bandwidth, being proportional to the square of

the capacitance and to the cube of the bandwidth (Smith & Personick 1980).

The choice between a bipolar and a MOS input transistor depends on the required bandwidth and the constraints on power consumption. The noise performance of a MOS input is better at frequencies up to a few hundred MHz (Kasper 1988). The total capacitance in the input node in our application is quite high, so that due to the noise gain peaking shown in Fig. 18, the input-referred noise voltage of the core amplifier is often the dominant noise source. It is therefore important to minimize the input-referred noise voltage of the input transistor by using a bipolar transistor with multiple interdigitated emitter and base stripes, or a MOS transistor with a very large transconductance. In practise, the bias current of a MOS input transistor must be much higher than that of a bipolar one, resulting in a higher power consumption.

Both types of input transistor are used here. In practise bipolar ones are preferable above ~50 - 100 MHz, because they make it much easier to implement a stable wideband response, and the penalty in noise performance is marginal. At lower frequencies the properties of MOS transistors are sufficiently good and their advantage in noise performance is more pronounced.

3.3.7. Differentiality

The majority of transimpedance preamplifiers have single-ended inputs and outputs. In some systems the signal is converted to a differential one in the voltage amplifier following the preamplifier (Meyer & Blauschild 1986). However, most preamplifier structures could easily be converted to fully differential ones. To the best of the author's knowledge a differential input was first proposed in his Paper II. Differentiality would bring several advantages: reduced sensitivity to disturbances, improved common mode rejection, improved linearity, reduced inductance of the input bondwires due to mutual inductance etc. The effect of differential input on noise performance must be considered case by case. On the one hand, the structure of the core amplifier is more complicated, e.g. a common emitter input must be converted to a differential pair, resulting in increased input-referred noise current and voltage. On the other hand, the effect of parasitic capacitances to the ground is halved, as shown in Fig. 19, which reduces the noise gain peaking of the input-referred noise voltage of the core amplifier ($A(s)$ in Fig. 18), and therefore also the output noise. The net effect depends on which of the noise sources is the dominant one, and

on the ratio of the parasitic capacitances to the diode capacitance.

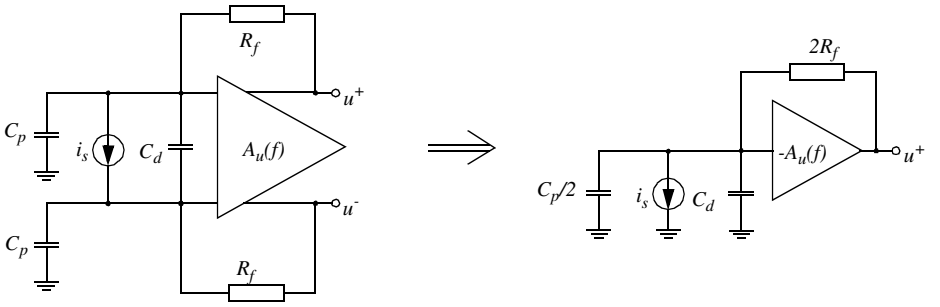

Fig. 19. A differential transimpedance preamplifier and the corresponding half-circuit.

3.4. Gain control

The dynamic range of the optical input signal in laser rangefinding applications often exceeds that of the receiver channel. If optimum accuracy is aimed at, one of the linear timing discrimination schemes presented in Chapter 4.1 should be used. As most of these schemes require that the signal should be preserved undistorted, the dynamic range of the input signal needs to be reduced by means of gain control. The signal amplitude varies mainly as a function of the measurement range and the reflectivity of the target, so that the variation is often slow enough for gain control to be used (Kilpelä *et al.* 1998). The gain control should not affect the propagation delay or the shape of the pulses, however, nor lead to any deterioration in the noise properties of the amplifier channel. The structure of the amplifier channel, the type of signal in the channel and possible places for gain control are shown in Fig. 20.

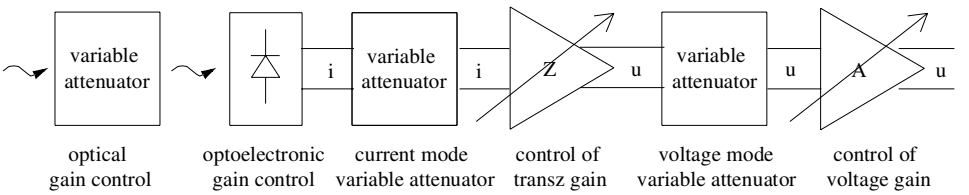

Fig. 20. Signal types and the possible modes of gain control in different parts of the receiver channel.

The dynamic range of the incoming light signal can be reduced with optical gain control structures such as a neutral density filter or a variable iris. Furthermore, the optics can be designed so that the field of view of the transmitter optics only partly overlaps with that of the receiver optics, the fraction depending on the distance (Wang *et al.* 1991). These optical

gain control structures are often slow and bulky, however, and may require a high control voltage. Moreover, the methods using a variable iris or partly overlapping fields of view may run into problems with the nonuniform cross-section of the laser beam (Vanderwall *et al.* 1974, Kilpelä *et al.* 1992). The shape of the light pulse is different in different parts of the beam, which means that, as the receiver diode sees a varying part of the beam as a function of distance or the setting of the iris, the timing point changes. In systems using an APD the avalanche gain can be controlled by changing the bias voltage. The accurate control range is quite limited, though. For example, a gain variation of 1:2 results in an error of only +/- 1.5 mm (Koskinen *et al.* 1989), but for a gain variation of 1:8 the error is increased to several decimetres (Määttä 1995).

Electronic gain control integrated within the receiver channel is desirable, because it is fast and saves space and power. From the noise performance point of view, it would be best to control the gain as late in the amplifier channel as possible, so as to minimize the degradation of the SNR. The gain must be controlled before any distortion occurs, however, and so several gain control blocks in different places may be needed. In practise the dynamic range of the transimpedance preamplifier in high frequency applications is limited to ~60 dB or so, which may not be enough in all applications, and thus gain control may already be needed in the transimpedance preamplifier or even in front of it. The accurate operating region of linear timing discrimination schemes is often limited to 20 dB ... 40 dB, which is even less than that of the preamplifier, so that it is advantageous to control the gain after the preamplifier as well.

3.4.1. Use of a current mode variable attenuator

A current mode variable attenuator, either a multiplier cell or an agc cell (Gilbert 1968), as shown in Fig. 21, can be placed between the photodetector and the transimpedance preamplifier (see Fig. 20). To the best of the author's knowledge this was first proposed by the author and was first reported in Palojärvi *et al.* (1997b). Of the two structures shown in Fig. 21, the agc cell has a better noise performance and dynamic range (Sansen & Meyer 1974), whereas the multiplier cell has a constant output common mode current, which makes cascading of the amplifier stages easier. Due to the common base connection of the input transistors, both structures have a very wide bandwidth. The linearity of the cells is limited by the base resistance of the quad transistors, capacitive feedthrough across them and the finite output conductance of the current sources (Sansen & Meyer 1973).

Very good performance has been achieved using a multiplier cell in the input of the receiver of a time-of-flight laser rangefinder, as reported in Paper V. The noise performance of the front end was not compromised and the delay variation was only +/-6 ps (corresponding to +/- 1 mm in distance) in a gain range from 1 to 1/15. In minimum attenuation mode the cell reduces to a common base buffer. The good noise properties in this mode result from the buffering action of the common base configuration, i.e. the high capacitance in the input node is isolated from the input of the transimpedance preamplifier. The good delay stability results from three facts: 1) the signal current flows through a similar path regardless of the gain setting, 2) the bandwidth of the gain control cell is so high that small changes in it do not affect the total bandwidth, and 3) the pole frequency in

the input node does not change with the gain setting. The only drawback of the structure is the extra negative power supply needed to generate the low noise bias current sources shown in Fig. 21.

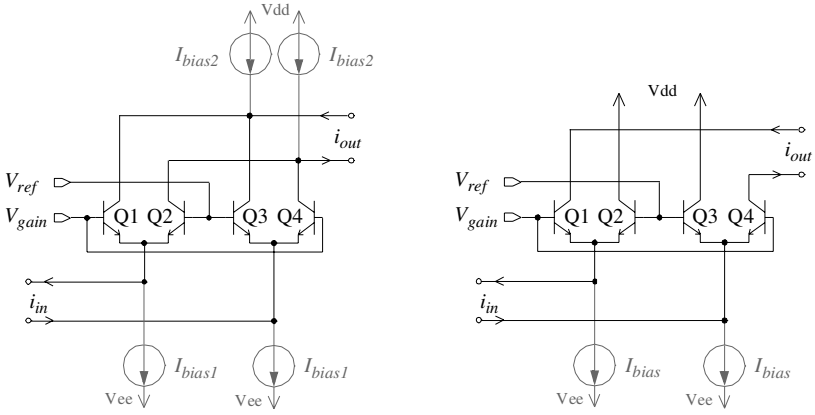

Fig. 21. Current mode gain control cells.

3.4.2. Control of transimpedance gain

If the current mode gain control scheme described above cannot be used for some reason, it is desirable to implement gain control in the transimpedance preamplifier. It is very difficult, however, to control the transimpedance gain without the bandwidth or propagation delay of the signal changing with the gain. Changing the value of the feedback resistor (Scheinberg *et al.* 1991, Meyer & Mack 1994, Paper I) affects the impedance and pole frequency in the input node, while controlling the gain of the core amplifier changes the bandwidth and shape of the frequency response (Yamashita 1986). Van den Broeke & Nieuwkerk (1993) used a current mode preamplifier and implemented gain control by steering a varying portion of the input signal current past the amplifying element. Again, it is difficult to keep the bandwidth and delay constant. All in all, it appears that no satisfactory ways of extending the dynamic range of the preamplifier using gain control have been devised so far.

3.4.3. Voltage mode variable attenuator

Gain control between the preamplifier and the voltage amplifier, where the signal is a voltage, can be realized with a voltage mode variable attenuator. One possible structure is a resistive divider, such as the R-2R ladder shown in Fig. 22. In this structure the attenuation can be changed in discrete steps, as opposed to the continuous range of values

of the current mode structures described above. On the one hand this is a limitation, but on the other hand it is easier to implement a specific attenuation value, e.g. 1/2, 1/4, 1/8. Moreover, the attenuation can be directly controlled digitally.

The R-2R ladder has good noise properties, because low signals are passed unattenuated through the first switch, and a wide linear range, as only passive components are used in the actual division. Furthermore, the bandwidth of the ladder can be made larger than that of the rest of the channel by using low valued resistors, so that small changes in bandwidth have little effect on the total bandwidth. The resistances together with the distributed capacitance of the resistors and the parasitic capacitances of the switch transistors nevertheless form a distributed RC delay line, so that the delay of the signal depends on the attenuation setting. Minimum-sized switches should be used to minimize the parasitic capacitances, and the resistances should be in the low kΩ range to keep the error caused by the intrinsic delay in the resistors in the millimeter range.

A variable R-2R ladder attenuator was used in the circuit documented in Paper III, for instance. The delay of the signal changes by +/-75 ps (corresponding to +/-11 mm in distance) in a gain range from 1 to 1/52, the delay being largest with the maximum attenuation. The delay variation can be reduced by adding extra delay with resistors R_c, as shown in Fig. 22, but it is difficult to achieve accurate compensation. The delay stability of the voltage mode attenuator appears to be inferior to that of the current mode described earlier, and therefore it is advantageous to use a current mode attenuator in front of the preamplifier if the extra power supply can be afforded.

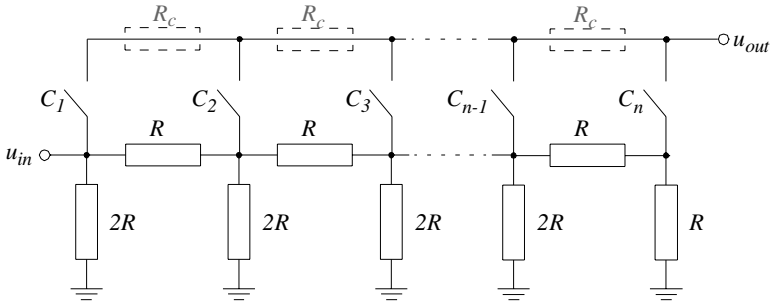

Fig. 22. A variable R-2R ladder attenuator (resistors R_c are only for delay compensation).

3.4.4. Control of voltage gain

The voltage amplifiers following the preamplifier can be implemented in two ways, either using a core amplifier and global feedback, or using an open loop amplifier with only local feedback. In the former case the gain can be controlled simply by changing the feedback factor, e.g. the configuration of the resistive feedback network can be changed with switches. However, if voltage mode techniques are used, as in basic noninverting and inverting feedback amplifiers, the gain and bandwidth are usually related, i.e. the product of gain and bandwidth is constant (Sedra & Smith 1987). This constraint is alleviated when a current feedback operational amplifier is used as the core amplifier (Bowers 1990).

Global feedback cannot always be used in wideband applications, because the GBW of the core amplifier may not be large enough to support stable feedback. A widely used wideband voltage amplifier topology is the double-stage transconductance-transimpedance amplifier (Cherry & Hooper 1963), where the input voltage signal is first converted to current in a transconductor and then back to voltage in a transimpedance amplifier. The bandwidth is wide, because only local feedback is used, and because the loading effects between the stages are reduced owing to the impedance mismatch (Reimann & Rein 1987, Möller *et al.* 1994). In the double-stage amplifier the gain control can be implemented in current mode between the stages using the previously described agc or multiplier cells, as in Meyer & Mack (1991). Other usable structures are the Gilbert quad (Sansen & Meyer 1974), or one of the more recently developed multiplier structures, such as the one given in Zarabadi & Ismail (1993).

The double-stage transconductance-transimpedance amplifier structure was used in the postamplifier of most of the receiver channels designed in this work, because it is easier to achieve the required GBW, especially in CMOS implementations. The channels then consist of alternating transimpedance and transconductance amplifiers in cascade, and the signal is converted successively from current to voltage and from voltage to current, as shown in Fig. 23. The gain control was usually implemented with a voltage mode variable attenuator between the transimpedance preamplifier and the postamplifier, and in a few cases a current mode variable attenuator was used in front of the preamplifier as well. The voltage mode attenuators will probably be replaced with current mode ones, as shown in Fig. 23, because the measurements have shown that the delay stability of the current mode attenuator is better than that of the voltage one.

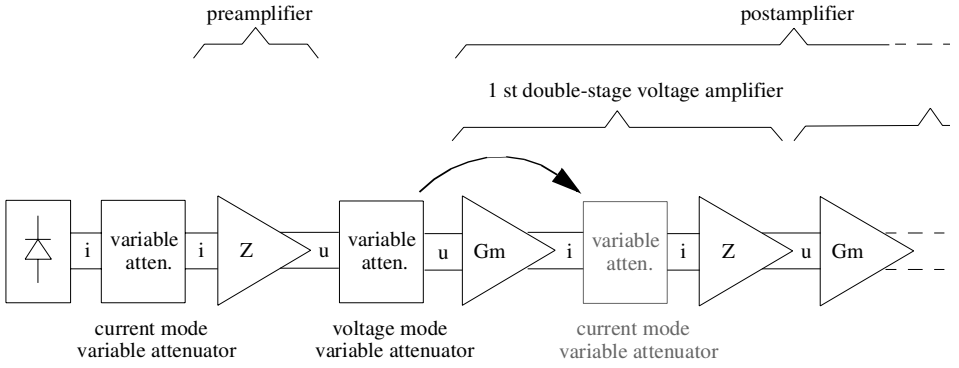

Fig. 23. An amplifier channel consisting of alternating transimpedance and transconductance amplifiers. Gain control can be implemented in current mode alone.

3.5. Amplitude measurement

The gain of the amplifier is controlled based on amplitude information provided by a peak detector, which measures the pulse amplitude at the output of the postamplifier. In some applications the amplitude information is used to compensate for variation in the timing

point with pulse amplitude as well, in which case accurate amplitude measurement is required. The peak detector can be considered a special case of a sample and hold circuit. In sample and hold circuits the variation in the input signal is followed in both directions during the tracking mode, and the circuit is switched to hold mode with an external control signal such as a clock pulse. In a peak detector the input signal is followed in only one direction and the transition to hold mode occurs automatically. Due to the similarities in their operation, similar techniques and circuit structures can be used in their implementation.

Ideally, the peak detector should follow the input signal accurately and without any delays in one direction, and the droop rate of the output should be infinitely low in the hold mode. The peak detector can be implemented using either an open or closed loop architecture (Razavi 1995), as shown in Fig. 24. The open loop architecture is composed of a rectifying element, a hold capacitor and a buffer amplifier, while in the closed loop architecture the rectifying element is controlled with an amplifier which compares the input voltage with that in the hold capacitor. The open loop architecture is faster and simpler, but it is also less accurate, and small pulses may not be detected at all, especially in CMOS implementations. The closed loop structure is more accurate, but it is slower and prone to peaking due to the delay in the feedback loop.

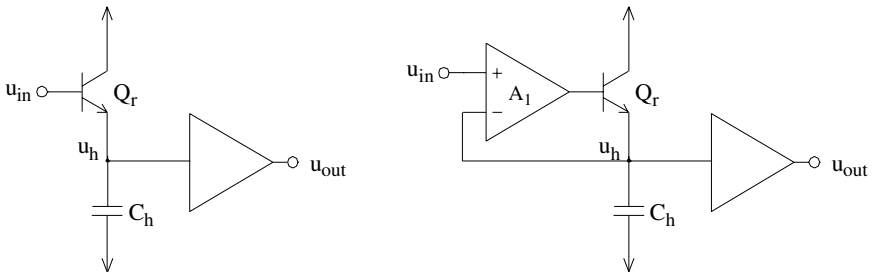

open loop architecture closed loop architecture

Fig. 24. Peak detectors using open and closed loop architectures.

The closed loop architecture was used in this work to achieve better accuracy. A multistage structure, as shown in Fig. 25, allows both short acquisition time and low droop rate to be achieved simultaneously. The first stage is designed to be as fast as possible, and the following stages have a gradually lower droop rate. Each of the stages comprises a differential pair amplifier, a transistor acting as a rectifier and a hold capacitor. The first stage has a small hold capacitor, so that the peak of a short pulse can be detected accurately. The feedback path is unbuffered to make it short and fast, so as to minimize the delay and overshoot, but the hold time is short, because the differential pair of the amplifier measuring the voltage of the hold capacitor saturates at the falling edge of the input pulse, which increases the base current i_{b1}. Nevertheless, the hold time is long enough for the second stage to sample the detected peak voltage. The second stage has a larger hold capacitor, and the feedback path is buffered with a fast emitter follower, and thus the droop rate is reduced. The last stage has the largest hold capacitor and the feedback path is buffered with a source follower, so that the leakage current and droop rate are very small.

It is advantageous to connect small current sources from nodes u_1, u_2 and u_{out} to ground to keep the rectifying transistors forward-biased in the quiescent state, so that they can react faster to the input pulse. In bipolar implementations the base currents i_{b1} and i_{b2} serve this purpose in the first two stages. The extra current source of the last stage can be shut down with the timing pulse, so as to minimize the droop rate. The same current source can be used to reset the last stage between pulses, while the first two stages are automatically reset by the base currents i_{b1} and i_{b2}. The hold capacitors are connected to the positive power supply instead of ground, so that the charging currents flow through a very short loop and do not generate disturbances in the common substrate.

The delays in the feedforward and feedback paths of each of the feedback loops should be matched to prevent excessive overshooting, i.e if the delay in the feedforward path is short, that in the feedback path should be short as well.

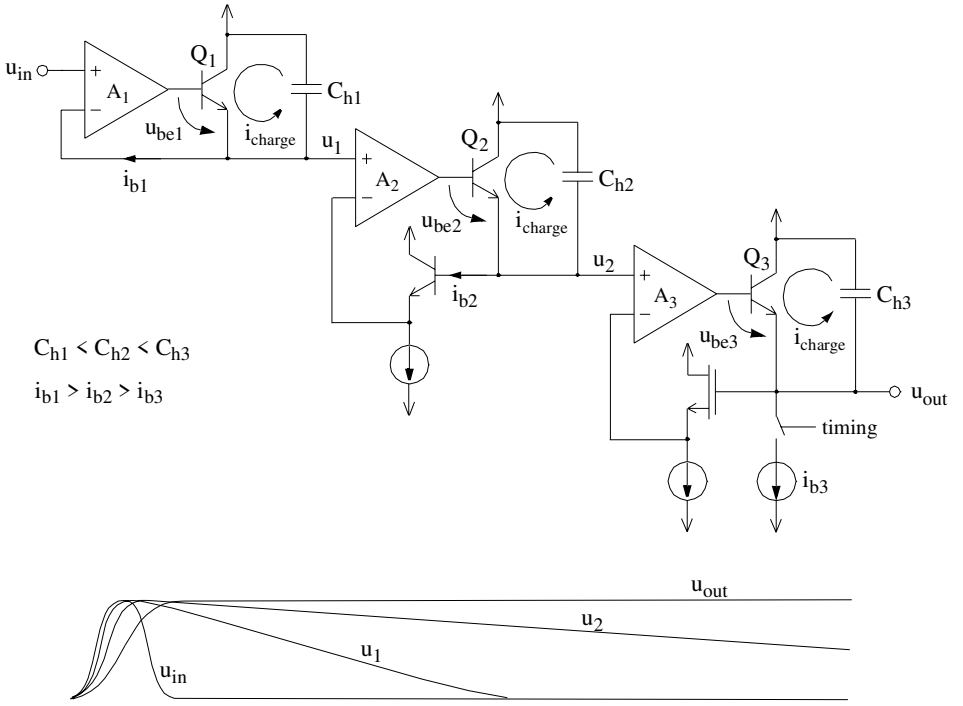

Fig. 25. Structure and operation of a multistage peak detector.

4. The timing discriminator

The timing discriminator is used to generate an accurately timed logic-level pulse from an analog input pulse. The distance measurement accuracy aimed at is only a small fraction of the width of the analog pulse, e.g. in a typical application an accuracy of better than 1 cm is required while the half-value width of the laser pulse is 1.5 m, so that the timing pulse must be generated from a specific point of the input pulse. The timing discriminator comprises a pulse shaper generating a zero crossing and a timing comparator, as shown in Fig. 10. The accuracy of the timing discrimination is mainly limited by walk error caused by the amplitude variation in the input pulses and jitter caused by noise (Gedcke & Williams 1968).

In some applications, such as fast scanning radars, it is not possible to use gain control, and thus the amplitude of the input pulses varies over a wide range. Even if gain control is used, there is some amplitude variation between the laser pulses, and therefore either the timing discrimination scheme must be insensitive to amplitude variation, or the amplitude of the pulses must be measured and correction tables used.

Even if the timing discrimination scheme itself is not sensitive to amplitude variation, the delay in the timing comparator will vary with the amplitude of the input signal. The rate of change in the delay is largest when the slope and over/underdrive of the input signal are small, so it is important to use a scheme which produces an output signal with a sufficiently fast edge and large enough over and underdrive. Furthermore, the delay variation can be reduced by increasing the bandwidth of the comparator.

4.1. Timing discrimination schemes

4.1.1. Leading edge discriminator with constant threshold

Various timing discrimination schemes have been used in nuclear physics and in radar applications, for example, the simplest one being a leading edge detector with a constant

threshold voltage, as shown in Fig. 27 a). This scheme is sensitive to variation in the pulse amplitude, so that to achieve good accuracy the amplitude of each pulse must be measured and the result corrected with tables.

The walk error in leading edge discrimination with a constant threshold can be estimated by means of a simple piecewise linear model, as shown in Fig. 26.

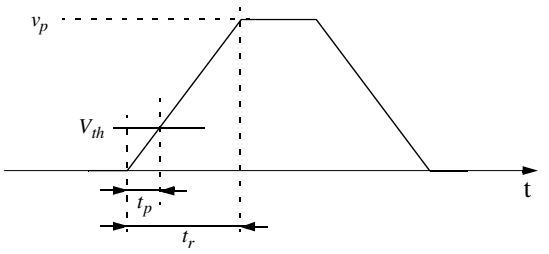

Fig. 26. Simple model used to estimate the error in a leading edge discrimination scheme.

Using the notation in Fig. 26, the timing point is

$$t_p = V_{th} t_r \frac{1}{v_p} , \qquad (11)$$

where t_p is the timing point, V_{th} is the threshold voltage, v_p is the peak amplitude of the pulse and t_r is the rise time of the pulse. If the rise time of the pulse is 1 ns and the threshold is 50 mV, for example, an amplitude variation from 100 mV to 2 V results in a timing point variation from 500 ps to 25 ps. This walk error can be compensated for, if the pulses do not vary too much in shape and if the amplitude of the signal can be measured accurately enough. Differentiating (11) with respect to the amplitude of the pulse gives

$$dt_p = -\frac{V_{th} t_r}{v_p^2} dv_p . \qquad (12)$$

Thus, with the parameter values given above, an error of only 1 mV in the amplitude measurement of a 100 mV pulse causes an error of 5 ps, which corresponds to ~1 mm in distance.

When the amplitude is higher than about 2 V, the amplifier channel and peak detector are saturated, so that the exact amplitude can no longer be measured. Fortunately, the variation in the timing point is small with larger signals.

A BiCMOS receiver channel designed for an application where the amplitude of the input signal varies over a very wide range and where gain control cannot be used to reduce the signal dynamics is described in Section 5.3.1. As none of the linear timing discrimination schemes could be used, a leading edge timing discriminator with a constant threshold voltage and compensation based on amplitude measurement was employed.

4.1.2. Linear timing discrimination schemes

Several techniques have been developed for reducing sensitivity to amplitude variation. In the case of signal independent noise an optimum transfer function from the precision point of view can be derived systematically, as presented in Section 3.1. The use of this transfer function results in a bipolar output pulse with the zero crossing at the timing point, which is also advantageous as far as walk error is concerned. The optimum transfer function is not always realizable, however, so that other schemes had to be developed.

Discrete component realizations are often based on the use of delay lines, one of the most widely used methods being the constant fraction (CF) discriminator, where an attenuated input pulse is compared with a delayed one (Gedcke & McDonald 1968, Maier & Sperr 1970, Spieler 1982). The attenuation factor is typically 20 % and the delay is equal to the rise time of the pulse. By using a shorter delay a true-constant-fraction and amplitude-and-rise-time-compensated (ARC) scheme can be implemented (real ARC only if the leading edge is linear) (Paulus 1985). The input pulse can also be differentiated and then compared with a delayed input pulse (Kinbara & Kumahara 1969), or the input pulse can be shaped (stub-clipped) with shorted delay lines (ORTEC AN-42, Gedcke & McDonald 1968).

The methods listed above extract the timing from the leading edge of the pulse. Trailing edge discrimination can be implemented by stretching and attenuating the input pulse and comparing it to the original one (ORTEC AN-42). In Määttä (1995) the input pulse is compared to a delayed one, the delay being equal to the half-value width of the input pulse. In this way the timing is generated using both the leading and trailing edges.

Integration of the timing discrimination schemes described above is difficult, because it is not easy to achieve good quality delay lines with high bandwidth and low attenuation in an integrated circuit. Transmission lines take up a lot of space, and suffer from the resistance of the metal lines and losses in the semiconducting substrate. Active delay filters costructed with OTA-C techniques, for example, require elaborate real-time tuning schemes to stabilize the delay, and have rather limited bandwidth and dynamic range (Nauta 1990). Therefore alternative methods must be used in integrated realizations.

The signal processing operations which can be performed in integrated circuits with wide enough bandwidth and dynamic range include passive filtering and simple arithmetic operations such as inversion, summation and taking a logarithm. Furthermore, passive distributed RC delay lines can be used to generate short delays, of the order of 1 ns (Simpson *et al.* 1996). The achievable performance of integrated timing discriminators using lumped elements such as resistors, capacitors and amplifiers has been shown to be comparable to that of discrete component implementations using delay lines (Nowlin 1992, Binkley 1994).

One of the timing discriminators used in integrated circuits is a highpass filter, as shown in Fig. 27 b) (Turko 1992, Simpson *et al.* 1995). This works well with symmetric pulses, but if the trailing edge is markedly slower than the leading edge, both the walk error and jitter are larger than those of the leading edge discriminator (Simpson *et al.* 1995). The cut-off frequency should be designed to give large enough under and overdrive in the input of the timing comparator to minimize the walk error. The optimal cut-off frequency from the jitter point of view depends on the dominant noise source, and optimization is easiest with Monte Carlo simulations. The highpass filter can be used in other discrimination

schemes as well. The highpass filtered pulse can be compared to the original pulse (Tanaka *et al.* 1992) or to an attenuated pulse, as shown in Fig. 27 c) (Nowlin 1992, Binkley 1994).

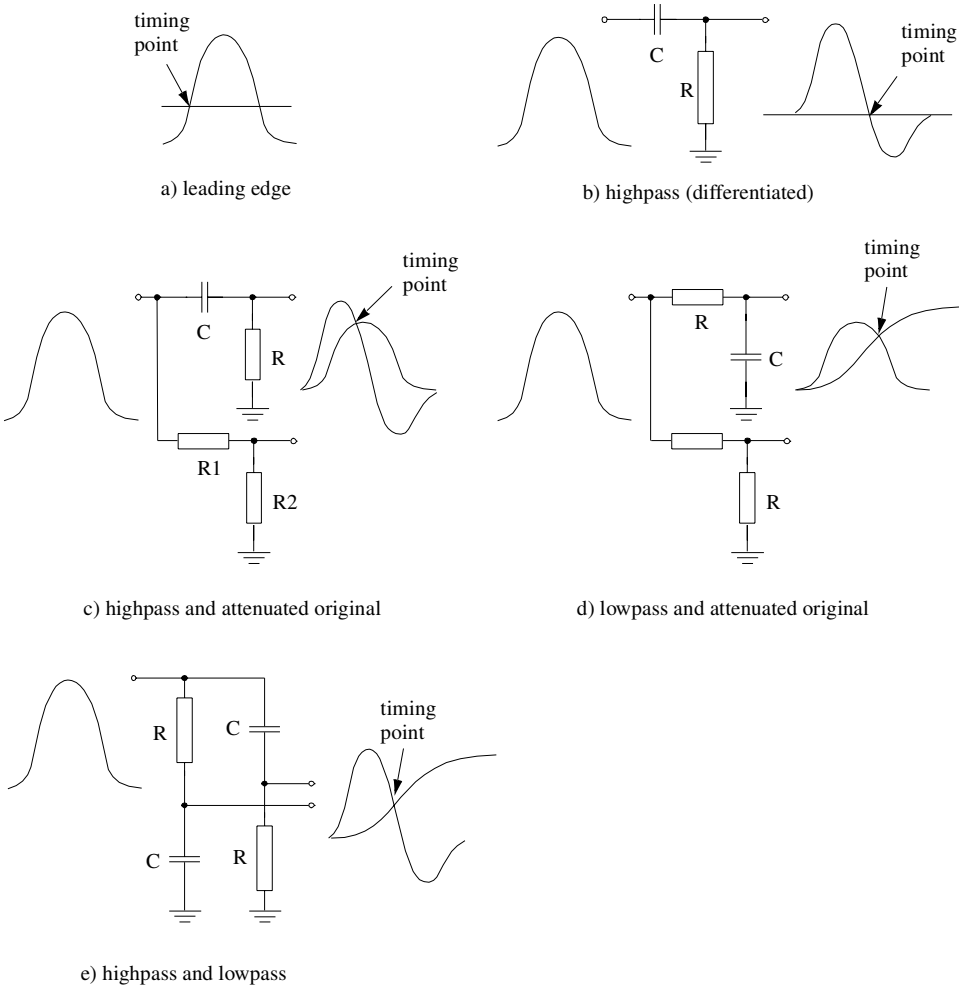

Fig. 27. Integrated timing discriminators.

The integrated equivalent to the CF discriminator is a method in which a lowpass filtered pulse is compared to an attenuated one, as shown in Fig. 27 d) (Binkley 1994). The lowpass filter is used to create a delayed version of the pulse, the problem being that the rise time of the pulse is increased in the process. In Simpson *et al.* (1996) the delay is achieved with a passive distributed RC delay line composed of a resistive stripe of polysilicon on top of a thin oxide and polysilicon plate (capacitor structure), yielding improved performance relative to a lowpass filter implemented with lumped elements. A method in which a highpass filtered pulse is compared with a lowpass filtered version is shown in Fig. 27 e). This method resembles the one used by Kinbara & Kumahara (1969), except that the delay

line is replaced with a lowpass filter.

Differential versions of the highpass and highpass/lowpass discriminators were used here. In the case of the pulse shown in Fig. 9, for instance, the optimal frequency response given by (8) and shown in Fig. 11 is approximated with 3 cascaded first order lowpass sections (preamplifier and 2 cascaded voltage amplifiers), which produce the -60 dB/decade roll-off at high frequencies, followed by one first order highpass section (highpass timing discriminator), which produces the +20 dB/decade rise at low frequencies (Paper IV). The notches at high frequencies would have been too difficult to produce accurately and robustly, and were thus ignored. The time constants were selected based on walk and jitter simulations.

4.2. The timing comparator

The output of the timing discriminator described above is an analog signal with a zero crossing (or two signals crossing each other) at the timing point. This signal needs to be converted to a digital timing pulse, because time measurement circuits often require digital input signals. This is usually done with a timing comparator, which should ideally have an infinitely large gain and bandwidth, but limited output swing. In practise, however, conversion of analog input signal with a varying amplitude to a digital pulse is quite difficult, as the delay in a practical comparator varies with the rate of change, overdrive and to some extent underdrive of the input signal (Turko *et al.* 1990). Furthermore, the input offset voltage of the comparator causes significant error in a timing discriminator (Binkley & Casey 1988).

4.2.1. Comparator structures

One possible structure for a fast comparator, which was used in this work, too, is shown in Fig. 28. The comparator consists of a few amplifying stages, a latch and a buffer stage in the output. The gain stages typically comprise a differential pair amplifier buffered with an emitter/source follower. The optimal load resistance and swing for each stage can be estimated with the equations given by Fang (1990), for example. To maximize GBW it is advantageous to use a large number of low gain stages in cascade (Simpson *et al.* 1995).

A latch is often used to maximize the speed, owing to the positive feedback (Arbel 1980, Gao *et al.* 1996). The input offset associated with a latch is reduced by using a few fast amplifying stages, and possibly offset compensation circuitry, in front of it, as shown in Fig. 28 (Razavi & Wooley 1992). An added advantage of a latch is that the outputs of the comparator change state only once, which reduces switching noise. This is important in the arming comparators used to enable the timing comparator shortly before the timing point. Furthermore, it is important to minimize switching in the start channel so that the stop channel is not disturbed.

One widely used technique for improving the speed is to first force the operating points of the amplifying stages and the latches to the middle of their swing so that the gain and

bandwidth are maximized and then trigger the comparator with the clock signal. This technique is difficult to use in a timing discriminator, however, because the exact time of arrival of the input pulse in not known beforehand.

Both emitter/source follower and open collector/drain output stages have been used, the advantage of the latter being the more symmetrical differential output voltages achieved, the smaller current consumption (Rein & Hauenschild 1990) and better stability. Furthermore, an open collector/drain stage generates less disturbances than an emitter/source follower.

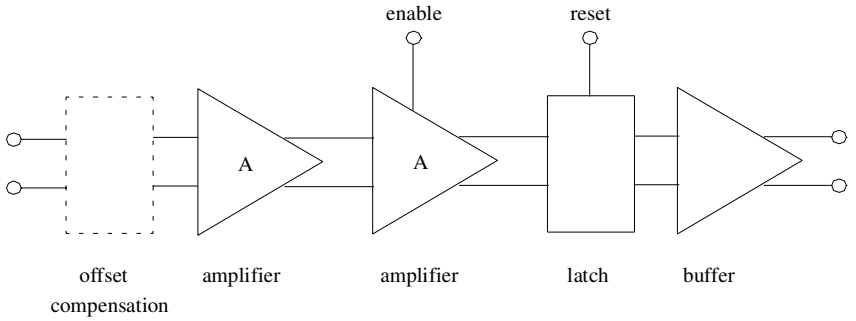

Fig. 28. Typical structure of a fast comparator.

4.2.2. Delay variation in comparators

Accurate modeling and analysis of the operation of a comparator is quite difficult, because the change of state of a comparator is a nonlinear large signal process. For example, the operation region of some active devices may change from cut-off to saturation and further to a linear region, and the comparator may operate in a linear, swing-limited or slew-rate limited region depending on the magnitude and rate of change of the input signal. Models of varying accuracy and complexity are presented in the literature.

According to a simple model presented in (Paulus 1985, ORTEC AN-42), the delay in a comparator is composed of a charge-sensitive and a fixed component. The former arises from the need to exchange charge in the input devices, e.g. to charge/discharge the base region of bipolar transistors, while the latter models the delay in the later stages (Binkley & Casey 1988). Van Valburg *et. al* (1993) and Plassche (1994) modeled the comparator with a limiting amplifier followed by a band-limiting stage. The model has been used to predict the nonlinearity of AD converters caused by delay variation in the comparator.

In a more complicated large signal model taking into account the impedance of the signal source, overdrive conditions, the rate of change of the signal, the bandwidth of the comparator etc. presented by Moscovici (1995), the comparator has at least three possible operation regions. With small input signals it operates in the linear region, and the step response is that of a simple lowpass filter. With larger input signals it may operate in a swing-limited region, where the step response first follows that of a lowpass filter but the output becomes clamped before reaching the equilibrium, so that the comparator appears

to be operating faster. With even larger signals the operation of the input stage may be limited by its slew rate.

According to a simple model based on linear small signal operation, the delay t_{dcomp} has a varying component which is inversely proportional to the square-root of the rate of change of the input signal and a fixed component t_{dmin} caused by delays in the amplifiers (Arbel 1980), i.e.

$$t_{dcomp} \approx t_{dmin} + \frac{B}{\sqrt{\frac{dv_{in}}{dt}}}, \tag{13}$$

where B is a constant depending on the structure, bandwidth etc. of the comparator. This model seems to work fairly well with large signals, too (Kilpelä *et al.* 1998).

4.2.3. Compensation for delay variation

The walk error caused by the delay variation in the comparator can be compensated for with correction tables, provided that the amplitude of the input pulses can be measured accurately. Alternatively, the walk error can be partially compensated for with a small offset voltage in series with the input of the comparator (Kinbara & Kumahara 1969). An offset voltage of the right polarity produces a walk error that is inversely proportional to the rate of change of the signal (Määttä 1995) and is of opposite polarity to the walk error caused by the comparator, i.e.

$$t_{doffset} \approx -\frac{V_{offset}}{\frac{dv_{in}}{dt}}, \tag{14}$$

where $t_{doffset}$ is the change in the timing point caused by the offset voltage V_{offset}. The cancellation is not exact, as shown in Fig. 29, because the dependences of the walk errors on the rate of change of the signal are different, but the residual error is largest with small signals, where the increasing jitter prevents the use of the discriminator in any case.

A complete differential timing discriminator, e.g. that used in the circuit described in Paper VII, composed of an arming/noise comparator, highpass/lowpass timing discriminator, timing comparator and walk error compensation, is shown in Fig. 30. The delay in the arming comparator should be minimized to allow sufficient settling of the timing comparator between the arrivals of the arming pulse and the timing pulse. To this end it is advantageous to apply the arming/enable pulse to the second or even later stage of the timing comparator. It is important to minimize the disturbances generated by the arming comparator, as it switches quite close to the timing point. The floating offset voltages can be generated by leading the output current of a D/A converter through small resistors in series with the inputs of the comparators. The arming and timing comparators can be partly

merged to save space and power consumption (Simpson *et al.* 1995).

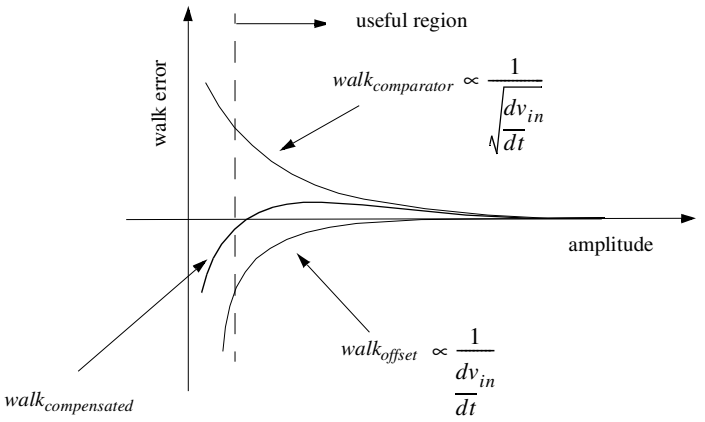

Fig. 29. Walk compensation with constant offset voltage.

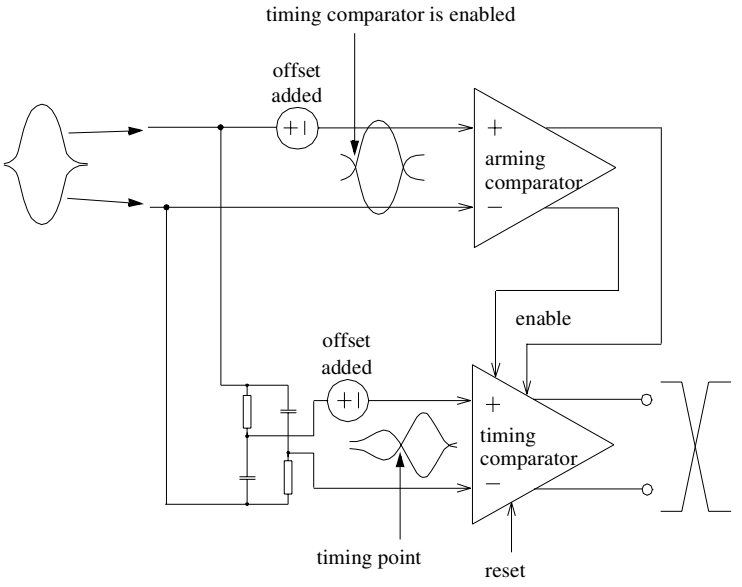

Fig. 30. A differential highpass/lowpass timing discriminator with walk compensation together with arming/noise and timing comparators.

5. Circuit implementations

A number of test circuits have been designed for various applications with different goals in mind, using CMOS, BiCMOS and bipolar technologies and in frequency ranges from about 5 MHz to about 4 GHz. Selected circuits together with experimental results are described in the following.

Sections 5.1.1 to 5.1.4 describe CMOS and BiCMOS receiver channels designed with the aim of achieving millimetre-level accuracy over a wide input signal dynamic range. Gain control was used to reduce the dynamics of the input signal, and the timing was discriminated with a linear discrimination scheme to minimize the walk error. Averaging was used to achieve the required precision. Section 5.1.5 describes a receiver channel, in which the main goal was to further improve the accuracy, i.e. to reduce both walk error and jitter by using very short laser pulses with fast edges. The circuit was implemented in a fast bipolar array to achieve the required wide bandwidth.

The main goal when designing the BiCMOS receivers described in Sections 5.2.1 and 5.2.2 was maximization of the measurement range to noncooperative targets. To this end noise in the receiver channel had to be minimized by optimizing the size and bias current of the input transistors and by limiting the bandwidth of the amplifier channel. The increased measurement range was achieved at the expense of reduced accuracy.

Chapter 5.3.1 describes a BiCMOS receiver channel designed for a fast scanning application, in which the amplitude of the input signal varies in a very wide range and where gain control cannot be used to reduce the signal dynamics. Therefore none of the linear timing discrimination schemes was usable and a leading edge timing discriminator with a constant threshold voltage was used instead.

5.1. Wideband linear receiver channels

High speed, high performance analog circuits have traditionally been realized in bipolar technology due to the superior performance (larger transconductance, voltage gain, bandwidth etc.) of bipolar transistors over MOS transistors. The increasing demands being

made on fast digital VLSI circuits has nevertheless led to the rapid development of CMOS processes, which has narrowed the gap between bipolar and CMOS technologies. Furthermore, the need to integrate whole systems on fewer chips has led to the development of circuit techniques which enable the use of CMOS processes in high performance applications, especially in the field of telecommunications. Therefore the first receiver channels were designed using CMOS technology.

5.1.1. A 65 MHz single-ended CMOS amplifier channel

A single-ended amplifier channel realized in a 1.2 μm CMOS process is described in Paper I. The circuit was designed to provide information on the accuracy of the simulation models and on the performance achievable in a standard CMOS process. The specifications were prepared with decimetre-level measurement accuracy in mind.

The amplifier channel consists of a transimpedance preamplifier with gain control, a voltage mode gain control cell and a voltage amplifier. The preamplifier comprises a wideband core amplifier and a linearized floating MOS feedback resistor, and the transimpedance gain can be controlled by changing the value of the feedback resistor and by shunting part of the input current past it. The voltage mode gain control cell is a R-2R variable ladder attenuator and the voltage amplifier comprises two cascaded double-stage transconductance-transimpedance amplifiers.

The measured performance, BW ~ 65 MHz, i_n ~ 7 pA/$\sqrt{Hz}$ and Z_{max} ~ 250 kΩ, agrees well with the simulations, but the frequency response peaks at higher gains, as shown in Fig. 8 of Paper I, which shows that cross talk between stages is a serious problem in single-ended, high-gain wideband structures. Nevertheless, the measurements indicated that the intended accuracy was achievable, provided that the interferences could be reduced. The next step was to improve the stability and to design a timing discriminator.

5.1.2. A 60 MHz differential CMOS receiver channel

The CMOS receiver channel described in Paper II was implemented in a 1.2 μm process and comprised a differential amplifier channel, a peak detector and a differential highpass timing discriminator (the arming and timing comparators are single-ended). A differential amplifier structure is used to reduce the stability problems encountered in the circuit described above and to improve its linearity. Results of measurements performed on the amplifier channel are described in Paper II and results obtained with the timing discriminator in Ruotsalainen *et al.* (1995). The results are summarized in Table 1 for convenience.

The frequency response shows no peaking in spite of the much larger transimpedance than in the circuit described in Section 5.1.1, which confirms the advantage of the differential amplifier structure. Furthermore, the noise performance of the amplifier channel is improved, owing to the larger input transistors and the increased bias current in them. However, the circuit suffers from a large drift with temperature and supply voltage,

and the usable input signal range of the timing discriminator is quite limited due to a slow timing comparator. Moreover, the single-ended structure of the arming and timing comparators results in deteriorated single shot precision at higher gains, and false triggerings of the timing comparator caused by the switching noise of the arming comparator prevent use of the maximum transimpedance.

Table 1. Measurements performed on the 60 MHz differential CMOS receiver channel.

bandwidth	60 MHz
maximum transimpedance	1.27 MΩ
input-referred noise	4.5 pA/$\sqrt{Hz}$
delay variation with gain control	+/- 50 ps (Z_{tot} = 120 kΩ – 550 kΩ)
walk error of the timing discriminator	+/- 60 ps in the range from 0.5 V to 2.2 V
average drift with temperature	54 ps/°C in the range 0°C - +50°C
drift with supply voltage	2.3 ns/V
single shot precision, 1σ (SNR[a] = 250)	66 ps

a. peak signal voltage to rms noise of the electronics ratio

The measured delay variation in the gain control cell, the walk error and the single shot precision indicate that decimetre-level accuracy can be achieved with CMOS technology. To achieve centimetre-level accuracy, the drift with temperature and supply voltage needs to be reduced and the speed of the comparator needs to be improved to reduce the walk error. The next circuits were designed using a BiCMOS process because the higher transconductance and speed of bipolar transistors helps to improve the speed of the timing comparator, especially with smaller input pulses, and therefore to reduce the walk error.

5.1.3. A 160 MHz differential BiCMOS receiver channel

A differential BiCMOS receiver channel implemented in a 1.2 µm process and comprising a voltage amplifier channel with variable gain, a differential highpass timing discriminator and a peak detector is described in Paper III. The bandwidth of the receiver channel was increased to 160 MHz to improve the single shot precision. The circuit was designed to be used with an external preamplifier, so that the properties of the receiver, such as bandwidth and total transimpedance, could be adjusted to different applications. A commercial preamplifier with a bandwidth of 100 MHz was used in the measurements.

The measurement results reported in Paper III are summarized in Table 2. The drift in the delay with temperature as given in Paper III includes the drift of an ECL comparator

(AD96687) buffering the output signal from the timing comparator, which was not measured at the time. The drift of two comparators of the same type was measured afterwards and found to be about 1 ps/°C in the temperature range from -40°C to +20°C, and about 4 ps/°C in the range from +20°C to +60°C. Taking this into account, the average drift of the receiver channel with temperature is estimated to be of the order of 1 ps/°C in the temperature range from -40°C to +60°C.

Table 2. Measurements performed on the 160 MHz differential BiCMOS receiver channel.

bandwidth	160 MHz
maximum gain	23
delay variation with gain control	+/- 75 ps (A = 0.44 – 23 i.e. 1:52)
walk error of the timing discriminator	+/- 30 ps in the range from 50 mV to 3.3 V
average drift with temperature	2.2 ps/°C in the range -40°C - +60°C
average drift with supply voltage	300 ps/V
single shot precision, 1σ	266 ps @ SNR = 20 33 ps @ SNR = 250

Compared to the CMOS realizations, the use of a BiCMOS process resulted in a smaller walk error and a wider usable signal range, especially as much smaller signals could be handled owing to the faster and more sensitive timing comparator. Furthermore, the drift with temperature and supply voltage was significantly reduced.

A prototype of a laser rangefinding device (Palojärvi 1995, Palojärvi 1997a) has been implemented employing two of these receiver channels (start and stop channels) and an integrated CMOS time-to-digital converter as described by Räisänen-Ruotsalainen *et al.* (1995). The device has an accuracy of +/- 35 mm in a measurement range of 1 m to 20 m to non-cooperative targets and in a temperature range of -10°C to +30°C. The measurement takes 200 ms with a pulsing frequency of 2.1 kHz. The accuracy is limited by the effects associated with the nonuniform cross-section of the laser beam. The device uses two-axis optics, and the receiver diode sees a varying part of the laser beam as a function of distance from the target. This means that the optical stop pulse differs in shape from the start pulse. Moreover, the stop pulse changes in shape with the measurement range, leading to linearity errors.

Most of the problems encountered in the first circuits, such as large drift and walk error, were solved by using differential structures and a BiCMOS process, and the intended centimetre-level accuracy was achieved. The problem of a very wide dynamic range of input signals in typical applications nevertheless remained, so that the main goal was now to increase the dynamic range of the receiver channel. The dynamic range of wideband transimpedance preamplifiers is often limited to about 40 dB (SNR > 10), which is not always enough. Gain control was therefore needed in the preamplifier or in front of it.

5.1.4. A 170 MHz differential BiCMOS receiver channel

The differential receiver circuit described in Paper IV was implemented in a 0.8 µm BiCMOS process and contains two receiver channels, one for the start signal and the other for the stop signal, and a peak detector. Each receiver channel comprises a transimpedance amplifier channel with variable gain and a differential highpass timing discriminator. Gain control is realized with a current mode gain control cell (see Fig. 21 a)) in front of the preamplifier and a voltage mode gain control cell (see Fig. 22) between the preamplifier and the voltage amplifier.

The goal was to achieve millimetre-level measurement accuracy in a wide dynamic range by means of accurate gain control, and to minimize the drift with temperature and supply voltage by having both the start and stop channels on the same chip. In a practical measurement event the correct gain level is first set by sending a few pulses to the target and changing the gain based on the amplitude information provided by the peak detector. The peak detector is then disabled to reduce interferences and the actual distance measurement is carried out.

The layout of the receiver circuit is shown in Fig. 31. The start and stop channels are identical, in order to match the drifts in the delays with the temperature and supply voltage. The start channel is placed on the top of the circuit and the stop channel on the bottom, and the digital control register is placed between them to increase their separation and thereby to reduce interference between channels. The amplifier channels are placed to the left and the timing discriminators to the right. The cells are laid out symmetrically and placed in straight rows to reduce disturbances and their effect inside the channels. Moreover, each cell has a separate power supply and ground, wired next to each other to reduce the total wire inductances owing to the effect of mutual inductance. The differential inputs, and the differential outputs, are also placed next to each other for the same reason. The outputs of the timing comparators are of the open collector type with small output swing, to increase the symmetry of the output signals and minimize disturbances.

Measurements of the circuit are described in Paper IV and Paper V and are summarized in Table 3. There were some problems with false triggerings caused by interferences at maximum gain, which were thought to be caused by the package parasitics (44-pin ceramic leaded chip carrier). Unpackaged chips were therefore also tested. These were bonded directly onto a ceramic substrate with minimum length bondwires and the power supplies were filtered with miniature RF capacitors placed right next to the chip. These measures solved the interference problems. Otherwise the performance of the packaged and unpackaged circuits was similar, which shows the low sensitivity of the common base input to parasitic capacitances. The single shot precision, and the drift with temperature and

supply voltage listed in Table 3, were measured using unpackaged circuits.

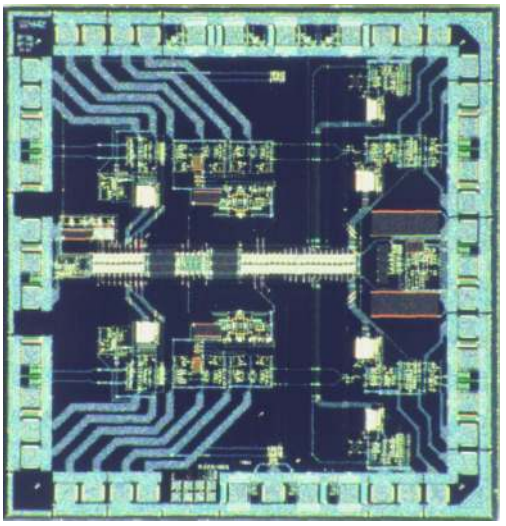

Fig. 31. Photograph of the receiver circuit.

Table 3. Measurements performed on the 170 MHz differential BiCMOS receiver channel.

bandwidth	170 MHz
maximum transimpedance	260 kΩ
input-referred noise	6 pA/$\sqrt{Hz}$
delay variation with current mode gain control	+/- 6 ps (A_i = 1 – 1/15)
delay variation with voltage mode gain control	+/- 10 ps (A_u = 1/4 – 1/16)
walk error of the timing discriminator	+/- 12 ps (u_{in} = 250 mV - 2.6 V)
drift with temperature, 1 channel	7 ps/°C (average in the range -40°C - +60°C)
drift with temperature, 2 channels	0.6 ps/°C (average in the range -40°C - +60°C)
drift with supply voltage, 1 channel	125 ps/V
drift with supply voltage, 2 channels	50 ps/V
single shot precision, 2 channels, 1σ	240 ps @ SNR(start) = 125 & SNR(stop) = 20, 58 ps @ SNR(start) = 125 & SNR(stop) = 250

Again the drifts with temperature include that of the ECL comparators (AD96687) driving the time-to-digital converter (Määttä *et al.* 1988). The estimated drift of one channel with temperature is of the order of 5 ps/°C, when the drift of the ECL comparator is eliminated. The drift is higher than that of the channel described in Section 5.1.3, because this 170 MHz circuit includes an internal preamplifier. The drift with temperature in the case of 2 channels is caused by mismatches in the start and stop receiver channels. In this case the effect of the drifts of the ECL comparators is more difficult to estimate, but the 0.6 ps/°C given in Table 3 is probably mostly due to the receiver channel (measurements indicate that the mismatches of the drifts of the ECL comparators is of the order of 0.2 ps/°C).

The measured single shot precision is shown in Fig. 32. This includes the jitter of the start and stop channels, and that of the time-to-digital converter, ~ 15 ps. The signal amplitude of the start channel was set to a value lying in the flat part of the walk curve so as to minimize the delay variation caused by pulse-to-pulse amplitude variation, the SNR of the start signal then being ~ 125. The jitter of the start channel limits the single shot precision to ~ 55 ps when the SNR of the stop channel is high.

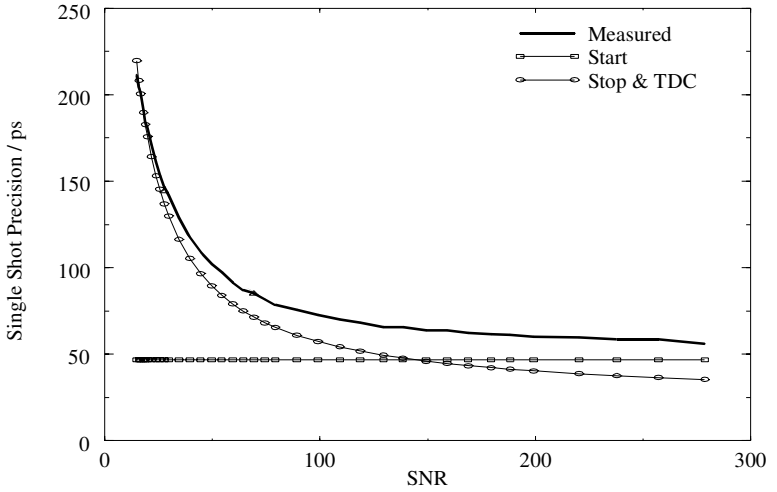

Fig. 32. Single shot precision of the receiver circuit. The measured single shot precision includes the jitter of the start and stop channels and TDC, the estimates for which are also shown in the figure (SNR is the peak amplitude of the pulse divided by the measured electronic noise of the receiver channel).

The current mode gain control cell in front of the preamplifier works very well. The delay variation is only +/-6 ps (corresponding to +/- 1 mm in distance) in a gain range from 1 to 1/15 and the noise properties are not compromised. According to simulations, the accurate gain control range can be increased to more than 1:20 by redesigning the circuit which generates the voltage controlling the attenuation of the cell (V_{gain} in Fig. 21 a)). The voltage steps are now too large at higher attenuation levels. The gain of the voltage mode gain control cell can be varied in the range 1 to 1/16, but there is a small design error in the R-2R ladder which causes excess delay variation when the gain is changed from 1 to 1/4,

so that the usable range is only from 1/4 to 1/16.

When using gain control the total walk error is less than +/- 30 ps (+/- 4.5 mm in distance) given a signal that varies in the range 0.73 μA (SNR = 10) to 0.45 mA (total range of 1:624). According to the simulations, the range can be increased to more than 1:1000 by correcting the error in the voltage mode gain control cell. An even better performance may be achievable if the voltage mode gain control cell is replaced with a current mode one, as shown in Fig. 23.

The precision of the measurement can be improved by, for example, a factor of 100 by averaging 10 000 measurements, which takes 1 s with a typical pulsing frequency of 10 kHz. In this way a worst case precision (SNR = 10) of about +/- 2.2 mm (+/- 3σ) can be achieved. Integration of the start and stop channels on the same chip reduces the drifts with temperature and supply voltage. The delay varies about 60 ps (+/- 9 mm in distance) in a temperature range of 100 °C, and about 63 ps (+/- 9.5 mm in distance) when the supply voltage varies from 4.75 V to 5.25 V (10 %). In practise the supply voltage variation, and therefore the associated drift as well, can be made negligible by using stabilized power supplies.

The total accuracy, taking into account walk error, jitter (3σ) and drift with temperature, is about +/- 16 mm (average of 10000 measurements) when the signal in a range of 1:624 and the temperature varies in a range of 100°C. The largest error, +/- 9 mm, is caused by drift with temperature. By measuring the temperature and using correction tables it may be possible to achieve an accuracy of better than +/- 10 mm.

The interference between channels has been measured by feeding input pulses to the start channel and observing the output of the stop amplifier channel with an oscilloscope. No sign of disturbances can be seen in the stop channel at the time of the start pulse, which indicates that the substrate and switching noise generated in the start channel do not disturb the stop amplifier channel.

A new prototype of a laser rangefinder employing this receiver channel and an integrated BiCMOS time-to-digital converter is being designed. The receiver PCB of the device is shown in Fig. 1 b). The main objective is to determine the achievable performance of a miniaturized rangefinder in the presence of various disturbances. Testing of the receiver channel showed that disturbances generated by the laser pulser are a serious problem and may ultimately limit the accuracy, especially as the pulser and the receiver channel must be placed next to each other. Furthermore, it is important to measure the effect of interferences between the start and stop channels in short measurement ranges.

This circuit requires accurate gain control and averaging of several measurements to achieve centimetre/millimetre-level accuracy. Measurements could be made faster by improving the single shot precision by using shorter laser pulses with very fast edges. This would reduce the walk error as well.

5.1.5. A 4 GHz differential bipolar receiver channel

A differential bipolar receiver channel implemented with a fast analog array and comprising a transimpedance amplifier channel with current mode gain control and a highpass timing discriminator is described in Paper VI. The main goal was the

minimization of walk error and timing jitter by using very fast laser pulses. A single shot precision of ~1 mm in the edge detection method requires a bandwidth of the order of 5 GHz, as shown in Section 2.3.1. A laser pulse compatible with this bandwidth has a FWHM of ~ 100 ps. The techniques used to generate very short pulses of sufficient intensity using semiconductor lasers are documented by Vainstein & Kostamovaara (1998) and Vainstein *et al.* (1998).

Since the high bandwidth and fast pulses preclude the use of packaged photodetector and receiver circuits, a ceramic hybrid was designed, as shown in Fig. 33. A small MSM photodetector chip, RF supply bypass capacitors and terminating resistors are placed next to the receiver chip and bonded with minimum length wires to minimize inductances and parasitic capacitances.

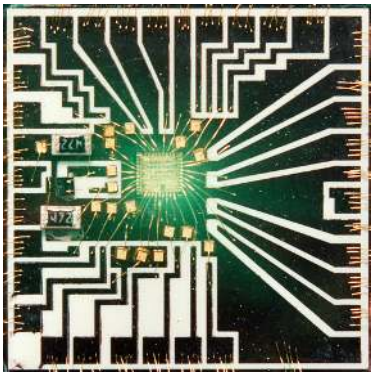

Fig. 33. A hybrid comprising the receiver channel, the MSM photodetector and a few passive components.

Measurements of the amplifier channel are described in Paper VI and are repeated in Table 4. Preliminary measurement results of the timing discriminator are also given.

Table 4. Measurements performed on the 4 GHz differential bipolar receiver channel.

bandwidth	2.5 MHz, estimated to correspond to an internal bandwidth of 4 GHz
maximum transimpedance	11 kΩ
input referred noise	8 pA/$\sqrt{Hz}$
walk error of the timing discriminator	+/- 1.5 ps (u_{in} = 65 mV - 650 mV, 1:10) +/- 6 ps (u_{in} = 40 mV - 800 mV, 1:20)
single shot precision, 1σ	below 21ps @ SNR > 10

The walk error of the timing discriminator at two walk compensation voltages is shown

in Fig. 34. A very small walk error of +/- 1.5 ps, corresponding to ~0.23 mm, is achieved in a signal amplitude range of 1:10. The increase in walk error at high amplitudes is partly caused by loading effects of the measurement setup, so that the actual range is even wider. The measured single shot precision, 21 ps (corresponding to 3 mm in distance), is limited by the measurement setup, i.e. the start channel, which is a discrete component implementation having a bandwidth of 500 MHz, and the TDC.

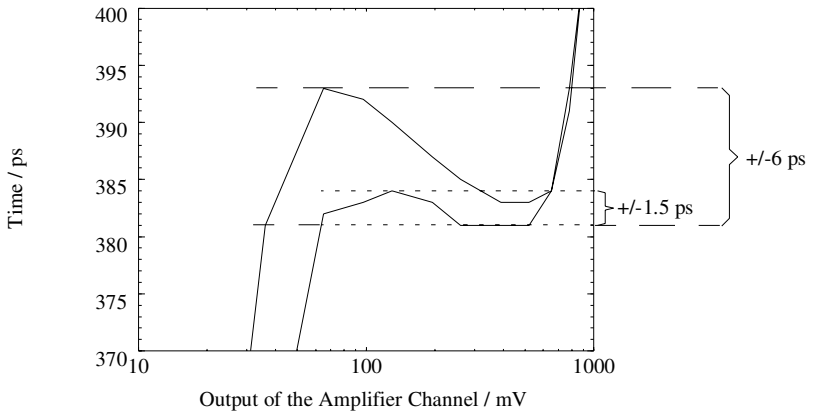

Fig. 34. Walk error of the timing discriminator at two compensation voltages.

The experimental results show that careful circuit and hybrid design can permit sub-100 ps pulses to be handled. The simulations and measurements suggest that millimetre-level single shot measurement accuracy is a realistic goal.

The use of very short pulses may significantly simplify the structure of the receiver channel. The walk error is reduced to a level which enables the use of a leading edge discriminator even when millimetre-level accuracy is required, which results in a wide dynamic range without gain control structures or walk compensation. The wider bandwidth and higher noise density than in the 170 MHz circuit described in the previous section nevertheless results in higher noise, the minimum acceptable signal current of the 4 GHz circuit being 5 μA (SNR = 10) versus the 0.73 μA of the 170 MHz circuit. Thus the improved accuracy is achieved at the expense of reduced measurement distance.

5.2. Low-noise linear receiver channels

The circuits described in this section were designed for an application in which a decimetre-level accuracy and a maximum measurement range of up to about 100 m to noncooperative targets was required. The measurement device was to consist of inexpensive components such as a laser diode with only one emitting stripe, a PIN photodiode and small-sized plastic lenses. Since the output power of the laser and the sensitivity of the photodiode are low, the amplitude of the input signal current of the receiver channel is low, too. Therefore the main goal in the designing of the circuits was

the minimization of noise in the receiver channel. This was achieved by limiting the bandwidth of the amplifier channel to about 10 MHz and optimizing the size and bias current of the input transistor. As the bandwidth is lowered, correspondingly slower laser pulses must be used, i.e. the pulses have a risetime and half-value width of about 30 ns and 50 ns. The use of pulses with slower edges results in increased walk error and jitter.

5.2.1. A 10 MHz differential BiCMOS receiver channel

The differential BiCMOS receiver channel described in Paper VII was implemented in a 1.2 μm process and comprised a transimpedance amplifier channel, a peak detector and a highpass/lowpass timing discriminator.

In low frequency applications the noise performance of a MOS input transistor is usually better than that of a bipolar one (Kasper 1988). Simulations suggest, however, that the differences in this case are fairly small. Bipolar input transistors were used because MOS transistors with the same noise performance would have required about an order of magnitude higher bias currents (~ 200 μA versus ~ 2 mA).

A highpass/lowpass timing discriminator with a corner frequency of 2 MHz was used. As the light pulses are slower and the amplifier bandwidth is reduced compared to the receivers described in Sections 5.1.1 to 5.1.4, the slope of the input signal of the timing discriminator is lower, which results in a larger walk error and jitter. Furthermore, with minimum signals, when the ratio of the slope of the signal to the noise is smallest, the noise shifts the mean value of the timing point earlier, which is manifested as an additional walk error. This walk error depends on the absolute amplitude of the input current signal of the receiver channel, as opposed to the walk error caused by the timing discrimination scheme and timing comparator, which depends on the amplitude of the voltage signal to the input of the timing discriminator.

The measurement results are described in Paper VII and are repeated in Table 5. The capacitance of the photodiode was 0.8 pF. The input-referred noise of the receiver channel can be calculated to be ~ 2.8 nA. In practise a minimum SNR of about 10 is required for reliable detection, so that the minimum input signal is ~ 28 nA. The maximum achievable measurement range can be estimated with the radar equation (6). If $i_{signal}(PIN)$ = 28 nA, P_T = 10 W, τ_T = 0.85, τ_R = 0.6 (filter included), ε = 0.1, r = 2.5 cm and R_0 = 0.5 A/W, the maximum measurement range is ~ 75 m.

By comparison, the maximum measurement range of the 170 MHz circuit described in Section 5.1.4 would be only ~ 14 m under the same conditions, i.e. about one fifth of the range achieved with this circuit. The increased measurement range is achieved at the expense of reduced accuracy, the walk error being larger by about a factor of four and the jitter by about a factor of three larger.

The aim was now to further increase the measurement range by reducing the noise of the receiver channel. Furthermore, the drift with temperature and supply voltage needed to be

reduced.

Table 5. Measurements performed on the 10 MHz differential BiCMOS receiver channel.

bandwidth	10 MHz
transimpedance	340 kΩ - 2.7 MΩ
input-referred noise	0.9 pA/$\sqrt{Hz}$
delay variation with voltage mode gain control	+/- 100 ps (A_u = 1 − 1/8)
walk error of the timing discriminator	+/- 50 ps (u_{in} = 150 mV - 2.5 V)
drift with temperature	100 ps/°C (average in the range -40°C - +60°C)
drift with supply voltage	1.25 ns/V
single shot precision, 1σ	650 ps @ SNR = 20, 180 ps @ SNR = 250

5.2.2. A 5 MHz differential BiCMOS receiver channel

The differential receiver circuit described in Paper VIII was implemented in a 0.8 μm BiCMOS process and contains two receiver channels, one for the start signal and the other for the stop signal, and a peak detector. Each receiver channel comprises a transimpedance amplifier channel with variable gain and a differential highpass timing discriminator. The start and stop channels were located on the same chip in order to minimize the drifts with temperature and supply voltage.

The measurement results given in Paper VIII are reproduced in Table 6. The measured bandwidth of the amplifier channels is 5 MHz instead of the design goal of 10 MHz, which is a result of increased capacitance in the input nodes of the preamplifier. The receiver channels were originally designed for a diode capacitance of 0.8 pF, but were tested with larger diodes having a capacitance of 2 pF. Furthermore, the capacitance of the I/O protection diodes was 3.1 pF/pad, which was about three times higher than estimated.

The input referred noise was reduced from the 0.9 pA/$\sqrt{Hz}$ of the 10 MHz channel to about 0.6 pA/$\sqrt{Hz}$ with a more aggressive design of the preamplifier. The noise bandwidth of the preamplifier was reduced by lowering the bandwidth of the core amplifier, but this also reduced the phase margin of the preamplifier and increased the risk of stability problems with a worst case combination of process parameters and temperature. Thus both the gain and bandwidth of the core amplifier were made programmable, so that the

preamplifier can always be stabilized.

Table 6. Measurements performed on the 5 MHz differential BiCMOS receiver channel.

bandwidth	5 MHz
maximum transimpedance	8.4 MΩ
input-referred noise	0.6 pA/$\sqrt{Hz}$
walk error of the timing discriminator	+/- 150 ps (u_{in} = 100 mV - 2.5 V)
drift with temperature, 1 channel	160 ps/°C average in the range -20°C - +60°C
drift with temperature, 2 channel	60 ps/°C average in the range -20°C - +60°C
drift with supply voltage, 1 channel	1050 ps/V
drift with supply voltage, 2 channel	90 ps/V
single shot precision, 2 channel, 1σ	1060 ps @ SNR = 20, 175 ps @ SNR = 250

The high total transimpedance and long optical pulses cause some interference problems between channels at short measurement ranges. The total length of the optical pulses used with the receiver is above 70 ns, which corresponds to over 10 m in distance. When the measurement range is of the order of the pulse length or lower the start pulse is still travelling in the channel when the stop pulse arrives. With the maximum gain, crosstalk causes false triggerings and deteriorates the accuracy. This is not a problem in a practical measurement situation, however, as the maximum gain is used only when the input signal is low due to the long measurement range.

Owing to the lower noise density and bandwidth compared with the 10 MHz channel described in Section 5.2.1, the input-referred noise is halved, being ~ 1.3 nA. This can be estimated to result in an increase of ~ 40 % in the maximum measurement range. On the other hand, the lower bandwidth increases the walk error and jitter by about 50 %. The noise causes an additional walk error with minimum input signals, just as with the 10 MHz circuit.

A new version of the circuit has been designed with a measured bandwidth of 15 MHz and an input-referred current noise of ~ 0.6 pA/$\sqrt{Hz}$ (unpublished work). Some modifications had to be made to achieve the same input-referred noise current density despite the larger bandwidth. The bipolar input transistors were replaced with less noisy MOS transistors, but at the expense of higher current consumption. In the older 5MHz version of the circuit the postamplifier consists of two cascaded voltage amplifiers, so that the noise bandwidth is limited by two real poles at the same frequency. In the newer 15 MHz version of the circuit the postamplifier has been designed to have the response of

a second order Butterworth lowpass filter. The complex poles result in a sharper roll-off above the cut-off frequency, so that the high frequency noise is more effectively filtered. To reduce the parasitics, the circuit was not packaged, but instead a bare chip was bonded on a ceramic substrate.

5.3. A receiver channel with a wide input signal dynamic range

While the circuits described in the previous Sections rely on gain control and linear signal processing to achieve good accuracy over a wide dynamic range, the one described in this section was designed for an industrial scanning application where the dynamic range of the signal was very wide, about 1:20 000, and gain control could not be used to reduce this dynamics. Therefore none of the timing discrimination schemes based on linear signal processing could be used, but instead a leading edge timing discriminator with a constant threshold voltage was tried. This resulted in increased walk error, which in this application limits the measurement accuracy to a few centimeters when pulses with a rise time of ~1 ns and a half-value width of ~4 ns are used.

Later on it may be possible to reduce the walk error by using very short pulses (FWHM < 100 ps) and a correspondingly faster receiver channel, so that a leading edge discriminator can be used even when millimetre-level accuracy is required. This would simplify the receiver channel considerably, as no gain control structures or walk compensation would be needed.

5.3.1. A 250 MHz differential BiCMOS receiver channel

This receiver channel consists of a differential transimpedance amplifier channel, a peak detector, an rms-meter and a timing discriminator (unpublished work). The goal was to achieve centimetre-level single shot distance measurement accuracy. The device scans the surrounding area continuously, so there is no time to measure the received amplitude and adjust the gain between distance measurements. The required measurement frequency is so high that it prohibits extra scannings to provide an “amplitude view” of the environment. Furthermore, the gain cannot be adjusted based on the amplitude of the previously received pulse, because the signal amplitude may vary in a wide range from one measurement to another due to small objects with widely differing reflectivities in the field of view.

A simplified block diagram of the circuit is shown in Fig. 35. The amplifier channel, timing comparator and peak detector are similar to those used in the circuit described in Section 5.1.4. An rms-meter is used to measure the noise of the output signal of the amplifier channel between distance measurements and the peak detector measures the amplitude of every pulse. This means that the SNR and precision of each measurement can be estimated. The variable R-2R ladder attenuator shown in the figure is used only to test and calibrate the peak detector and rms-meter during operation (a small sector of the scanning field is reserved for calibration and testing). Only the mid-gain is used in the actual measurement.

A leading edge timing discriminator with a constant threshold voltage is used. In this scheme it is sufficient to amplify the smallest pulses to a level which can be detected with a comparator. Clipping of the high amplitude pulses does not matter. The use of a constant threshold leads to a large walk error, however, which needs to be compensated with correction tables. The compensation is accurate only when the signal is in the linear range of the amplifier channel, so that the peak of the pulse can be measured accurately.

The circuit contains only a stop channel, the start signal being taken electrically from the laser pulser. This does not reduce the accuracy or increase the drift too much, because the device is calibrated continuously.

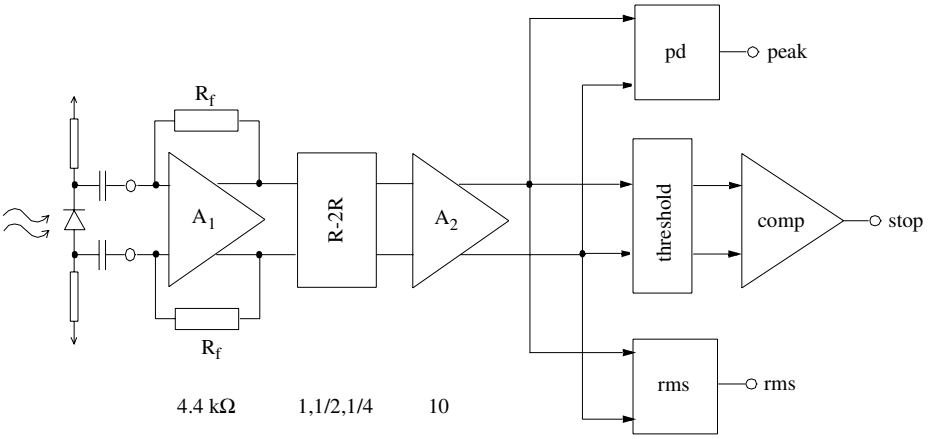

Fig. 35. Simplified block diagram of the receiver circuit.

The receiver hybrid designed for the measurements, as shown in Fig. 36, comprises the receiver channel, an APD in the middle and a few passive components such as coupling and supply bypass capacitors and biasing resistors.

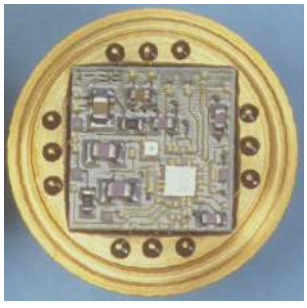

Fig. 36. A receiver hybrid comprising a receiver channel, photodetector and a few passive components.

The walk error at different temperatures is shown in Fig. 37 a). The amplitude of the optical input pulses has been varied in a range of ~ 1:4000, which according to calculations corresponds to input pulse amplitudes ranging from ~ 4 µA to ~ 16 mA. The peak of the output pulse of the amplifier channel was measured with the peak detector. The amplifier channel and peak detector can handle linearly output pulses with amplitudes of up to 1900 mV, which corresponds to an input pulse amplitude of ~ 95 µA. With higher input pulse amplitudes both the amplifier channel and the peak detector are saturated. The walk error is seen to be about 200 mm in the range ~ 4 µA to ~ 95 µA and about 70 mm in the range ~ 95 µA to ~ 16 mA.

The error after walk and temperature compensation is below +/- 35 ps, as shown in Fig. 37 b). With small amplifier output signals, below ~ 400 mV, the accuracy of the peak detector limits that of the compensation. When the amplitude of the pulses is above ~ 1900 mV, the peak detector cannot provide accurate amplitude information. In that range the compensation is performed by adding/subtracting a fixed value from the distance measurement result so that the peak-to-peak error is minimized. Hence the jump in the curves around 1900 mV.

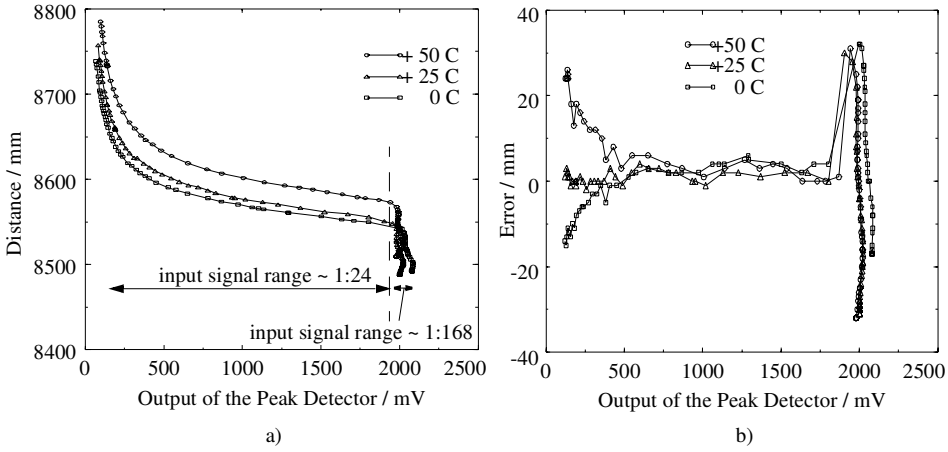

Fig. 37. a) Uncompensated distance measurements at different temperatures as a function of the measured pulse amplitude and b) error of the temperature and walk compensated distance measurements.

The single shot precision at different temperatures is shown as a function of the amplitude in the input of the timing discriminator in Fig. 38. The single shot precision is better than +/- 9.5 mm when the peak of the pulse is higher than 80 mV. The jitter of the

TDC, which is included in the figure, limits the precision at high signal amplitudes.

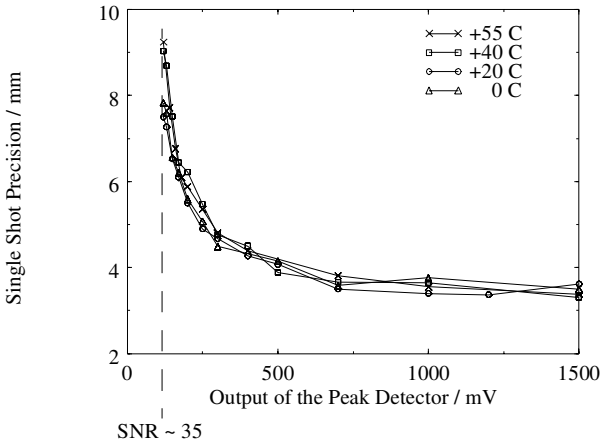

Fig. 38. Single shot precision of the measurements (single shot precision of the TDC, 3.75 mm, is included).

The measurements are listed in Table 7. The accuracy of a single measurement is better than +/- 65 mm, including walk error (amplitude varies in the range 1:4000), drift with temperature (ambient temperature varies in the range 0 °C to + 50 °C) and jitter (+/- 3σ and SNR > 35).

Table 7. Measurements performed on the 250 MHz differential BiCMOS receiver channel.

bandwidth (C_d ~2 pF)	250 MHz
transimpedance	10 kΩ, 20 kΩ, 40 kΩ
input-referred noise	7 pA/$\sqrt{Hz}$
error after walk and temperature compensation	< +/- 35 mm (i_{in} = 1:4000)
single shot precision, 1σ	< +/- 9.5 mm @ SNR > 35

The circuit achieves the intended centimetre-level single shot accuracy over a very wide dynamic range. Due to the wide bandwidth, the jitter is smaller than that of the 170 MHz receiver channel, but the walk error is larger because of the leading edge timing discrimination and limited accuracy of the peak detector with small input pulses.

5.4. Interference issues

The various parasitics and interference problems associated with packaging have a

significant effect on the performance of the receiver of the laser radar, and may in some cases be the main factor limiting the accuracy. The interferences may appear as random noise, and thus increase the jitter, or they may cause systematic delay variation. Both ceramic leaded chip carriers (CLCC) and bare chips bonded directly on the PCB or a ceramic substrate were used in this work. Packaged circuits were preferred because they are easier to handle and mount on the PCBs than bare IC chips. The lack of established and supported models for the substrate and packages prevents accurate estimation of the effect of electrical and magnetic interferences. Silicon foundries often provide the designer with simulation models of some of their packages, but neither the major suppliers of design software nor the silicon foundries have good models for the substrate or automatic tools for extracting model parameters from a circuit layout.

Inside the receiver channel the main sources of disturbance are the fast switching arming comparator and peak detector, which inject current spikes to the supply wires and the common substrate and produce large voltage swings and current spikes in the output bondwires. A laser radar contains several other switching circuits as well, such as the laser pulser, which handles very fast, large current pulses, the switching regulators and the high voltage generators, which transmit interferences via electric and magnetic fields.

The most sensitive part of the receiver channel is the preamplifier. The internal interferences are mainly picked up from the common substrate capacitively and through the substrate contacts. Both external and internal disturbances are picked up capacitively and inductively by bondwires. Another sensitive component is the timing comparator, which may be disturbed by switching of the arming comparator and peak detector just before the timing point.

Both circuit and layout techniques were used to solve these interference problems, the most important being differential structures and signal processing, and current steering operation with small voltage swings (Shin & Hodges 1989). The layout of differential circuits was made symmetrical and the layout cells placed in straight lines (Reimann & Rein 1987). Differential inputs and outputs were used because they are less susceptible to disturbances than single-ended ones.

The bondwire inductances and the parasitic and supply bypass capacitances form resonance circuits between the external and internal power supplies, and current spikes drawn by the circuit cause voltage dips and ringing in the internal supplies. The inductances were reduced by using multiple bonds (Abidi 1984). The amplitude of the dips could also have been reduced by increasing the internal bypass capacitor, but this would have brought the resonance frequency down closer to the signal frequencies. Each circuit block has separate supplies and a separate bias current to reduce crosstalk caused by the changing voltage drops in common inductances and resistances. According to simulations, each amplifying stage in the timing comparator even needs to be biased separately to prevent delay variations caused by interstage coupling through bias lines.

The bonding scheme was designed to minimize the interferences, and inputs and outputs were located on opposite sides of the circuit (Jindal 1987b), preferably in the middle of the package, where the wires were shortest. Differential signals, and the power supplies, were routed to adjacent pins so that the total inductance in the loop was minimized due to the mutual inductance. The inductance of the power supply lines could be further reduced by placing a bypass capacitor in the cavity next to the chip (Ishihara *et al.* 1992). Inputs and outputs were surrounded by ground wires to reduce coupling to other signals. Single-ended

signals, such as the output from the peak detector, were located next to a ground wire, because this minimizes the inductance of the loop (Verghese *et al.* 1995).

The substrate of current CMOS and BiCMOS processes is often composed of a thin (< 10 μm), lightly doped epitaxial layer on top of a thick (~ 500 μm), highly doped bulk. Due to its high doping and great thickness, the resistance of the bulk is low, so in effect it acts like a single node (Su *et al.* 1993). Switching in one part of the circuit couples to the common bulk through the thin high resistive epitaxial layer, spreads across the whole circuit and then couples capacitively or through substrate contacts to sensitive nodes in other parts of the circuit. The situation becomes even worse with scaling of technologies (Verghese *et al.* 1995).

Shielding guard structures were used around sensitive parts, such as the preamplifier and the timing comparator, and cells that disturb each other were placed far apart. These methods are not very efficient, however, especially when the bulk is highly doped (Su *et al.* 1993). In fact, improperly used guard rings may even make things worse. The most effective way to reduce crosstalk is to connect the bulk node to a quiet ground, and to minimize the inductance of this ground connection by attaching the chip to the cavity of the package with conducting glue and then connecting the cavity to one or more of the package leads with thick plugs (Su *et al.* 1993).

5.5. More advanced technologies and their potential

For cost reasons the receiver channels designed here were implemented in standard silicon-based CMOS, BiCMOS or bipolar processes. The performance of the receiver channel could be improved by using one of the more advanced technologies, such as silicon-germanium (SiGe), gallium-arsenide (GaAs) or indium phosphate (InP). The main features of some of these processes from the point of view of the present application are discussed briefly in this chapter.

SiGe heterobipolar transistor (HBT) technology is a viable solution for demanding medium-cost applications, because SiGe HBTs can be incorporated as add-ons to existing silicon-based BiCMOS processes with only a couple of extra processing steps (Harame *et al.* 1995). It can nevertheless provide highly improved properties relative to silicon bipolar transistors, such as higher transition frequency f_t (Baureis *et al.* 1993), higher current gain β, increased Early voltage V_A, reduced base transit time (Harame *et al.* 1995) and lower base resistance (Gao *et al.* 1996). All these properties would be very useful when designing key circuit blocks for receiver channels, such as low-noise wideband preamplifiers and ultrafast comparators.

Other possible technologies, though more expensive ones, are the GaAs and InP-based metal semiconductor field effect transistor (MESFET) and high electron mobility transistor (HEMT) processes. GaAs-based processes offer transistors with high f_t and a low noise figure, but MESFETs in particular suffer from low transconductance, poor matching and large variations in process parameters (Burns 1995). InP-based HEMT processes have the advantage that high quality photodetectors can be integrated on the same chip with the signal processing electronics (Yano *et al.* 1990, Lee *et al.* 1990). This would simplify the receiver PCB, and could result in a larger achievable bandwidth and lower noise as a result

of reduced parasitics.

GaAs-based HBTs offer high speed but suffer from high base-emitter voltage (V_{be} > 1.4 V). Furthermore, the current gain is high only at high current densities, which leads to temperature problems, especially as the thermal resistance of GaAs is high (Poulton *et al.* 1995). Compared to GaAs, InP-based HBTs have the advantages of a lower base-emitter voltage (V_{be} = 0.7 V), better thermal conductivity and higher current gain at low current densities (Jensen *et al.* 1995).

The SiGe and InP HBT technologies appear to be the most interesting ones for this application. The possibility of integrating high quality photodetectors favors the InP technology, whereas the SiGe technology would probably be less expensive. Furthermore, a SiGe HBT BiCMOS process is similar to a conventional silicon BiCMOS process, so that minimal redesign would be needed, as similar circuit techniques and structures could be used.

6. Discussion

The goal of this work was to develop integrated electronics for the receiver of a portable laser radar. To that end, several receiver channels were implemented with different specifications, as described in Chapter 5. The long-term aim is the implementation of a small-sized laser radar with a minimum number of components.

Two means of processing the analog input pulse were used here. In the first scheme the pulse was processed in a strictly linear manner with a variable gain amplifier channel followed by an amplitude-insensitive timing discriminator, while in the second scheme the pulse was amplified in an amplifier channel with a fixed gain and the timing point discriminated with a leading edge discriminator having a constant threshold voltage. The first scheme, based on linear signal processing, is often more accurate and was therefore used in most of the circuits described here, but it is more difficult to implement and typically requires gain control circuitry with a stable delay and bandwidth. The problem with the second scheme is the large walk error, which, when using pulses with a rise time of ~1 ns and a half-value width of ~4 ns, limited the measurement accuracy to a few centimeters. The experimental results described in Chapter 5 nevertheless show that sub-100 ps pulses can be handled with careful circuit and hybrid design. In this way the walk error of the leading edge discriminator can be significantly reduced, and simulations and measurements suggest that millimetre-level single shot measurement accuracy is a realistic goal. This may considerably simplify the structure of the receiver channel, as a wide dynamic range can be achieved without gain control structures or walk compensation.

Fully differential structures, including the transimpedance preamplifier, were used here, as those entail certain advantages: reduced sensitivity to disturbances, improved common mode rejection, improved linearity, reduced inductance of the input bondwires due to mutual inductance etc. The majority of transimpedance preamplifiers in common use have single-ended inputs and outputs, but most of the structures could easily be converted to fully differential ones.

In many applications the dynamic range of the input signal exceeds that of the receiver channel, so that gain control is needed. Electronic gain control integrated within the receiver channel is preferable over optical gain control from the point of view of space and power consumption. Both current and voltage mode gain control structures were designed,

and the delay stability of the current mode attenuator based on a multiplier structure was found to be better than that of the voltage one composed of a resistive divider.

The current mode gain control scheme in front of the transimpedance preamplifier developed in this work deserves special attention. The dynamic range of the preamplifier can be significantly increased using this scheme, and at least in our application, the bandwidth or noise performance of the preamplifier did not deteriorate. The delay variation was only +/-6 ps (corresponding to +/- 1 mm in distance) in a gain range from 1 to 1/15.

Both MOS and bipolar input transistors were used in the transimpedance preamplifier, the choice being dependent on the required bandwidth and the constraints on power consumption. The noise performance of a MOS input is better at frequencies up to a few hundred MHz, but the bias current of a MOS input transistor has to be much higher than that of a bipolar one, resulting in a higher power consumption. Furthermore, it is easier design a preamplifier with stable gain using bipolar transistors owing to the larger achievable GBW.

Both CMOS and BiCMOS processes have been used in the practical implementations. The measured delay variation of the gain control cell, the walk error and the single shot precision indicate that decimetre-level accuracy can be achieved with 1.2 µm CMOS technology. In the BiCMOS implementations (0.8 µm process) the higher transconductance and speed of bipolar transistors helps to improve the speed of the timing comparator, especially with smaller input pulses, and therefore to reduce the walk error. Consequently centimetre/millimetre-level accuracy was achieved.

In addition to reduced size, integration of the receiver electronics brings other advantages such as reduced disturbances and timing errors associated with the input/output (I/O) buffering, circuit packages and wiring on a PCB. Furthermore, more complicated functions can be incorporated in the receiver channel without increasing the area or complexity of the system to any considerable extent. This helps to improve the performance and versatility of the measurement devices.

Integration of the receiver channel introduces special problems of its own, however. Most of the circuit blocks have to be full-custom designed, which is time-consuming, and many components used in discrete implementations, such as accurate passive components or delay lines, are not available, so that alternative circuit techniques must be developed and used. Packaging of the receiver channel entails problems, as well. The integrated circuit is fabricated on a semiconducting substrate, and the interactions of the various blocks on this common substrate are difficult to model accurately.

It is difficult to compare the properties of the amplifier channels constructed here with those reported in the literature (Ingels *et al.* 1994, Meyer & Mack 1994, Vanisri & Toumazou 1995, Ayadi *et al.* 1997), because the areas of application and specifications, such as diode capacitances, parasitics, bandwidths and stability criteria, are so different. Higher frequencies and much smaller photodiodes are used in fiberoptic communications, for instance. Also, performance can be measured and specified in many different ways. For example, noise performance may be measured with or without a diode in the input, the output noise may be measured at one spot frequency or integrated over a certain frequency range, and peaking may be used to increase the bandwidth etc.

Comparison of timing discriminators is equally difficult. The walk error and jitter depend on the shapes and widths of the optical pulses, the frequency response and bandwidth of the amplifier channel preceding the timing discriminator, the properties of the

dominant noise source etc. The measured walk error of the highpass timing discriminator in most of the receiver channels designed here nevertheless seems to be in line with that of other implementations and discrimination schemes (Tanaka *et al.* 1992, Turko 1992, Simpson *et al.* 1995, Simpson *et al.* 1996).

6.1. Comparison with a discrete component implementation

Since the techniques developed in this work can be used to replace discrete component sub-systems with integrated ones in existing measurement devices, it is appropriate to compare the performance of integrated receiver channels with that of discrete component implementations. The main features of the 170 MHz receiver channel described in Section 5.1.4 and those of a discrete component receiver channel used in a commercially available measurement device as described by Määttä et al. (1990), Määttä et al. (1993), Määttä (1995) and Kilpelä et al. (1998) are listed in Table 8.

Table 8. Comparison of the performance of integrated and discrete component implementations of the receiver channel (C_d = 1.6 pF).

property	integrated realization	discrete realization
bandwidth	170 MHz	100 MHz
max. transimpedance	260 kΩ	150 kΩ
input-referred noise	6 pA/$\sqrt{Hz}$	6.6 pA/$\sqrt{Hz}$
delay variation with current mode gain control	+/- 6 ps (A_i = 1 − 1/15)	-
delay variation with voltage mode gain control	+/- 10 ps (A_u = 1/4 − 1/16)	several cm (1 cm = 70 ps) (A_u = 1 − 1/4)
walk error of the timing discriminator	+/- 12 ps (u_{in} = 250 mV - 2.6 V)	+/- 43 ps (u_{in} = 200 mV - 2 V)
temperature drift	0.6 ps/°C (average in the range -40°C - +60°C)	~ 0.75 ps/°C (average in the range -10°C - +35°C)
single shot precision 2 channel, 1σ	240 ps @ SNR(start) = 125 & SNR(stop) = 20, 58 ps @ SNR(start) = 125 & SNR(stop) = 250	250 ps (SNR = 20) 73 ps (SNR = 250)
area	chip size ~ 3 mm x 3 mm PCB size ~ 25 mm x 25 mm	1 x Euro1-size PCB 100 mm x 160 mm
power consumption	~ 270 mW	~ 5 W

The amplifier channels have similar transimpedances, bandwidths and input-referred

noise densities, and the single shot precision of the timing discriminator is almost the same in each case. Therefore the sensitivities of the receivers, and hence their maximum measurement ranges, are comparable. The dynamic range of the integrated receiver channel, however, is much wider owing to the superior gain control circuitry and significantly smaller walk error of the timing discriminator. When gain control is used, the total walk error of the integrated receiver channel is less than +/- 30 ps with a signal varying in the range 1:624, whereas the walk error of the discrete component implementation is +/- 43 ps with a signal varying in the range of 1:10. The walk error of the discrete component implementation can be reduced by using a faster timing comparator, and a walk error of about +/- 10.5 ps in a signal range of 1:10 has been achieved in practise (Kilpelä et al. 1998).

Probably the most pronounced improvement introduced by the use of integrated technology is the significantly reduced size and power consumption. This, along with the fact that the increased dynamic range may enable the elimination of optical gain control structures, may considerably simplify rangefinding devices. Moreover, the small size permits the integration of an array of photodetectors, receiver channels and TDCs, and working in parallel, on one chip. This may enable the realization of three dimensional object recognition and machine vision systems of new a kind, without complicated mechanical scanning structures.

6.2. Future development

The next major goal in the development of a portable laser radar is integration of the whole receiver electronics, including the photodetector, receiver channel, TDC and the required control electronics, on one chip, preferably using silicon or silicon-germanium technology. This would reduce the size and complexity of the measurement device, and could reduce the disturbances associated with the transmission of signals between circuits. An example of a current receiver hybrid used together with an integrated TDC circuit is shown in Fig. 39 a), and the goal, in which the entire receiver electronics is fitted in a single compact package, is shown in Fig. 39 b).

Integration of the photodetector would reduce the problems caused by the bondwire inductances and the various parasitic capacitances associated with the PCB, package and I/O cells. Silicon-based integrated photodetectors suffer from low sensitivity, however (Ayadi *et al.* 1997), the responsivity of a pn diode being only about 0.25 A/W at a wavelength of 850 nm (Palojärvi *et al.* 1997c). This detracts from their usability. As an option, a flip chip photodetector mounted directly on the receiver chip may be a viable solution in the future.

Integration may also cause some interference problems, especially if a fast digital clock signal is needed in the TDC. Another alternative is to use a multichip module, so that the receiver and TDC chips are placed next to each other and connections are made directly with bonding wires. Interference problems should be less severe, as the substrates of the

chips are separated.

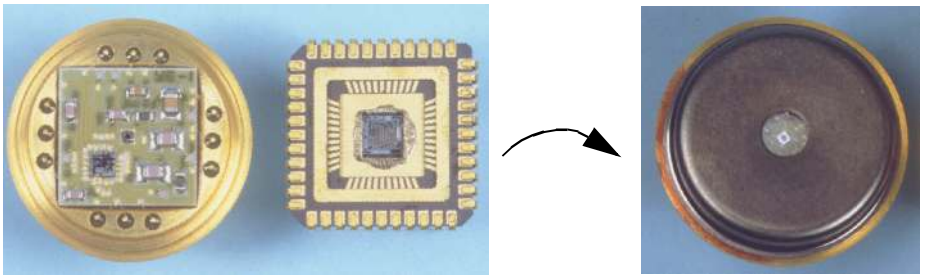

a) b)

Fig. 39. The next step in the development of a portable laser rangefinder, from a receiver hybrid and a packaged TDC (Räisänen-Ruotsalainen *et al.* 1998b) a) to fully integrated receiver electronics b).

Another goal is simplification of the system by using very short laser pulses (FWHM < 100 ps). The walk error may be reduced to a level, which enables the use of a leading edge discriminator with constant threshold even when millimetre-level accuracy is required. This would result in a wide dynamic range without gain control structures or walk compensation. SiGe heterobipolar transistor (HBT) technology is a viable solution for implementing the faster electronics needed to handle the shorter pulses, as it can provide transistors with improved properties compared to silicon bipolar transistors, hopefully at a reasonable extra cost. Furthermore, a SiGe HBT BiCMOS process is similar to a conventional silicon BiCMOS process, so that minimal redesigning would be needed, as similar circuit techniques and structures can be used. New silicon-based deep sub-micron processes are another option, but the maximum allowable supply is being scaled down with the linewidth and is currently around 3 V or even lower, which may cause problems.

7. Summary

The thesis describes the development of integrated structures and circuit implementations for the receiver channel for portable pulsed time-of-flight laser rangefinders to be used in industrial measurement applications where the measurement range is from ~ 1 m to ~ 100 m to noncooperative targets and the required measurement accuracy is from a few millimetres to a few centimetres. Alternative circuit structures are discussed, concentrating on the preamplifier, gain control circuitry and timing discriminator, which are the key circuit blocks from the performance point of view. Several circuit implementations for different applications are presented, together with experimental results.

The receiver channel is used to convert the current pulse from a photodetector to a voltage pulse, amplify it, discriminate the timing point and produce an accurately timed logic-level pulse for a time-to-digital converter. The length of the laser pulse, typically 5 ns, is large compared to the required accuracy, 1 mm corresponding to ~ 7 ps, so that a specific point in each pulse, such as the peak, has to be discriminated. The main factors limiting the accuracy of the receiver channel of a pulsed TOF laser radar are amplitude variation in the input signal, which causes systematic error, and noise, which causes random errors. Furthermore, temperature and supply voltage variation cause systematic errors, and electrical disturbances may cause both random and systematic errors. Since the amplitude of the input pulses varies over a wide range as a function of the measurement range etc., the gain of the amplifier channel needs to be controlled. Furthermore, the discrimination scheme should be insensitive to the amplitude variation of the input signal in order to minimize walk error, and the amplifier channel should have low noise to minimize timing jitter.

Two means of processing the analog input pulse are used here. In the first scheme the pulse is processed in a strictly linear manner with a variable gain amplifier channel followed by an amplitude-insensitive timing discriminator, while in the second scheme the pulse is amplified in an amplifier channel having a fixed gain and the timing point is discriminated with a leading edge discriminator with a constant threshold voltage. The first scheme, based on linear signal processing, is often more accurate and is therefore used in most of the circuits described here, but it is more difficult to implement and typically requires gain control circuitry with a stable delay and bandwidth. The problem with the

second scheme is the large walk error, which, when using pulses with a rise time of ~1 ns and a half-value width of ~4 ns, limits the measurement accuracy to a few centimetres. The experimental results nevertheless show that with careful circuit and hybrid design sub-100 ps pulses can be handled. This enables the walk error of the leading edge discriminator to be significantly reduced, and the simulations and measurement results suggest that millimetre-level single shot measurement accuracy is a realistic goal. This may considerably simplify the structure of the receiver channel, as a wide dynamic range can be achieved without gain control structures or walk compensation.

A special feature of laser rangefinders in typical industrial measurement applications is that photodiodes with a large active area and large capacitance need to be used. The large capacitance has a significant effect on the performance and design of the preamplifier. The diode and parasitic capacitances, along with the bondwire inductances, limit the achievable bandwidth and transimpedance, deteriorate the noise performance and stability, and may cause resonances and peaking in the frequency response.

New circuit techniques and structures, such as a fully differential transimpedance preamplifier and a current mode gain control scheme, have been developed in the course of this work. The differentiality provides several advantages: reduced sensitivity to disturbances, improved common mode rejection, improved linearity, reduced inductance of the input bondwires due to mutual inductance etc. The dynamic range of the preamplifier can be significantly increased by using the current mode gain control scheme, and at least in this application, the bandwidth and noise performance of the preamplifier do not deteriorate. The delay variation is only +/-6 ps (corresponding to +/- 1 mm in distance) in the gain range 1 to 1/15. The electronic gain control structures enable the elimination of awkward optical ones in some applications, which along with the small size and power consumption, owing to the use of integrated technology, considerably simplifies the rangefinding devices.

Both CMOS and BiCMOS processes are used in the practical implementations. The measured delay variation in the gain control cell, the walk error and the single shot precision indicate that decimetre-level accuracy can be achieved with 1.2 µm CMOS technology. In the 0.8 µm BiCMOS implementations the higher transconductance and speed of bipolar transistors helps to improve the speed of the timing comparator, especially with smaller input pulses, and therefore the walk error is reduced. For instance, one of the BiCMOS circuits is a differential receiver channel with a bandwidth of 170 MHz, input-referred noise of 6 pA/$\sqrt{Hz}$ and maximum transimpedance gain of 260 kΩ. By using gain control and linear signal processing an accuracy of about +/- 7 mm (average of 10000 measurements) can be achieved, taking into account walk error (input signal amplitude varies in the range 1:624) and jitter (3σ).

Another BiCMOS circuit designed for an industrial scanning application in which the dynamic range of the signal is very wide and gain control cannot be used to reduce it, uses a leading edge timing discriminator with a constant threshold voltage. The accuracy of a single measurement is better than +/- 65 mm, including walk error (amplitude varies in the range 1:4000), drift with temperature (ambient temperature varies in the range 0 °C to + 50 °C) and jitter (3σ and SNR > 35).

The achievable performance level using integrated circuit technology is comparable or superior to that of the previously developed, commercially available discrete component implementations, the most pronounced improvement being the significantly reduced size

and power consumption and the wider dynamic range, owing to the current mode gain control scheme developed in this work.

The next major goal in the development of a portable laser radar is integration of the whole receiver electronics, including the photodetector, receiver channel, TDC and the required control electronics, on one chip, preferably using silicon or silicon-germanium technology. Another goal is simplification of the system by using very short laser pulses (FWHM < 100 ps). The walk error may be reduced to a level which enables the use of a leading edge discriminator with constant threshold even when millimetre-level accuracy is required. This would result in a wide dynamic range without gain control structures or walk compensation. SiGe heterobipolar transistor (HBT) technology is a viable solution for implementing the faster electronics needed to handle the shorter pulses, as it can provide transistors with improved properties compared to silicon bipolar transistors, hopefully at a reasonable extra cost.

References

Abidi AA (1984) Gigahertz transresistance amplifiers in fine line NMOS. IEEE Journal of Solid-State Circuits, 19(6): 986-994.

Abidi AA (1987) On the noise optimum of gigahertz FET transimpedance amplifiers. IEEE Journal of Solid-State Circuits, 22(6): 1207-1209.

Abraham M (1982) Design of Butterworth-type transimpedance and bootstrap-transimpedance preamplifiers for fiber-optic receivers. IEEE Transactions on Circuits and Systems, 29(6): 375-382.

Acuity Research, Inc. (1995) Using the AccuRange 4000. Product information.

Ahola R (1979) Design of the transmitter and receiver of a laser rangefinder system for moving targets. (Liikkuvan kohteen Laser-etäisyysmittauslaitteiston lähettimen ja vastaanottimen suunnittelu). Dipl. Eng. thesis, University of Oulu, Department of Electrical Engineering.

Aiki M (1985) Low-noise optical receiver for high-speed optical transmission. IEEE Journal of Lightwave Technology. 3(6): 1301-1306.

Araki T & Yoshida H (1996) Optical distance meter using a pulsed laser diode and fast avalanche photo diodes for measurements of molten steel levels. Transactions of the ASME, 118: 800-803.

Arbel AF (1980) Analog signal processing and instrumentation. Cambridge University Press, Cambridge, USA.

Athanasious & Papoulis (1984) Probability, random variables, and stochastic processes. McGraw-Hill, New York, USA.

Automotive Engineering (1997) Scanning laser radar for on-the-road distance measuring. July, 49-52.

Ayadi K, Kuijk M, Heremans P, Bickel G, Borghs G & Vounckx R (1997) A monolithic optoelectronic receiver in standard 0.7-µm CMOS operating at 180 MHz and 176-fJ light input energy. IEEE Photonics Technology Letters, 9(1): 88-90.

Banu M & Tsividis Y (1982) Floating voltage-controlled resistors in CMOS technology. Electronics Letters 18(15): 678-679.

Baureis P, Göttler D, Oehler F & Zwicknagl (1993) Monolithic high gain DC to 10 GHz direct coupled feedback transimpedance amplifier using AlGaAs/GaAs HBT's. Proc. Nineteenth European Solid-State Circuits Conference, Sevilla, Spain: 126-129.

Bertolini G (1968) Pulse shape and time resolution. In: Bertolini G & Coche A (eds) Semiconductor detectors. North-Holland Publishing, Amsterdam, Holland.

Binkley DM & Casey ME (1988) Performance of fast ECL voltage comparators in constant-fraction discriminators and other timing circuits. IEEE Transactions on Nuclear Science, 35(1): 226-230.

Binkley DM, Simpson ML and Rochelle JM (1991) A monolithic, 2 µm CMOS constant-fraction discriminator for moderate time resolution systems. IEEE Transactions on Nuclear Science, 38(6): 1754-1759.

Binkley DM (1994) Performance of non-delay-line constant-fraction discriminator timing circuits. IEEE Transactions on Nuclear Science, 41(4): 1169-1175.

Bowers DF (1990) Applying "current feedback" to voltage amplifiers. In: Toumazou C, Lidgey FJ & Haigh DG (Eds) Analogue IC design: the current-mode approach. Peter Peregrinus Ltd, London, United Kingdom.

Bosch T, Servagent N, Chellali R & Lescure M (1996) A scanning range finder using the self-mixing

effect inside a laser diode for 3-D vision. Proc. IEEE Instrumentation and Measurement Technology Conference, Brussels, Belgium, 226-231.
Burns LM (1995) Applications for GaAs and Silicon Integrated Circuits in Next Generation Wireless Communications Systems. IEEE Journal of Solid-State Circuits, 26(3): 184-191.
Chang ZY & Sansen WMC (1991) Low-noise wide-band amplifiers in bipolar and CMOS technologies. Kluwer Academic Publishers, Boston, Massachusetts, USA.
Cherry EM & Hooper DE (1963) The Design of Wide-Band Transistor Feedback Amplifiers. Proceedings I.E.E, 110(2):375-389.
CRC Press, Inc. (1993) CRC Handbook of Chemistry and Physics. Boca Raton, Florida, USA.
Das MB, Chen JW & John E (1995) Designing optoelectronic integrated circuit (OEIC) receivers for high sensitivity and maximally flat frequency response. IEEE Journal of Lightwave Technology, 13(9): 1876-1882.
Dixon R (1994) Spread spectrum systems with commercial applications. John Wiley & Sons, Inc., New York, USA.
EG&G Optoelectronics Canada (1994) Short form catalog, emitters and detectors. Quebec, Canada.
El-Diwany MH, Roulston DJ & Chamberlain SG (1981) Design of low-noise bipolar transimpedance preamplifiers for optical receivers. IEE Proceedings, Part G, 128(6): 299-305.
Fang W (1990) Accurate analytical delay expressions for ECL and CML circuits and their applications to optimizing high-speed bipolar circuits. IEEE Journal of Solid-State Circuits, 25(2): 572-583.
Fleischer BM (1994) Jitter in relaxation oscillators. UMI Dissertation Services, Michigan, USA.
Gatti E & Svelto V (1966) Review of theories and experiments of resolving time with scintillation counters, 43: 248-268.
Gao W, Snelgrove WM & Kovacic SJ (1996) A 5-GHz SiGe HBT return-to-zero comparator for RF A/D conversion. IEEE Journal of Solid-State Circuits, 30(10): 1088-1095.
Gedcke DA & McDonald WJ (1968) Design of the constant fraction of pulse height trigger for optimum time resolution. Nuclear Instruments and Methods 58: 253-260.
Gedcke DA & Williams CW (1968) High resolution time spectroscopy 1. Scintillation detectors. ORTEC Application note.
Ghausi MS & Kelly JJ (1968) Introduction to distributed parameter networks: with application to integrated circuits. Holt, Rinehart and Winston, New York, USA.
Gilbert B (1968) A precise four-quadrant multiplier with subnanosecond response. IEEE Journal of Solid-State Circuits, 3(4): 365-373.
Gray PR & Meyer RG (1984) Analysis and design of analog integrated circuits. John Wiley & Sons, Singapore.
Gruss A, Carley R & Kanade T (1991) Integrated sensor and range-finding analog signal processor. IEEE Journal of Solid-State Circuits, 26(3): 184-191.
Hamano H, Yamamoto T, Nishizawa Y & Oikowa Y (1991) 10 Gbit/s optical front end using Si-bipolar preamplifier IC, flipchip APD, and slant-end fibre. Electronics Letters, 27(18): 1602-1605.
Harame DL, Comfort JH, Cressler JD, Crabbe EF, Sun JY-C, Meyerson BS & Tice T (1995) Si/SiGe epitaxial-base transistors - part I: materials, physics, and circuits. IEEE Transactions on Electron Devices, 42(3): 455-468.
Haykin H (1983) Communications systems. John Wiley & Sons, Singapore.
Heikkilä J (1997) Accurate camera calibration and feature based 3-D reconstruction from monocular image sequences. Acta Univ Oul C 108.
Hewlett-Packard Inc. Time interval averaging. Application note 162-1.
IEEE, The Institute of Electrical and Electronics Engineers, Inc. (1984) IEEE Standard Dictionary of Electrical and Electronics Terms. New York, USA.
Ingels M, Van der Plas G, Crols J & Steyaert M (1994) A CMOS 18 THzΩ 240 Mb/s transimpedance amplifier and 155 Mb/s LED-driver for low cost optical fiber links. IEEE Journal of Solid-State Circuits, 29(12): 1552-1559.
Ishihara N, Sano E, Imai Y, Kikuchi H & Yamane Y (1992) A design technique for a high-gain, 10-GHz class-bandwidth GaAs MESFET amplifier IC module. IEEE Journal of Solid-State Circuits, 27(4): 554-562.
Jindal RP (1984) Noise Associated with Distributed Resistances of MOSFET Gate Structures in Integrated Circuits. IEEE Transactions on Electron Devices, 31(10): 1505-1509.
Jindal RP (1985a) Noise Associated with Substrate Current in Fine-Line NMOS Field-Effect Transistors. IEEE Transactions on Electron Devices, 32(6): 1047-1052.
Jindal RP (1985b) Distributed Substrate Resistance Noise in Fine-Line NMOS Field-Effect Transistors. IEEE Transactions on Electron Devices, 32(11): 2450-2453.

Jindal RP (1986) Hot-Electron Effects on Channel Thermal Noise in Fine-Line NMOS Field-Effect Transistors. IEEE Transactions on Electron Devices, 33(9): 1395-1397.
Jindal RP (1987a) General noise considerations for gigabit-rate NMOSFET front-end design for optical-fiber communication systems. IEEE Transactions on Electron Devices, 34(2): 305-309.
Jindal RP (1987b) Gigahertz-band high-gain low-noise AGC amplifiers in fine-line NMOS. IEEE Journal of Solid-State Circuits, 22(4): 512-521.
Jensen JF, Raghavan G, Cosand AE & Walden RH (1995) A 3.2-GHz second-order delta-sigma modulator implemented in InP HBT technology. IEEE Journal of Solid-State Circuits, 30(10): 1119-1127.
Kaisto I, Kostamovaara J, Moring I & Myllylä R (1990) Laser rangefinding techniques in sensing of 3-D objects. Proc. SPIE, Santa Clara, California, USA, 1260: 122-133.
Kaisto I, Kostamovaara J, Manninen M & Myllylä R (1993) Laser radar based measuring systems for large scale assembly applications. Proc. SPIE, Brighton, United Kingdom, 2088: 121-131.
Kasper BL (1988) Receiver design. In: Miller SE & Kaminow IP (eds) Optical fiber telecommunications II. Academic Press Inc., San Diego, California, USA.
Kilpelä A, Vainshtein S, Kostamovaara J & Myllylä R (1992) Subnanosecond, high power laser pulses for time-of-flight laser distance meters. Proc. SPIE, Boston, Massachusetts, USA, 1821: 365-374.
Kilpelä A, Ylitalo J, Määttä K & Kostamovaara J (1998) Timing discriminator for pulsed time-of-flight laser rangefinding measurements. Review of Scientific Instruments 69(5) 1978-1984.
Kinbara S & Kumahara T (1969) A leading-edge time pickoff circuit. Nuclear Instruments and Methods 69: 261-266.
Koskinen M, Ahola R, Kostamovaara J & Myllylä R (1989) Automatic gain control electronics for fast pulsed time-of-flight laser rangefinding. Proc. ISA, ISA Galgary'89 Symposium, Galgary, Canada: 295-303.
Kostamovaara J, Määttä K, Koskinen M and Myllylä R (1992) Pulsed Laser Radars with High-Modulation-Frequency in Industrial Applications. Proc. SPIE, Laser Radar VII: Advanced Technology for Applications, Los Angeles, California, USA, 1633: 114-127.
Kuriyama Y, Akagi J, Sugiyama T, Hongo S, Tsuda K, Iizuka N & Obara M (1995) DC to 40-GHz broad-band amplifiers using AlGaAs/GaAs HBT's. IEEE Transactions on Solid-State Circuits, 30(10): 1051-1054.
Lee WS, Spear DAH, Agnew MJ, Dawe PJG & Bland SW (1990) 1.2 Gbit/s fully integrated transimpedance optical receiver OEIC 1.3 - 1.55 μm transmission systems. Electronics Letters, 26(6): 377-379.
Leti, Microchip Laser Range-Finder, Product Information, Grenoble, France.
Lindblom L, Edwards IK (1991) Analog position-sensing photodetectors: New life for an old technology. Photonics Spectra, 25(11): 149-156.
Loinaz MJ & Wooley BA (1995) A CMOS multichannel IC for pulse timing measurements with 1-mV sensitivity. IEEE Journal of Solid-State Circuits, 30(12): 1339-1349.
Maier MR & Sperr P (1970) On the construction of a fast constant fraction trigger with integrated circuits and application to various photomultipliertubes. Nuclear Instruments and Methods 87: 13-18.
Meyer RG & Blauschild (1991) A wide-band low-noise monolithic transimpedance amplifier. IEEE Journal of Solid-State Circuits, 21(4): 530-533.
Meyer RG & Mack WD (1991) A DC to 1-GHz differential monolithic variable-gain amplifier. IEEE Journal of Solid-State Circuits, 26(11): 1673-1680.
Meyer RG & Mack WD (1994) A wideband low-noise variable-gain BiCMOS transimpedance amplifier. IEEE Journal of Solid-State Circuits, 29(6): 701-706.
Moscovici A (1995) Understanding comparator dynamic response. Electronic Design, 43(16):77-84.
Muoi TV (1984) Receiver design for high-speed optical-fiber systems. Journal of Lightwave Technology, 2(3):243-267.
Määttä K, Kostamovaara J & Myllylä R (1988) Time-to-digital converter for fast, accurate laser rangefinding. Proc. SPIE International Conference on Industrial Inspection (ECO1), Hamburg, FRG, 1010: 60-67.
Määttä K, Kostamovaara J & Myllylä R (1990) On the measurement of hot surfaces by pulsed time-of-flight laser radar techniques. Proc. SPIE International Conference on Industrial Inspection II (ECO3), Hague, The Netherlands, 1265: 179-191.
Määttä K, Kostamovaara J & Myllylä R (1993) Profiling of hot surfaces by pulsed time-of-flight laser range finder techniques. Applied Optics, 32(27): 5334-5347.
Määttä K (1995) Pulsed time-of-flight laser rangefinding techniques and devices for hot surface

profiling and other industrial applications. Acta Univ Oul C 81.
Määttä K & Kostamovaara J (1997) High accuracy liquid level meter based on pulsed time of flight principle. Proc. SPIE, Europto Series, Munich, Germany, 3100: 268-277.
Möller M, Rein H-M & Wernz H (1994) 13 Gb/s si-bipolar AGC amplifier IC with high gain and wide dynamic range for optical-fiber receivers. IEEE Journal of Solid-State Circuits, 29(7): 815-822.
Nowlin CH (1992) Low-noise lumped-element timing filters with rise-time invariant crossover times. Review of Scientific Instruments, 63(4): 2322-2326.
ORTEC AN-42, Principles and applications of timing spectroscopy. Application note 42.
Palojärvi P (1995) Electronic and optical realization of integrated laser radar. (Integroidun lasertutkan optinen ja elektroninen toteutus.) Dipl. Eng. thesis, University of Oulu, Department of Electrical Engineering.
Palojärvi P, Määttä K & Kostamovaara J (1997a) Integrated time-of-flight laser radar. IEEE Transactions on Instrumentation and Measurement IM-46(4): 996-999.
Palojärvi P, Ruotsalainen T & Kostamovaara J (1997b) Electronic gain control with constant propagation delay for integrated transimpedance preamplifiers. Proc. 40th Midwest Symposium on Circuits and Systems, Sacramento, California, USA, 1: 225-228.
Palojärvi P, Ruotsalainen T, Simin G & Kostamovaara J (1997c) Photodiodes for High-Frequency Applications Implemented in CMOS and BiCMOS Processes. Proceedings of SPIE, Sensors, Sensor Systems, and Sensor Data Processing, Munich, Germany, 3100: 119-126.
Park SM & Toumazou C (1998) Low noise current-mode CMOS transimpedance amplifier for giga-bit optical communication. Proc. IEEE International Conference on Circuits and Systems, Monterey, California, USA., 1:293-296.
Paulus TJ (1985) Timing electronics and fast timing methods with scintillation detectors. IEEE Transactions on Nuclear Science 32(3): 1242-1249.
Pearson T & Beckwith D (1992) MC10/100H640 clock driver family I/O spice modeling kit. Motorola application note AN1400.
Personick SD (1973) Receiver design for digital fiber optic communications systems, I & II. The Bell System Technical Journal, 52(6):843-886.
Pietruszynski DM, Steininger JM & Swanson EJ (1988) A 50-Mbit/s CMOS monolithic optical receiver. IEEE Journal of Solid-State Circuits, 23(6): 1426-1433.
Poulton K, Knudsen KL, Corcoran JJ, Wang K-C, Nubling RB, Pierson RL, Chang M-C, Asbeck PM & Huang RT (1995) A 6-b, 4 GSa/s GaAs HBT ADC. IEEE Journal of Solid-State Circuits, 30(10): 1109-1118.
Razavi B (1995) Principles of data conversion system design. IEEE Press, New York, USA.
Razavi B & Wooley BA (1992) Design techniques for high-speed, high-resolution comparators. IEEE Journal of Solid-State Circuits, 27(12): 1916-1926.
Rehak P (1983) Detection and signal processing in high-energy physics. In. Bologna G & Vincelli M (ed.) Data acquisition in high-energy physics. North-Holland, Amsterdam, Netherlands.
Reimann R & Rein H-M (1987) Bipolar high-gain limiting amplifier IC for optical-fiber receivers operating up to 4 Gbit/s. IEEE Journal of Solid-State Circuits, 22(4): 504-511.
Rein H-M (1990) Silicon bipolar integrated circuits for multigigabit-per-second lightwave communications. IEEE Journal of Lightwave Technology, 8(9): 1371-1378.
Rein H-M & Hauenschild J (1990) Suitability of present silicon bipolar IC technologies for optical fibre transmission rates around and above 10 Gbits/s. IEE Proceedings, Part G, 137(4): 251-260.
Rogers DL (1984) Transimpedance input stage for current amplifiers. IBM Technical Disclosure Bulletin, 27(4B): 2521-2522.
Rüeger JM (1990) Electronic distance measurement. Spinger-Verlag, Berlin Heidelberg, Germany.
Ruotsalainen T, Palojärvi P & Kostamovaara J (1995) BiCMOS and CMOS timing detectors for the receiver of a portable laser rangefinding device. Proc. 38th Midwest Symposium on Circuits and Systems, Rio de Janeiro, Brazil, 2: 1022-1025.
Räisänen-Ruotsalainen E, Rahkonen T & Kostamovaara J (1995) A Low-Power CMOS Time-to-Digital Converter. IEEE Journal of Solid-State Circuits, 30(9): 984-990.
Räisänen-Ruotsalainen E (1998) Integrated time-to-digital converter implementations. Acta Univ Oul C 122.
Räisänen-Ruotsalainen E, Rahkonen T & Kostamovaara J (1998a) Integrated Time-to-Digital Converters Based on Interpolation. Journal of Analog Integrated Circuits and Signal Processing, 15(1): 49-57.
Räisänen-Ruotsalainen E, Rahkonen T & Kostamovaara J (1998b) A Time-to-Digital Converter with 35 ps Resolution and 2.5 ms Range. Proc. 41th Midwest Symposium on Circuits and Systems, Notre Dame, Indiana, USA.

Samuels M, Patterson S, Eppstein J & Fowler R (1992) Low cost, handheld lidar system for automotive speed detection and law enforcement. Proc. SPIE, Laser Radar VII, Los Angeles, California, USA, 1633: 147-159.

Sansen WMC & Meyer RG (1973) Distortion in bipolar transistor variable-gain amplifiers. IEEE Journal of Solid-State Circuits, 8(4): 275-282.

Sansen WMC & Meyer RG (1974) An integrated wide-band variable-gain amplifier with maximum dynamic range. IEEE Journal of Solid-State Circuits, 9(4): 159-166.

Scheinberg N, Bayruns RJ & Laverick TM (1991) Monolithic GaAs transimpedance amplifiers for fiber-optic receivers. IEEE Journal of Solid-State Circuits, 26(12): 1834-1839.

Scott MW (1990) The United States of America as represented by the Department of Energy, assignee. Range imaging laser radar. US patent 4.935.616.

Sedra AS & Smith KC (1987) Microelectronic circuits. Holt, Rinehart and Winston. Inc., New York, USA.

Senior JM (1992) Optical fiber communications, Principles and practice. Prentice Hall, London, United Kingdom.

Shin HJ & Hodges DA (1989) A 250-Mbit/s CMOS crosspoint switch. IEEE Journal of Solid-State Circuits, 24(2): 478-485.

Sibley MJN, Unwin RT, Smith DR, Boxall BA & Hawkins RJ (1984) A monolithic transimpedance preamplifier for high speed optical receivers. British Telecom Technology Journal 2(3): 64-66.

SICK, Proximity Laser Scanner, Product Information, SICK AG, Waldkirch, Germany.

Simpson ML, Britton CL, Wintenberg & Young GR (1995) An integrated, CMOS, constant-fraction timing discriminator for multichannel detector systems. IEEE Transactions on Nuclear Science 42(4): 762-766.

Simpson ML, Young GR, Jackson RG & Xu M (1996) A monolithic, constant-fraction discriminator using distributed r-c delay line shaping. IEEE Transactions on Nuclear Science 43(3): 1695-1699.

Simpson ML & Paulus MJ (1998) Discriminator design considerations for time-interval measurement circuits in collider detector systems. IEEE Transactions on Nuclear Science 45(1): 98-104.

Smith RG & Personick SD (1980) Receiver design for optical fiber communication systems. In: Kressel H (eds) Semiconductor devices for optical communication. Springer-Verlag, New York, USA.

Spieler H (1982) Fast timing methods for semiconductor detector. IEEE Transactions on Nuclear Science 29(3): 1142-1158.

Su DK, Loinaz MJ, Masui S & Wooley BA (1993) Experimental results and modeling techniques for substrate noise in mixed-signal integrated circuits. IEEE Journal of Solid-State Circuits, 28(4): 420-430.

Tanaka M, Ikeda H, Ikeda M & Inaba S (1992) Development of a monolithic constant fraction discriminator. IEEE Transactions on Nuclear Science 39(5): 1321-1325.

Thornber KK (1981) Resistive-gate-induced thermal noise in IGFET's. IEEE Journal of Solid-State Circuits, 16(4): 414-415.

Turko BT, Kolbe WF & Smith RC (1990) Ultra-fast voltage comparators for transient waveform analysis. IEEE Transactions on Nuclear Science, 37(29): 424-429.

Turko BT & Smith RC (1992) A precision timing discriminator for high density detector systems. IEEE Transactions on Nuclear Science 329(5): 1311-1315.

Unwin RT (1982) A high-speed optical receiver. Optical and Quantum Electronics, 14: 61-66.

Vainshtein SN & Kostamovaara JT (1998) Spectral filtering for time isolation of intensive picosecond optical pulses from a Q-switched laser diode. Journal of Applied Physics, 84(4): 1843-1847.

Vainshtein SN, Simin GS & Kostamovaara JT (1998) Deriving of single intensive picosecond optical pulses from a high-power gain-switched laser diode by spectral filtering. Journal of Applied Physics, 84(8): 4109-4113.

van den Broeke LAD & Nieuwkerk AJ (1993) Wide-Band Integrated Optical Receiver with Improved Dynamic Range Using a Current Switch at the Input. IEEE Journal of Solid-State Circuits, 28(7): 862-864.

van de Plassche R (1994) Integrated analog-to-digital and digital-to-analog converters. Kluwer Academic Publishers, Dordrech, the Netherlands.

Vanderwall J, Hattery WV & Sztankay ZG (1974) Subnanosecond rise time pulses from injection lasers. IEEE Journal of Quantum Electronics, 10:570-572.

Wang J, Määttä K & Kostamovaara J (1991) Signal power estimation in short range laser radars. Proc. LIA International Symposium on Optical Sensing and Measurement Symposuim (ICALEO'91), San Jose, California, USA, 73: 16-26.

Vanisri T & Toumazou C (1992) On the design of low-noise current-mode optical preamplifiers. Journal of Analog Integrated Circuits and Signal Processing, 2(3):179-195.

Vanisri T & Toumazou C (1995) Integrated high frequency low-noise current-mode optical transimpedance preamplifiers: theory and practice. IEEE Journal of Solid-State Circuits, 30(6):677-685.

van Valburg J & van de Plassche R (1993) High speed folding ADC's. In: Huijsing J, van der Plassche R & Sansen W (eds) Analog circuit design. Kluwer Academic Publishers, Dordrech, the Netherlands.

Vella-Coleiro GP (1988) Optimization of the optical sensitivity of p-i-n FET receivers. Electron Device Letters, 9(6):269-271.

Verghese NK, Schmerbeck TJ & Allstot DJ (1995) Simulation techniques and solutions for mixed-signal coupling in integrated circuits. Kluwer Academic Publishers, Boston, Massachusetts, USA.

Wilson B & Darwazeh I (1987) Transimpedance optical preamplifier with a very low input resistance. Electronics Letters, 23(4): 138-139.

Yamashita K, Kinoshita T, Takasaki Y, Maeda M, Kaji T & Maeda N (1986) A variable transimpedance preamplifier for use in wide dynamic range optical receivers. IEEE Journal of Solid-State Circuits, 21(2): 324-330.

Yano H, Aga K, Kamei H, Sasaki G & Hayashi H (1990) Low-noise current optoelectronic integrated receiver with internal equalizer for gigabit-per-second long-wavelength optical communications. IEEE Journal of Lightwave Technology, 8(9): 1328-1333.

Yano H, Sasaki G, Murata M & Hayashi H (1992) An ultra-high-speed optoelectronic integrated receiver for fiber-optic communications. IEEE Transactions on Electron Devices, 39(10): 2254-2259.

Zarabadi SR & Ismail M (1993) A 100 MHz BiCMOS four-quadrant multiplier/mixer. Proc. Nineteenth European Solid-State Circuits Conference, Sevilla, Spain: 130-133.

Ziemer R & Tranter W (1985) Principles of Communications. 2nd ed., Houghton Mifflin, Boston, USA.